TOXICOLOGICAL AND CHEMOTHERAPEUTIC EFFECTS OF ORAL CESIUM CHLORIDE IN PC-3 AND LNCAP PROSTATE CANCER HUMAN XENOGRAFTS

by

JONATHAN CEDRIC LOW

BSc, The University of British Columbia, 2004

A THESIS SUBMITTED IN PARTIAL FULFILLMENT OF THE REQUIREMENTS FOR THE DEGREE OF

MASTER OF SCIENCE

in

THE FACULTY OF GRADUATE STUDIES

(Pharmaceutical Sciences)

THE UNIVERSITY OF BRITISH COLUMBIA

April 2007

ABSTRACT

Purpose: High pH Therapy is an alternative cancer therapy involving the daily ingestion of concentrated dosages of cesium chloride (CsCl). Although the U.S. Food and Drug Administration has not approved the use of CsCl as a cancer treatment, individuals seeking this therapy need only search the internet to purchase CsCl solutions or tablets. Companies market these CsCl treatments by presenting the most recent CsCl cancer research, the majority of which is outdated and incomplete. The purpose of this study was to assess the therapeutic and toxicological effects of CsCl administration in mice bearing human prostate cancer tumors.

Methods: Three CsCl dose titration studies were completed in tumor bearing and non-tumor bearing athymic nude mice. All mice were administered either vehicle (controls), 150mg/kg, 300 mg/kg, 600 mg/kg, 800 mg/kg, 1000 mg/kg or 1200mg/kg of CsCl once daily by oral gavage for 30 consecutive days. Body mass was measured daily, food and water consumption were measured every two days, and tumor volume was measured twice weekly. Histopathological analysis was conducted on tissues collected from each of the studies. Serum AST, ALT and creatinine were also measured.

Results: Chronic administration of 800mg/kg to 1200mg/kg CsCl significantly reduced PC-3 tumor growth but had no effect on LNCaP tumor growth. In addition, tumor bearing and non-tumor bearing animals receiving these concentrated CsCl dosages (800mg/kg-1200mg/kg) developed bladder crystals and showed an increase in water consumption. An observed loss in body mass and an increased prevalence of post-mortem cardiac fibrin clots appeared to be dependent on the xenograft type and

concentration of CsCl administered. CsCl did not affect serum AST, ALT and creatinine levels in any of the treatment groups.

Conclusions: Although CsCl appears to have some therapeutic benefit in treating the PC-3 prostate cancer model, a number of toxicological effects were also observed linked to its administration, including loss of body mass, increase of water consumption, fibrin clot formation and bladder crystal formation.

TABLE OF CONTENTS

LIST OF TABLES

LIST OF FIGURES

LIST OF ABBREVIATIONS

ANOVA ---------- analysis of variance

AR ---------- androgen receptor

AST---------- aspartate aminotransferase

ALT ---------- l-alanine:2-oxoglutarate aminotransferase

AA ---------- atomic absorption

Cs ---------- cesium

CsCl ---------- cesium chloride

DHT ---------- dihydrotestosterone

DMEM ---------- dulbecco's modified eagle medium

DRE ---------- digital rectal examination

FBS ---------- fetal bovine serum

HPLC---------- high performance liquid chromatography

IL-6 ---------- interleukin-6

IL-1β ---------- interleukin-1β

LOD ---------- limit of detection

LOQ ---------- limit of quantification

NAD---------- nicotinamide adenine dinucleotide

NADH---------- reduced nicotinamide adenine dinucleotide

%CV---------- percent coefficient of variance

PSA---------- prostate specific antigen

RPMI ---------- roswell park memorial institute

STD---------- standard deviation

TNF-α ---------- tumor necrosis factor α

ACKNOWLEDGEMENTS

I would like to thank my supervisors, Dr. Emma Guns and Dr. Kishor Wasan. Dr. Guns provided a great environment to conduct my experiments and to learn new techniques. In addition, her enthusiasm, open mindedness and overall support have been crucial throughout my research. Dr. Wasan's vast experience and knowledge in pharmaceutical sciences have been pivotal to the success and rigor of my project. Thank you both for your contributions.

I would like to thank my committee members, Dr. Brian Rodrigues, Dr. Helen Burt, Dr. Marcel Bally, Dr. Stelvio Bandiera and Dr. Urs Hafeli for their suggestions and contributions to my project.

Lastly, I would like to thank my coworkers, past and present, at the Prostate Centre at VGH for their guidance and friendship: Dr. Simon Cowell, Andy Eberding, Yang Zhou, Catherine Wood, Alain Musende, Hans Adomat, Mary Bowen, Jennifer Locke, Dr. Ladan Fazli and Michael Blicker.

DEDICATION

This work is dedicated to…

My parents, Cedric and Pamela Low, my siblings, Christopher and Rachel Low, and to my girlfriend, Sarb Tatla. Their unwavering support has been crucial throughout my studies.

Section 1

Introduction

1.1 Project Overview

Prostate cancer is the most prevalent form of cancer in North American men. Like most cancers, the mechanism by which individuals develop this disease is poorly understood; likely there is some interplay between genetics and environment. The search for alternate treatments for advanced prostate cancer remains elusive. Although techniques exist to cure early stage, localized (stage T1-T3), hormone dependent prostate cancer, current treatments for advanced prostate cancer (stage T4-M) typically only increase life expectancy by months to one or two years.

A number of alternative cancer treatments exist, whose proponents often claim curative effects. However, most of these treatments have not been rigorously researched to support these claims. Regardless, a large proportion of cancer patients often purchase these alterative therapies once diagnosed with their disease. These alternative treatments are often self administered by the patient either while receiving their conventional therapy or alone as a single agent. Co-administration of alternative treatments with conventional cancer therapies may be dangerous, as possible interactions between the two therapies may lead to higher levels of toxicity than administration of either agent alone.

Cesium chloride (CsCl) is the main component of an alternative cancer treatment known as "High pH Therapy". According to Dr. Keith Brewer, the creator of this therapy, administration of CsCl can reduce tumor volume by increasing intracellular tumor pH in both man and mice (1). However, to date there is no published work by Dr. Brewer illustrating CsCl's ability to increase intracellular pH.

Although the US. Food and Drug Administration has not approved the use of CsCl as a cancer treatment, individuals seeking this therapy need only search the internet to

purchase CsCl solutions or capsules. Most of the companies that advertise on the internet, promote their products by citing the most current CsCl cancer research, the majority of which is outdated or incomplete (2-4).

There have been a limited number of preclinical and clinical studies conducted evaluating the therapeutic effects of CsCl. For the most part, the results from these studies provide support that CsCl may be able to treat different forms of cancer (5-10). However, the archaic cancer models and suboptimal experimental designs used in these studies reduce their credibility.

Studies investigating the toxicity of CsCl have revealed some inherent side effects, but have not produced a rigorous toxicological profile. In addition, the severity of these reported side effects appear to vary considerably from study to study; cardiac abnormalities in man and canines are the most severe effects attributed to CsCl administration (11-23). It should be noted that only a few case studies have reported patients with these cardiac abnormalities (15-23).

The lack of CsCl research is detrimental to the safety of consumers taking CsCl products, because the efficacy and toxicity of CsCl has not been fully delineated. The purpose of this research project was to assess the therapeutic effect of chronic daily administration of CsCl in mice bearing human prostate tumor xenografts. In addition, the toxicological profile of CsCl was also determined using tumor bearing and non-tumor bearing nude mice through histopathology and serum based toxicity assays.

1.2 Background

1.2.1. Cancer

Cancer is a disease which is typically characterized by unregulated cellular growth and proliferation that disrupts the function of normal bodily systems, potentially leading to the death of the host. The transition of a normal cell to that of a population of cancerous cells requires numerous rounds of mutation and proliferation in the midst of evading cellular regulatory circuitry. Hanahan and Weinburg described six physiological alterations that normal cells must undertake to become cancerous: growth signal self-sufficiency, antigrowth signal insensitivity, avoidance of apoptosis, infinite replicative capability, angiogenesis and the ability to metastasize (24). To date more than 100 different types of cancer have been identified (24). In 2002, it was predicted worldwide that 10.9 million people were diagnosed with cancer and 6.7 million people died of the disease (25).

1.2.2. Prostate Cancer

1.2.2.1 Epidemiology

Prostate cancer is the second most prevalent form of cancer in men and ultimately the fifth most prevalent form of cancer worldwide (25). In most developed countries, the incidence of prostate cancer has increased over time, while the mortality rate from this disease has decreased (26). These same trends are not observed in developing countries as a result of under funded health care systems and limited access to these health care

systems (26). Interestingly, the incidence of prostate cancer is quite low in most Asian countries including Japan (25). However, an increase in incidence is observed in individuals who emigrate from a low-risk country like Japan to a high-risk country like the United States (25). These results indicate the potential role of environmental factors influencing this disease (25).

In North America, prostate cancer is the most prevalent form of cancer in men as it contributes to 33% of all new cancer cases (26-29). It is now predicted that one in every six American men will develop prostate cancer sometime during their lifetime (30). Individuals with this disease have approximately a 9% mortality rate (29).

The main risk factors that have been associated with prostate cancer are genetics, race, age and diet (26, 27). The genetic predisposition of prostate cancer is not well understood. Although certain genes have been implicated as being important predisposing factors for prostate cancer, large inter-individual differences in the frequency of these genes provide evidence that prostate cancer is genetically a heterogeneous disease (26). Studies have suggested that genetic predisposition contributes to a large proportion (just under 50%) of prostate cancer cases (31, 32).

In the United States, African American men have consistently displayed the highest incidence of prostate cancer compared to men of other ethnicities (26, 27). This greater incidence observed in one race cannot be attributed to any one factor but rather has both genetic and environmental influences.

Prostate cancer has typically been described as a disease that affects elderly individuals; individuals less than 50 years old rarely display this disease (26). It has been

hypothesized that aging provides the time required for sufficient maladaptive cellular events to occur which contribute to the formation of cancer (33).

Diet has been linked with the incidence of prostate cancer. Specifically, it has been argued that the high fat North American diet increases the risk of prostate cancer. However, this idea has yet to be definitively proven (27).

1.2.2.2 Oncogenes and Tumor Suppressor Genes

The impact of specific oncogenes and tumor suppressor genes on the propagation of prostate cancer still remains poorly defined due to the genetic complexity of the disease. Oncogenes that have been linked to the development of prostate cancer include c-myc, ERBB2 and bcl-2. C-myc is transcription factor involved in the regulation of apoptosis, cellular proliferation and differentiation (34, 35). C-myc over-expression by gene amplification has been observed in some prostate cancer tumors (36). ERBB2 is a transmembrane phosphoprotein which is also involved in the regulation of apoptosis, cellular proliferation and differentiation (37, 38). ERBB2 over-expression has been observed in some prostate tumors, but it is likely not the product of gene amplification (36, 39). bcl-2, an antiapoptotic gene, was reported to be over-expressed in 33-50% of prostate tumors; much more frequently than c-myc and ERBB2 (40, 41).

Tumor suppressor genes that have been linked to the progression of prostate cancer are PTEN and P53. One should recall that both alleles must be silenced for complete inactivation of a tumor suppressor gene. Chromosome loss and point mutations have been observed in tumors for both PTEN and P53 (42-44). In the case of PTEN, if one allele is

inactivated by a point mutation, the inactivation of the second allele occurs by an unknown mechanism (45).

1.2.2.3 Androgens and the Androgen Receptor

Androgens are responsible for the growth, development and functioning of the prostate (46-48). Testosterone, the most prevalent androgen in males, is converted by 5α-reductase to 5α-dihydrotestosterone (DHT), which is the main ligand for the androgen receptor (46). Once bound to the androgen receptor in the prostate, DHT promotes cell proliferation and differentiation, while thwarting cell death (39). Most androgens are produced by the Leydig cells of the testes. The adrenal glands also produce a small amount of androgen.

The androgen receptor (AR) is expressed mainly by the luminal epithelial cells of the prostate (46). When no ligand is present, the AR remains in the cytoplasm (Figure 1). However, once the AR is bound to DHT, it relocates to the nucleus and is a transcription factor for androgen regulated genes (Figure 1) (49). Specifically, the receptor-ligand complex binds to androgen response elements, which are located upstream of the target genes' coding sequences. The activation of these target genes are not only regulated by the receptor-ligand complex but by other coactivators and repressors (50).

Due to the dependence of prostate cancer cells on androgens for growth, a treatment strategy known as androgen ablation therapy is administered to individuals with advanced prostate cancer. This therapy is not a cure as it ultimately selects for prostate cancer cells that can survive under low androgen levels. There are three postulated mechanisms described leading to the survival of these androgen independent cells. The

first mechanism describes that the cancer cells might not be completely androgen independent at all, but rather able to produce more androgen receptors via amplification of the androgen receptor gene (51). Greater numbers of AR would allow these cells to survive under low androgen levels. The second mechanism describes cancer cells with mutated androgen receptors that are able bind non-androgen molecules present in circulation (52-54). Once bound to the AR, these non-androgen molecules would initiate the same proliferate effects as when androgen binds the AR. The final mechanism proposes that non-cancer cells, like neuroendocrine cells, secrete neuropeptides that support the growth of the cancer cells (51).

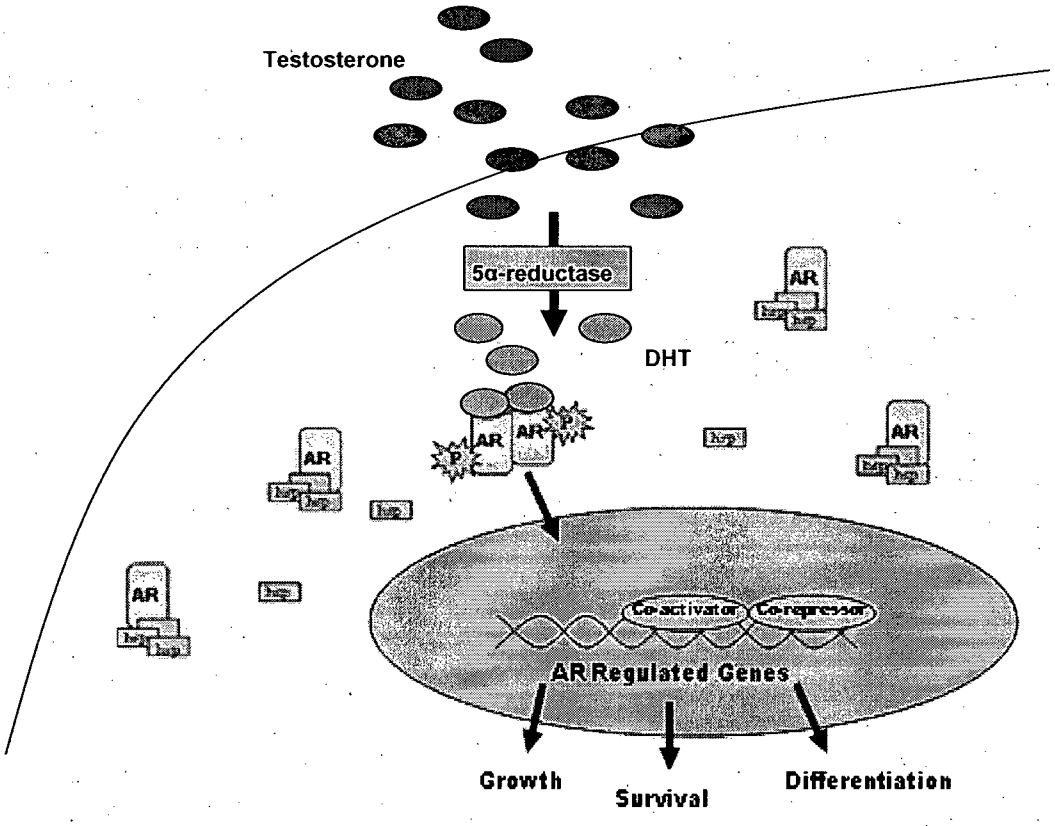

Figure 1. Image of the actions of the AR once bound by DHT. Once bound to DHT, AR dissociates from heat shock proteins, becomes phosphorylated and dimerizes (50). The DHT-AR complex binds to ARE with cofactors resulting in the transcription of specific genes (50). (Figure modified from Javidan et al., 2005 (50))

1.2.2.4 Diagnosis and Prostate Cancer Stages

The prostate is a walnut-shaped gland located under the bladder that envelops the urethra. The prostate is divided into five different lobes: anterior, median, posterior, and two lateral lobes. The primary function of the prostate is to produce fluid that is added the semen upon ejaculation (55). The prostate is surrounded by four distinct tissue areas: connective and fatty tissue (located on the rectal, lateral and anterior sides of prostate), seminal vesicles (located at the base of the prostate), bladder neck (located at the base of the prostate), and pelvis musculature (located on the apical side of prostate) (56).

There are two main tests used by physicians to diagnose prostate cancer; prostate specific antigen (PSA) tests and digital rectal exams (DRE) (57). The PSA test involves measuring PSA concentration in the blood. PSA, which is secreted by prostatic epithelial cells, tends to increase in individuals with prostate cancer due to the enlargement of the prostate (58). DRE is a more invasive test compared to the PSA test. This test requires access to the prostate by way of the rectum, in order to determine any structural irregularities indicative of prostate cancer. Only the two lateral and posterior lobes can be palpated using a DRE (57). If a positive result is obtained from either of these tests, a biopsy is normally performed to determine the presence and the extent of the cancer (57). The Gleason grading system is used by pathologists to determine the extent of cellular differentiation. According to this system, well differentiated cells are given a score of one, while poorly differentiated cells are given a score of five.

The TNM staging system was developed for physicians, to assess prostate cancer progression. The T stage refers to the form of cancer present within the prostate (Figure 2). The N stage refers to the progression of the cancer into the pelvic lymph nodes.

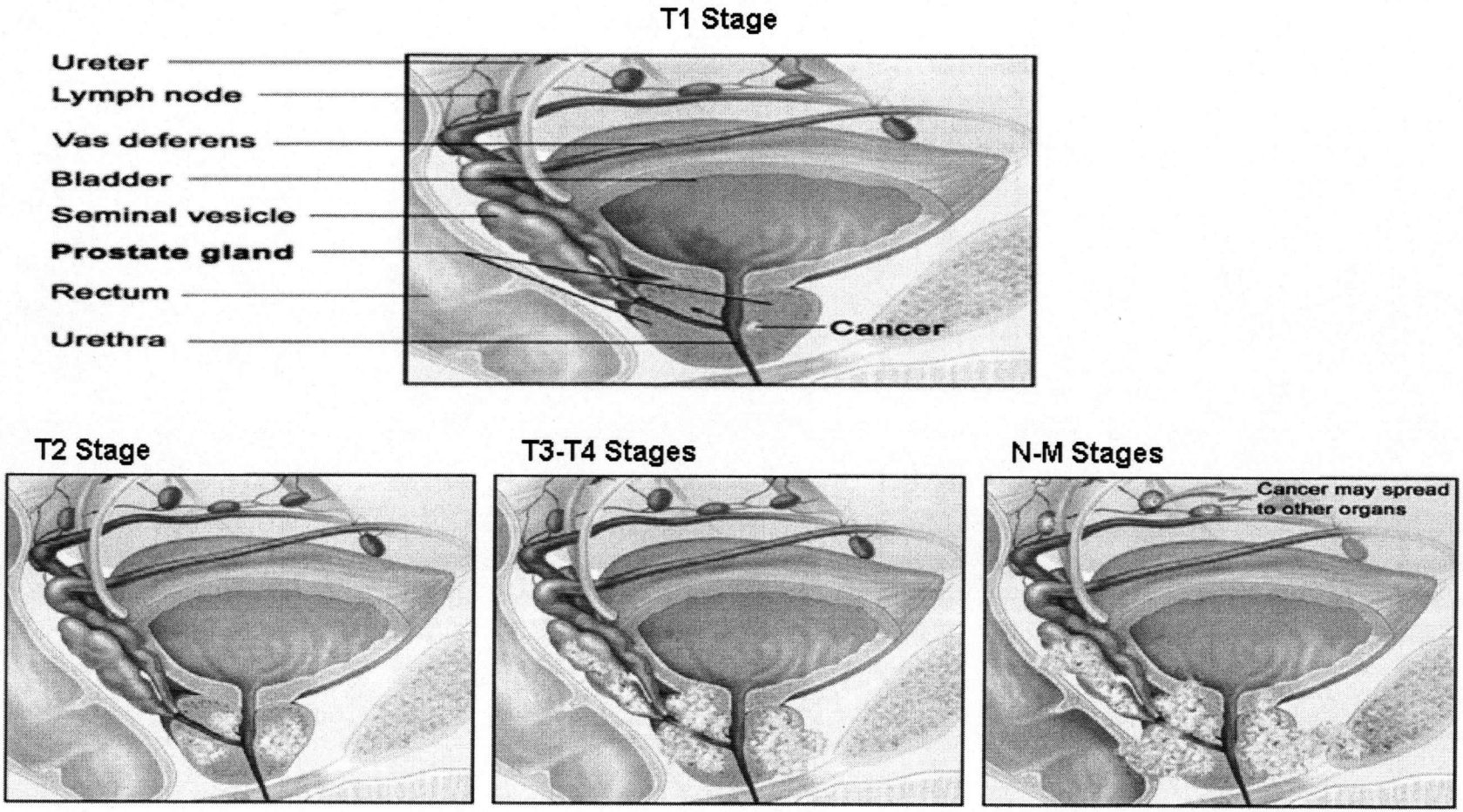

Figure 2. Image representing the progression of prostate cancer as described by the TNM staging system. (Figure modified from US. National Cancer Institute PDQ database website (59))

Finally, the M stage refers to the level of metastases that has occurred. Each of the stages described are further subdivided into sub-stages.

The T stage is further divided into the T1, T2, T3 and T4 sub-stages, each of which has their own sub-stages. The T1a and T1b stages refer to prostate cancer that is discovered by accident during a transurethral resection of the prostate in individuals who have benign prostate hyperplasia (56, 60). Using histopathological analysis, tumors which occupy $\leq$5% of the prostate are classified as T1a and tumors which occupy >5% of the prostate a classified as T1b (60). The T1c classification refers to elevated serum PSA levels (positive PSA test) (56, 60). Digital rectal exams are unable to detect tumors that are in the T1 stage (56).

The T2 sub-stages T2a, T2b and T2c refer to tumors that are detectable by the digital rectal exam (56, 60). T2a refers to a tumor that is constrained within a single lobe of the prostate and occupies less than 50% of the lobe (56). T2b refers to a tumor that is constrained within a single lobe of the prostate and occupies more than 50% of the lobe (56). T2C refers to the presence of cancer in both lobes of the prostate (56).

The T3 and T4 sub-stages refer to the invasion of the surrounding tissue of the prostate by the tumor. T3a and T3b sub-stages refer to a tumor that has spread to the connective and fatty tissue on one side or both sides of the gland respectively (60). The T3c sub-stage indicates that the tumor has invaded the seminal vesicles (60). The T4 sub-stage indicates that the tumor has progressed and invaded the bladder neck, rectum and/or the pelvis musculature (56, 60).

The N and M stages and sub-stages refer to various levels of invasion of the prostate cancer in pelvic lymph nodes and other sites outside the prostate. The N sub-stages refer

to gradual increases in the number of lymph lobes affected but also the size of tumors present within the lymph lobes. The M sub-stages refer to the presence of the cancer in bone, a main site for prostate cancer metastases, but also the presence of cancer in other distant sites.

1.2.2.5 Conventional Treatment

The treatment regimen administered to an individual with prostate cancer depends on a number of different factors including the progression of the cancer, health and age of patient, and degree of risk associated with each procedure. Early stage, localized (T1-T3), hormone dependent prostate cancer is normally treated with either external radiation therapy or a radical prostatectomy (55). Both of these procedures can essentially cure a patient if performed correctly, however, each runs the risk for possible mortality and morbidity (55, 61). Two additional procedures which are starting to be used more frequently for treating early stage prostate cancer are brachytherapy and cryotherapy. Brachytherapy involves the insertion of radioactive seeds (iodine-125 or iridium-192) into the prostate and other affected tissues rendering the death of the cancer cells over time (62). Cryotherapy involves the insertion of 17-gauge needles directly into the affected areas. These needles undergo several freeze-thaw cycles, resulting in the death of the cancer cells and surrounding tissue (63). A final option for patients with early stage prostate cancer is known as "watchful waiting", in which no treatment is administered and the cancer is monitored with subsequent PSA tests and DREs.

Hormone therapy, specifically androgen ablation therapy, is typically administered to treat advanced prostate cancer that has metastasized. Prostate cells are dependent on

androgens for proliferation, protein synthesis initiation and cell death inhibition (57). Thus, the removal of androgens through bilateral orchiectomy or administration of luteinizing hormone-releasing hormone agonists results in cell death (57). It should be noted that although androgen ablation therapy reduces androgen levels significantly, it does not remove androgens completely. The removal of androgens induces a high initial mortality rate in the cancer cell population, but ultimately selects for androgen independent (hormone refractory) cancer cell growth (64).

Once the prostate cancer has become hormone refractory, chemotherapy is often administered as a last resort, often with limited therapeutic effect. Docetaxel in combination with prednisone is currently the gold standard chemotherapeutic cocktail for advanced prostate cancer (51, 65, 66). In phase III clinical trials, patients administered the docetaxel based therapy showed greater survival compared to patients treated with a mitoxantrone based therapy (51, 65). It is believed that docetaxel binds directly to β-tubulin subunits promoting polymerization, which ultimately results in microtubule stabilization (51). As the cellular cytoskeleton no longer responds normally, the cell undergoes apoptosis (51).

1.2.3 Alternative Cancer Treatments

Advanced prostate cancer often does not respond well to chemotherapy. For this reason, along with the risks associated with other standard treatments, a number of prostate cancer patients turn to complementary or alternative self-treatments. Sometimes patients will even self medicate with these alternative therapies while receiving conventional therapy. A recent survey in British Columbia of 1108 men with prostate

cancer indicated that 39% of these individuals had used a complementary or alternative therapy (67).

Unfortunately, many alternative products have not been investigated rigorously, and it is relatively unknown whether they provide any benefit to the individual who is self-medicating. Fueled by the increased use of alternative therapies by cancer patients, a number of research facilities have begun to investigate these products. The purpose of these studies is to elucidate the therapeutic and toxicological effects of these agents, as well as determine their possible use in combination therapies with conventional treatments for cancer. "High pH Therapy" is an alternative cancer therapy that is built around the compound CsCl. Currently, the effects of CsCl alone and in combination with chemotherapeutic drugs are relatively unknown.

1.2.4 The Cesium Chloride Alternative Cancer Treatment

1.2.4.1 Historical use of Cesium Chloride: Brewer's "High pH Therapy"

In the early 1980's an alternative cancer therapy involving the use of CsCl was developed by the late Dr. Keith Brewer. The theoretical premise of this therapy was that CsCl could combat cancers through elevating intracellular tumor pH (1). Due to technological constraints, this CsCl induced change in tumor pH was never scientifically measured. However, firm on his theory, Brewer marketed this CsCl therapy under the name "High pH Therapy" (1).

Dr. Brewer began investigating CsCl after realizing its prevalence in several geographical areas with low cancer incidence (1). The groups of people living in these

areas had traditionally eaten food grown in the volcanic soil that was rich in cesium (Cs), and had inadvertently included Cs in their diets for generations (1).

The proposed mechanism of CsCl starts with the uptake of Cs by the cancer cells. Once inside the cells, Brewer believed that the Cs was able to facilitate an increase in the intracellular pH of the cells; that is, change the neutral to slight alkaline pH of normal cancer cells, to a basic pH of 7.5-9.0 (1). Brewer described that this proposed change in intracellular pH was not well tolerated by the cancer cells, resulting in many cells undergoing cell death (1).

To date, there have been no epidemiological studies conducted to determine the number of people who have used or are currently using CsCl. However, judging from the ample availability of CsCl products offered on the internet through multiple companies around the world, one could assume that a large number of people have tried to self-treat using this therapy (2-4). Dr. Abdul-Haqq Sartori, one of the main supporters of CsCl, has claimed to have treated more than 750 patients with his Enhanced CsCl therapy (68).

1.2.4.2 Reported Therapeutic Effects of Cesium Chloride

There have been only a few published studies evaluating the therapeutic effects of CsCl against cancer. The methodologies of most of these studies were not rigorously conducted or were hindered due to technology barriers.

In the one published clinical study on CsCl treatment, 50 terminal patients with generalized metastatic disease were given 6-9g of CsCl each day for three years (5). The results showed that 50% of these individuals were still alive at the end of the treatment (5). Pain also diminished in all patients within the first three days of the study (5).

Furthermore, autopsies of a few patients that had died during the treatment indicated very low levels of cancer tissue present (5). However, there was no control group in this study; every patient was treated with CsCl.

In vivo CsCl studies reported to date have used mice with surgically implanted murine sarcoma I, colon-38, or MT296 mammary tumors, or BZP-induced skin carcinoma. In these studies, a reduction in tumor volume was observed in animals that were administered daily intraperitoneal injections of 505.5mg/kg CsCl (1.1mg CsCl in combination with zinc and vitamin A for the animals with colon tumors) (6-10). One issue that arises when implanting or inducing tumors in animals is that some tumors fail to propagate due to factors independent of the drug; tumors fail to propagate in animals of treatment and control groups. With experimental designs that involve pretreatment of the animals with drug prior to tumor implantation or induction (as in the studies listed above), the researcher would not know whether the reduction in tumor volume observed in the treatment groups was completely related to the drug. Furthermore, there is no way of normalizing treatment groups in terms of tumor growth characteristics at the beginning of each of these studies; one would have to assume that all the tumors implanted or induced were the same size and had the same growth potential.

A few *in vivo* studies have also examined the impact of CsCl on mortality in tumor bearing animals. A study involving mice with SR-implanted tumors that received pretreatment with CsCl (505.5mg/kg) for 7 days prior to tumor inoculation, observed a reduction in tumor induced mortality rate compared to control animals (69). However, similar experiments conducted in rats bearing Novikoff Hepatoma showed opposite

results; there was less mortality in control animals compared to CsCl treated animals (70, 71).

Recently, our laboratory conducted the first CsCl study in a human derived cancer xenograft mouse model. Mice bearing a LNCaP prostate cancer xenograft treated with 150mg/kg CsCl daily via oral gavage had no significant reduction in tumor volume compared to control mice (72). No other dosages of CsCl were examined in this study. A reduction in tumor volume was only observed when 150mg/kg CsCl was administered in combination with vitamin D (72).

1.2.4.3 Reported Toxicological Effects of Cesium Chloride

In terms of toxicity, there appear to be some inherent side affects attributed to CsCl treatment, although the severity of these effects has not been resolved. Historically, the only adverse effects reported by patients were nausea, diarrhea, paresthesia (tingling of the skin), and hypokalemia (potassium deficiency) (5, 73). The consumption of high potassium foods was shown to reduce the onset of nausea and diarrhea (73).

Studies in canines have shown a link between CsCl administration and impaired cardiac function. It has been reported that canines administered concentrated dosages of CsCl experience long QT syndrome (abnormally long delay between ventricle depolarization and ventricle repolarization), torsades de pointes (ventricular tachycardia with irregular ventricle depolarization and ventricle repolarization) and various other cardiac arrhythmias (11-14). Interestingly, a few recent case studies have reported similar cardiac problems in patients self-administering CsCl (15-23). In one case study, a 43 year old woman who had been recently diagnosed with a brain tumor was admitted to hospital

after having two seizures (16). On arrival to the hospital, she had a third seizure and then suddenly collapsed due to ventricular tachycardia, for which defibrillation was administered (16). During her stay at the hospital she displayed ventricular tachycardia again on two separate occasions (16). Upon examination, the physicians found no evidence of heart disease (16). It was discovered that one day prior to her admittance to the hospital she had just finished a 9g/day 10 day regimen of CsCl treatment (16).

In mice, the acute LD_{50} dose of intraperitoneal administered CsCl was determined to be ~1.7g/kg (10, 74, 75). The acute LD_{50} dose of orally administered CsCl was determined to be 1.9-2.3g/kg (76, 77). Animals that died from the concentrated intraperitoneal injection of CsCl reportedly experienced respiratory failure followed by convulsions (10, 74). Animals that did not perish experienced copious salivation, increased urination, pilo-erection, central nervous system depression, and shallow, irregular breathing (10, 74).

Additional studies in mice investigated the impact of CsCl on development by replacing mothers' drinking water with 1M CsCl solution after giving birth. Male pups whose mothers consumed CsCl, had a decrease in brain mass and had lower body mass after breast-feeding was discontinued (weaning period), as compared to control pups (78-80). Similarly, male pups whose mothers consumed CsCl during pregnancy had a reduction in brain mass, but had increased spleen and testis mass (81, 82).

Studies investigating the effects of CsCl on murine bone marrow metaphase cells *in vivo* revealed that CsCl administration elicits clastogenic effects (chromosomal breakage) (83, 84). 125-500mg/kg CsCl administered orally resulted in chromosomal breaks and dicentrics in a dose dependent fashion within 6, 12, 18 or 24h (83, 84). A dose of 500mg/kg CsCl also reportedly reduced the mitogenic index of these bone marrow cells

24h after administration (83, 84). Several studies have demonstrated that the clastogenic effects of CsCl could be reduced, if animals were pretreated with vitamin C or Phyllanthus emblica fruit extract, or if CsCl was co-administered with chlorophyllin or calcium chloride (85-87).

Two additional studies analyzed the effects of CsCl on bone marrow erythrocytes. A dose of 1000mg/kg orally administered CsCl increased the prevalence of micronuclei in these cells 24 hours after administration (88). This same effect was not observed in animals administered 500mg/kg CsCl (88, 89).

1.2.4.4 Reported Biodistribution of Cesium Chloride

There have been a number of CsCl distribution studies completed in both man and animals. The average half life of CsCl was reported as 83-96 days in adult males and 65.5-77.2 days in adult females (90-93). One should note that half life appears to increase with body mass, indicating a possible rationale for the differences observed between males and females (91, 94).

Studies in humans reported that approximately 78% of ingested CsCl is absorbed into the blood (95). It appears that CsCl pharmacokinetics can be described by a two-compartment model; 6% is rapidly excreted with a half-life of 0.3 days, while the remaining 94% is slowly excreted over time (93, 95). According to a published pharmacokinetic model developed for CsCl distribution, CsCl is most concentrated in the heart, kidneys and liver after ingestion or intravenous injection (90). CsCl levels quickly drop in these organs within the first 24h and most of the CsCl is sequestered in the skeletal muscle for long term storage (19, 90).

The average half-life of CsCl in mice was determined to be 6.1 days (96). A subsequent experiment demonstrated that the pharmacokinetics of CsCl in mice could be described by a two-compartment model where 90% of CsCl is rapidly excreted in mice with a half-life of 2.83 days, while the remaining 10% is excreted more slowly with a half-life of 16.3 days (97). This is considerably different than the pharmacokinetic profile observed in humans.

CsCl retention studies in animals have shown varied results as different tissues have been examined within different studies. CsCl was reported to sequester mostly in the kidneys, small intestine and tumors, 14 min after intraperitoneal administration in mice bearing MT296 mammary tumors (98). However, when CsCl was administered orally to athymic nude mice bearing LNCaP tumors, it was concentrated mostly in the heart, liver, and kidneys within the first hour (72). Similar results have also been observed in studies involving rats (99, 100). CsCl concentrations in nude mice increased in the brain, spleen, prostate and tumors, and decreased in the heart, liver and kidneys over a 24h period (72). In non-tumor bearing mice chronically administered CsCl for 442 days, it was determined that CsCl concentrated in the muscle, heart and kidneys (101).

1.3 Rationale

A large number of patients have tried an alternative therapy to treat their cancer. The CsCl alternative cancer therapy requires patients to self-treat using high dosages (3-9g) of CsCl each day for extended periods of time (weeks to months). However, there have been no studies examining the therapeutic and toxicological effects of high (greater than 150mg/kg), repeated doses of orally administered CsCl in humans or human xenograft

models. Previous experiments involving tumor bearing mice, demonstrated that CsCl may have some therapeutic effect over a specific dose range. However, the design of these studies has failed to mimic the conditions under which cancer patients would administer this treatment; for example, patients would likely begin treatment after the diagnosis of cancer and not before. In addition, previous studies examining the toxicological effects CsCl have been very specific; the overall toxicity profile of CsCl throughout the body has not been documented, especially for chronic administration of CsCl over the long term.

The lack of research investigating CsCl as an alternative cancer treatment is deleterious to the safety of consumers self administering CsCl products. This study will provide the medical community with a comprehensive, rigorous evaluation of the therapeutic and toxicological effects of CsCl in human prostate tumor xenograft models. Furthermore, it will provide insight into the effects of this treatment against androgen dependent and androgen independent cancer.

1.4 Hypothesis

Daily administration of oral cesium chloride will have a therapeutic effect against human prostate tumor xenografts while eliciting some toxicity in the nude mouse model

1.5 Specific Aims

Aim 1:

To evaluate tumor growth and toxicity in the PC-3 and LNCaP human prostate tumor xenograft models, upon administration of escalating doses of CsCl to athymic nude mice.

Aim 2:

To analyze tissues obtained from the studies in Aim 1 to further investigate organ and tissue specific toxicity (histopathology and serum marker tests) in human prostate tumor xenograft bearing nude mice.

Section 2

Materials and Methods

2.1. Materials and Reagents

2.1.1. Instrumentation

Tumors volumes were measured using digital calipers. The mass of food, water and the mice themselves were monitored with an Acculab top loading balance (Bradford, MA, USA). Tissue sections, for histopathological analysis, were examined with a RT color-SPOT high resolution digital camera from Diagnostic Instrument. Inc. (Tampa, FL, USA), mounted on Olympus System light microscope model BX51 (Markham, ON, Canada). Semi-quantitative image analysis was performed using Image-Pro Plus version 4.5.1.22 from Media Cybernetics, (San Diego, CA, USA). AST and ALT assays were analyzed using a Bio-Tek Instruments Power Wave X with KC4 Kineticalc Version 2.6 Revision 3 software (Winooski, VT, USA). Serum creatinine was analyzed using a Waters 2695 Separations Module with a 3µm bore, 2.1x 50mm Waters Atlantis™ HILIC Silica column paired with a Waters 996 Photodiode Array Detector (Mississauga, On, Canada). The HPLC and detector were run using Empower Pro version 5.0 2002 software. All statistical analysis was conducted using SigmaStat 3.0 software.

2.1.2 Animals

All animal studies used 6-8 week old male athymic nude mice (HSD:Athymic Nude-FOXN1^{NU}) with body weights of 25-30g from Harlan Sprague Dawley, Inc (Indianapolis, IN, USA).

2.1.3 Chemicals and Reagents

Mouse LabDiet® 5058 was purchased from Jamiesons Pet Food Dist. (Delta, BC Canada). Cesium chloride (minimum 99%) was purchased from Sigma Aldrich (Oakville, ON, Canada). Dulbecco's Modified Eagle Medium (DMEM), Roswell Park Memorial Institute (RPMI) Medium 1640, Fetal Bovine Serum (FBS), 0.25% Trypsin, 1 mM ethylenediamine tetraacetic acid were purchased from Invitrogen, Inc (Burlington, ON, Canada). Eosin, Hematoxylin, HPLC grade water, HPLC grade acetonitrile, ammonium formate were purchased from Fischer Scientific (Ottawa, ON, Canada). Ethanol was purchased from Commercial Alcohols (Brampton, ON, Canada). Neutral Buffered Formalin 10% was purchased from EM Science (Fort Washington, PA, USA). The creatinine standard was purchased from Cayman Chemical (Ann Arbor, MI, USA). Infinity™ AST and ALT kits were purchased from Thermo Electron Corporation (Louisville, CO, USA).

2.2 Tumor growth and toxicity in the PC-3 and LNCaP human prostate tumor xenograft models, after administration of escalating doses of CsCl.

The effect of CsCl products on cancer patients is relatively unknown as there have been no rigorous studies conducted examining the therapeutic and toxicological effects of CsCl in humans or human xenograft models. Typically, for clinical drug investigation, Phase I and Phase II clinical trials are conducted as rigorous drug assessments in humans. Within these studies, the drug is administered at increasing concentrations to a small group of diseased or healthy patients to determine its therapeutic and toxicological effects. Although, CsCl must first be analyzed in a preclinical setting to delineate its

effects, the experimental design of these preclinical studies can mimic those of clinical drug trials. Within this aim, three animal studies were conducted to assess the actions of CsCl *in vivo*; the first study involved 56 animals bearing established PC-3 tumors, the second study involved 53 animals bearing established LNCaP tumors and the final study involved 41 non-tumor bearing animals. Figure 3 illustrates the timeline under which specific procedures were undertaken in each of the three animal studies. CsCl's therapeutic response was monitored in the two xenograft studies. As each of the chosen xenografts represents a different stage in prostate cancer progression, a response observed in either xenograft could provide pre-clinical evidence for the stage of progression at which CsCl is most efficacious. Acute toxicity was monitored in all three studies; both in tumor bearing and in non-tumor bearing animals. Acute toxicity observed in the animals of the two xenograft studies could be contributed to the combined effects of CsCl and each tumor. Alternatively, any acute toxicity observed in the non-tumor bearing animals was expected to be from CsCl alone as there would not be any influence from tumor burden.

Intra-study and inter-study comparisons between the three studies provided insight on the extent of CsCl's anticancer properties and acute toxicological effects relative to the concentration of CsCl administered and tumor model used. In addition, such comparisons allowed for tumor induced acute toxicity to be investigated.

2.2.1 Animal Husbandry

Once the nude mice arrived at The Prostate Center, they were placed in microisolator cages, 3 mice per cage, and were left to acclimatize to their new environment for two

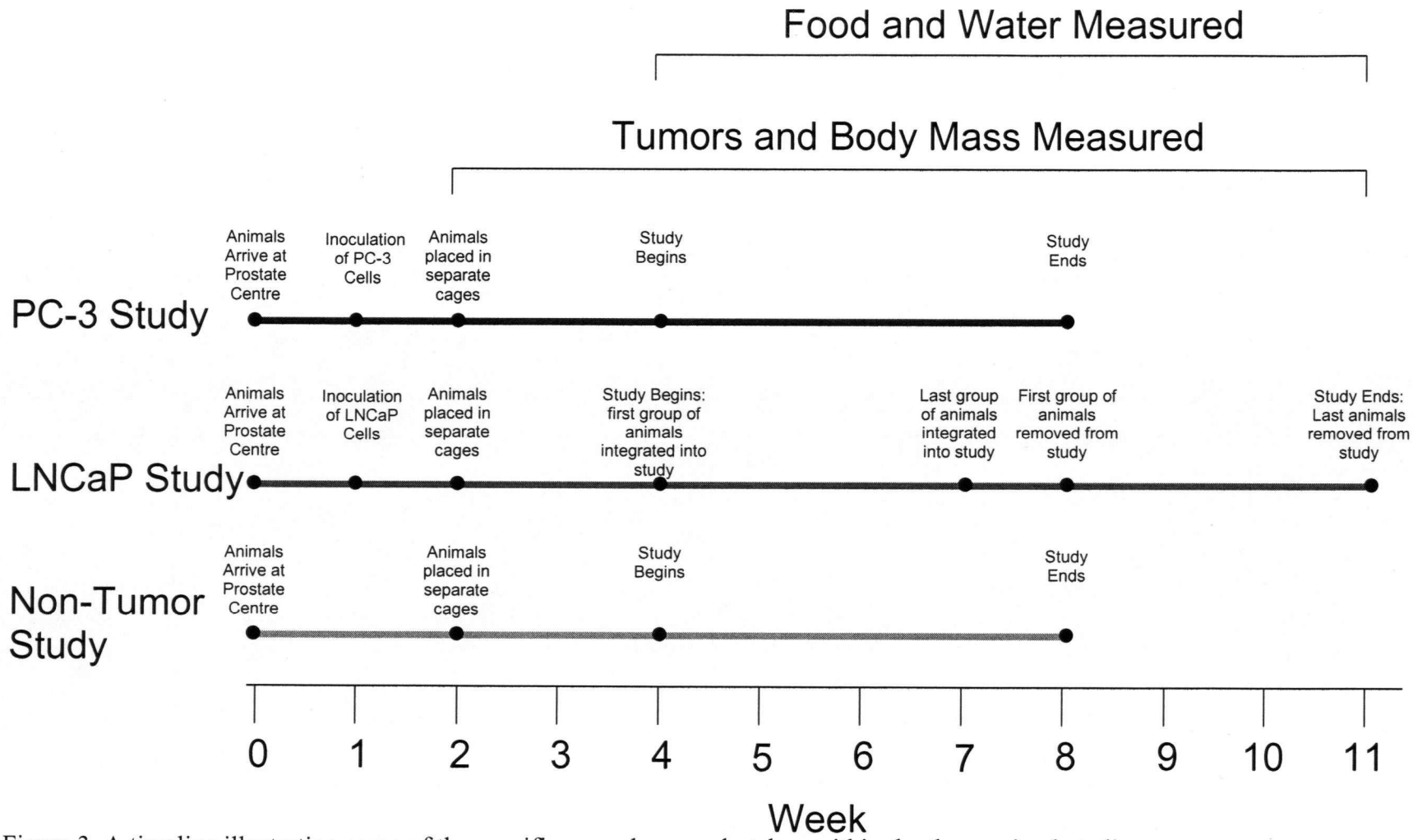

Figure 3. A timeline illustrating some of the specific procedures undertaken within the three animal studies.

weeks. The room environment in which the animals were housed had a controlled temperature of 19-25 °C, a 30-70% humidity and a 12-hour light cycle. Following the acclimatization process, mice were transferred into individual cages, and the husbandry duties (e.g. the changing of the cages, food and water) were passed from the animal care staff on to the researcher. The purpose of this exercise was to decrease the level of disturbance to each cage, in order to accurately assess water and food consumption as measures of acute toxicity for each mouse.

2.2.2 Cell Lines and Tumor Cell Inoculation

After the first week of the acclimatization period, mice of the PC-3 and LNCaP studies were inoculated subcutaneously with prostate cancer cells, and tumors were allowed to propagate. The PC-3 and LNCaP cell lines were chosen for these studies as they have been extensively characterized and are accepted models for prostate cancer both *in vitro* and *in vivo*. In addition, these two cell lines have molecular characteristics similar to prostate cancer cells observed clinically at different stages of the disease. Specifically, LNCaP cells have similarities to prostate cancer cells prior to androgen ablation therapy and PC-3 cells have similarities to prostate cancer cells post androgen ablation therapy. Using cell lines that represent different stages of prostate cancer progression is beneficial for this study, as it has not been documented at what stage prostate cancer patients are more likely to use CsCl treatments.

The LNCaP cell line originated in 1977 from a supraclavicular lymph node metastasis from a 50-year old Caucasian male and displays all the characteristics of a hormone responsive prostate carcinoma (102). It is fibroblastoid, androgen sensitive as it has a

mutated yet functional AR, and expresses PSA (102, 103). Following injection into athymic nude mice, LNCaP cells form tumors with variable growth rates and morphology. In comparison, the PC-3 cell line is representative of a hormone insensitive prostate cancer and was derived from a metastatic tumor (104). The PC-3 model has also been well characterized: the cells are androgen independent since they express very low levels of AR or do not express it at all, and they do not produce PSA (103-105). PC-3 tumors generally have a conserved shape, a greater growth rate and are typically less vascularized compared to LNCaP tumors.

The athymic nude mouse was used as the sole strain of mouse for the purposes of this project. This strain was selected due to its compatibility with the PC-3 and LNCaP cell lines in hosting subcutaneous human tumor xenografts.

The PC-3 and LNCaP cell lines respond quite differently when inoculated into the nude mouse model. Tumor propagation is never 100% for either cell line, however, inoculated PC-3 cells tend to form tumors more readily than LNCaP cells. For this reason 60 nude mice were inoculated subcutaneously with $2x10^6$ PC-3 cells in a single dorsal site. Of these, 56 animals had viable tumors on day 1 of the PC-3 study. Alternatively, for the LNCaP study, 70 nude mice were inoculated subcutaneously with $2x10^6$ LNCaP cells in two dorsal sites. Of these, 53 animals were incorporated into the LNCaP study. The PC-3 and LNCaP prostate cancer cells which were injected into the animals were originally cultured in DMEM and RPMI media, respectively, in the presence of 5% FBS. One senior animal technician was responsible for inoculating all of the animals to maintain the consistency of the method.

Once tumors became visible, their volumes were measured rigorously using calipers. This information, in addition to body mass values was crucial for allocating mice into treatment groups and ultimately determining the start dates of the PC-3 and LNCaP studies.

2.2.3 Integration of Animals into Each Study

In order to make comparisons between treatment groups within each study and between each of the three studies, animals were arranged into treatment groups so that day 1 values for tumor volume and body weight would not be statistically different when treatments groups were compared intra-study and inter-study. In other words, each treatment group had approximately the same tumor volume and body mass on day 1 as all the other treatment groups within the same study and between the three studies. In order to accomplish this standardization, animals of the three studies were not necessarily integrated into their respective studies on the same day. Animals of the PC-3 study were integrated into the study 4 weeks after their arrival at The Prostate Centre, since the tumors of each animal exceeded a predetermined volume (50-70mm^3). Alternatively, animals of the LNCaP study were integrated into the study in a staggered fashion because of the inter-variability of the LNCaP tumor's growth kinetics. As tumors reached a predetermined size (70mm^3), the respective animals were integrated into the study: the first animals were integrated into the study 4 weeks after their arrival at The Prostate Centre and the last animals integrated 7 weeks after their arrival at The Prostate Centre. Animals of the non-tumor bearing study were integrated into the study 4 weeks after their

arrival at The Prostate Centre, in order to maintain a consistent starting age with animals of the PC-3 and LNCaP studies.

In the PC-3 study, the homogeneous growth of the PC-3 tumors allowed for all of the animals to be integrated into the experiment on the same day. Mice were randomly distributed into the seven treatment groups according to their tumor volume and body mass (n=9 for control group, n=8 for the 150mg/kg, 300mg/kg, 600mg/kg, 800mg/kg, 1000mg/kg groups and n=7 for the 1200mg/kg group). Each treatment group had an average tumor volume of 82-107 mm^3 and an average body mass of 28.4-31.4g. Table 1 illustrates the average tumor volumes and body mass of animals within each of the seven treatment groups. Statistical analysis by one way analysis of variance (ANOVA) showed no statistical difference between any of the treatment groups in regards to average tumor volume or average body mass on day 1 of the study ($P>0.05$).

Table 1. Summary of the animal grouping within the PC-3 study.

Group	Tumor	CsCl Dose (mg/kg body wt)	Number of Mice/Group	Average Tumor Volume ±STD (mm^3) / Body Mass ±STD (g), on Day 1
1	PC-3	Vehicle (water)	9	101±57 / 30.1±2.4
2	PC-3	150.	8	102±68 / 31.4±2.3
3	PC-3	300	8	107±71 / 28.4±2.1
4	PC-3	600	8	95±61 / 28.9±1.7
5	PC-3	800	8	100±62 / 29.7±2.4
6	PC-3	1000	8	82±28 / 29.5±2.5
7	PC-3	1200	7	99±44 / 29.5±1.5

It was generally observed that LNCaP tumors have a highly variable growth rate, therefore mice were integrated into this experiment in a staggered fashion. Tumor volumes were monitored rigorously, until volumes greater than $70mm^3$ were observed, at which time the animals were allocated into one of the seven treatment groups (n= 8 for the control, 150mg/kg, 800mg/kg, 1000mg/kg groups, and n=7 for the 300mg/kg, 600mg/kg, 1200mg/kg groups). Body mass was also taken into consideration in determining the distribution of the animals into the treatment groups. Each treatment group had an average tumor volume of 96-115mm^3 and an average body mass of 25.8-28.5g on day 1 of the experiment. Table 2 illustrates the average tumor volumes and body mass of animals within each of the seven treatment groups. Statistical analysis by one way ANOVA showed no statistical difference between any of the treatment groups in regards to average tumor volume or average body mass on day 1 ($P>0.05$).

Table 2. Summary of the animal grouping within the LNCaP study.

Group	Tumor	CsCl Dose (mg/kg body wt)	Number of Mice/Group	Average Tumor Volume ±STD (mm^3) / Body Mass ±STD (g), on Day 1
1	LNCaP	Vehicle (water)	8	114±35 / 26.9±2.3
2	LNCaP	150	8	110±36 / 26.4±3.1
3	LNCaP	300	7	113±50 / 26±3.5
4	LNCaP	600	7	96±23 / 25.8±3.2
5	LNCaP	800	8	115±61 / 26.6±2.4
6	LNCaP	1000	8	108±32 / 28.5±2.1
7	LNCaP	1200	7	98±26 / 26.3±1.8

The 41 mice in the non-tumor bearing study were randomly distributed into the seven treatment groups according to body mass (n=6 for the control, 150mg/kg, 300mg/kg, 600mg/kg, 800mg/kg, 1000mg/kg groups, and n=5 for the 120 mg/kg group). The average body mass in each treatment group was 26.3-27.6g. Table 3 illustrates the average body mass of animals within each of the seven treatment groups. Statistical analysis by one way ANOVA showed no statistical difference between any of the treatment groups in regards to average body mass on day 1 of the study (P>0.05).

Table 3. Summary of the animal grouping within the non-tumor study.

Group	Tumor	CsCl Dose (mg/kg body wt)	Number of Mice/Group	Average Body Mass ±STD (g), on Day 1
1	None	Vehicle (water)	6	27.6±4.0
2	None	150	6	27.5±2.7
3	None	300	6	27.1±2.8
4	None	600	6	27.4±2.8
5	None	800	6	26.2±2.3
6	None	1000	6	26.6±2.1
7	None	1200	5	26.6±1.8

Comparison by one way ANOVA showed no statistical difference in average tumor volume in any of the treatment groups of the PC-3 and LNCaP studies on day 1 of each study (P>0.05). In terms of average body mass, only the 150mg/kg group of the PC-3 study was statistically different from other treatment groups of the LNCaP (150mg/kg,

300mg/kg , 600mg/kg , 800mg/kg and 1200mg/kg) and non-tumor (800mg/kg) bearing studies ($P>0.05$); all other treatment groups showed no statistical difference from other treatment groups between the three studies.

2.2.4 Dose Selection and Drug Administration

Most CsCl product instructions recommend that consumers use the product once or twice daily for months at a time via oral administration. In order to stay consistent with this drug regimen, animals were administered CsCl once daily via oral gavage. However, these animal experiments were limited to a 30 day duration due to growth of tumors within the control groups of the PC-3 and LNCaP studies.

The range of CsCl dosages was determined based on several factors: 150mg/kg appears to exhibit no toxicity in the nude mouse model based on previous studies in our laboratory; the oral LD_{50} of CsCl in mice is an acute dose of 2306mg/kg (77); the half-life of CsCl is ~3-6 days in mice (96, 97); a CsCl distribution study in mice conducted in our laboratory found that CsCl is retained in major bodily organs 24h after administration, indicating a potential additive accumulation of CsCl in these organs upon chronic dosing (72); companies advise patients to take 3-9g of CsCl per day, which in terms of body surface area translates to 527mg/kg-1581mg/kg in mice (for a 70kg human). Considering these factors, six dosages of CsCl were chosen to cover a range of 0-1200mg/kg CsCl to be dosed daily via oral gavage: vehicle (water), 150mg/kg, 300mg/kg, 600mg/kg, 800mg/kg, 1000mg/kg or 1200mg/kg.

Water was chosen as the vehicle for delivery of CsCl in this study, as it is often used as the vehicle for commercial CsCl products. In addition, CsCl is very soluble in water

allowing for homogenous drug administration. Water is also an inert substance, which will not contribute any therapeutic or toxicological effects; theoretically, the only effects observed in this study should be from CsCl.

Dosages administered were corrected on a daily basis for changes in body mass by changing the dose volume administered to the animals. Table 4 illustrates the dosage volumes administered according to the weight of a mouse.

Table 4. Dosage correction of vehicle and CsCl solutions to compensate for differences in animal body mass

Weight of animal (g)	Dosage administered (µl)
24±1.5	80
27±1.5	90
30±1.5	100
33±1.5	110
36±1.5	120

2.2.5 Measuring the Therapeutic Response of CsCl

The therapeutic effect of CsCl was monitored in the PC-3 and LNCaP studies by measuring tumor volumes. Calipers were used to determine the measurable linear axes and applying the formula $\pi/6$ x LxWxH (L:major axis, W:width, H:height). Tumor volume was measured twice weekly using calipers; once at the beginning of the week and once at the end of the week. In the LNCaP study, total tumor volume was not tracked on animals that had more than one tumor propagate. Only the tumor that was large enough

on day 1 of the study (greater than $70mm^3$) was tracked, as secondary tumors usually only became measurable as the study progressed. In addition, serum samples were removed from the LNCaP tumor bearing animals weekly via tail vein bleeds. The serum was intended to measure PSA, the levels of which are normally correlated to changes in tumor volume in the LNCaP xenograft model. However, these tests were not completed due to restrictions in study length resulting from toxicity in the LNCaP bearing animals, and the lack of an observed therapeutic effect from CsCl administration in this model.

2.2.6 Monitoring Acute Toxicity from CsCl

Three endpoints representing acute toxicity were measured for within each study: body mass was measured daily prior to dosing and food and water consumption were measured every two days. All three of these measurements were carried out using a top-loading scale. For body mass measurements, animals were placed directly on the scale. Food consumption was monitored by weighing the mass of all uneaten food pellets. Water consumption was monitored by weighing the mass of each water bottle; a decrease of 1g water would signify 1 ml of water consumed assuming that water has a density of ~1g/ml. Any animals displaying substantial decreases in body mass (>20% initial mass), shakiness, lethargy, and a decrease in food and water consumption were euthanized to minimize suffering, and their associated treatment group was no longer tracked throughout the study. Within these treatment groups that were no longer being tracked, animals that had not shown acute toxicity were treated until signs of toxicity were observed. Thus, not all animals within these groups were euthanized on the same day, but were instead euthanized when a specific threshold of toxicity was observed.

All tumor volume, body mass, food and water consumption measurements were conducted solely by the researcher. By allocating these measurements to a single individual, the data collected from these studies are more concise than if multiple researchers were making the measurements, as each would have their own measuring techniques.

2.2.7 Animal Euthanization and Tissue Harvesting

On the last day of each study, mice were euthanized approximately 24 hours after the last administration of vehicle or CsCl by carbon dioxide asphyxiation. Tumors, brains, hearts, lungs, livers, spleens, kidneys, small intestines, femurs, quadricep muscles and prostates were removed from each animal. On removal, each tissue was cut in half. One half was placed in formalin for histopathology and future tissue micro-array studies, and the other half was snap frozen for future Cs tissue distribution studies using atomic absorption (AA). Serum was collected from each animal via cardiac puncture for creatinine, AST (aspartate aminotransferase), ALT (L-alanine:2-oxoglutarate aminotransferase), and AA analysis. Figure 4 illustrates the tissues and organs removed from each of the animals in Aim 1, and shows the subsequent experiments both completed and postulated (grey boxes) involving these tissues and organs.

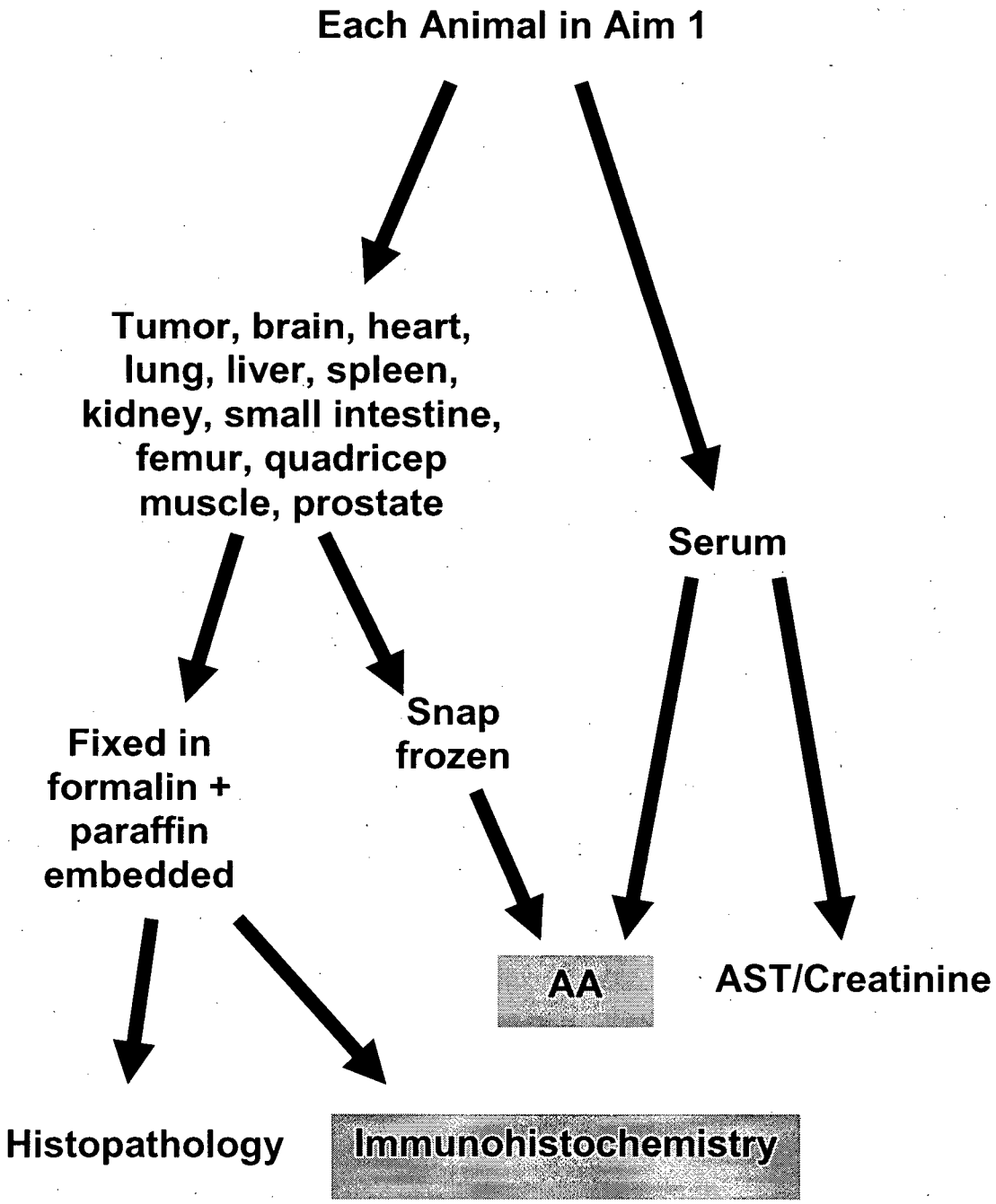

Figure 4. Analysis of tissues and serum obtained from the animals studies of Aim 1. Experiments designated in the grey boxes are part of future studies, the data of which will not be presented within this thesis.

2.3 Investigation of organ and tissue specific toxicity from CsCl (histopathology and serum marker tests) in human prostate tumor xenograft bearing nude mice

After completing a preclinical study, it is important to further investigate the toxicity of the compound administered; specifically, on different organs and tissues. The organ specific toxicity profile of a chemotherapeutic compound is crucial for determining cross reactivity with other agents, for designing potential detoxification measures, and for developing targeted drug carrier molecules (assuming the compound of interest has a therapeutic effect).

Aim 2 was designed to delineate the cause of potential acute toxicities and to develop an organ toxicity profile for CsCl through histopathological analysis and serum marker tests. As the use of the nude mouse model was consistent and conserved between the three studies, comparison could be made between treatment groups within the three studies and also between the three studies. By making such intra-study and inter-study comparisons, the extent of toxicity from each tumor alone, from CsCl alone, and from CsCl in combination with each of the tumor types was investigated.

2.3.1 Histopathology

Histopathology is regularly used to determine the toxicological profile of pharmacological agents and diseases. For histopathological analysis, brains, hearts, lungs, livers, spleens, kidneys, small intestines and quadriceps were collected from each mouse and transferred into 10% formalin. The formalin was removed after 48 hours of fixation and tissues were dehydrated in ethanol. For paraffin embedding, each tissue sample was enclosed in a plastic cassette, and placed in an ethanol bath. The cassettes were

subsequently taken to VGH Pathology Laboratory (Vancouver, BC, Canada) for the embedding process.

Once received from the pathology laboratory, the tissue containing paraffin blocks were placed on a cold plate for least one hour, and cut into 5 micron sections using a microtome. Each section was then placed on the surface of 45°C water bath for 45 min before mounting onto slides. Slides were incubated at 37°C over night. The slides were subsequently stained with hematoxylin and eosin. Each slide was analyzed for organ specific changes by a pathologist who was blinded to the treatment groups.

Analysis of all of the tissues collected would not be feasible in terms of cost and time constraints; thus, only the tissues of three animals from the control, 150mg/kg, 800mg/kg and 1200mg/kg groups from each of the three studies were analyzed initially. If the pathologist recognized any abnormalities in a specific organ or tissue of a specific animal, that organ or tissue of interest was analyzed in all animals of the control, 150mg/kg, 800mg/kg and 1200mg/kg of all three studies to increase the n-values and determine if the toxicological phenomenon was real.

2.3.2 Serum AST and ALT Analysis

Serum Aspartate Aminotransferase (AST) and L-Alanine:2-Oxoglutarate Aminotransferase (ALT) levels were measured as secondary measures of organ and tissue toxicity. AST is present in the liver, heart, kidney, skeletal muscle and erythrocytes (106). Damage to any of these organs and tissues results in the release of AST into the blood, and thus, increases blood AST concentrations (106). ALT is concentrated in the

liver (107). Damage to the liver results in release of ALT into circulation, and thus, increases blood ALT concentration.

Standard AST and ALT kinetic assay kits (Infinity™ AST Liquid Stable Reagent and Infinity™ ALT Liquid Stable Reagent, respectively) were implemented in 96-well plates to quantify AST and ALT serum levels. Plates were scanned using a Power Wave X microplate reader linked with KC4 Kineticalc. Both of these assays measure their respective markers indirectly by monitoring absorbance at 340nm which represents reduced nicotinamide adenine dinucleotide (NADH), and decreases in signal intensity as NADH is oxidized to nicotinamide adenine dinucleotide (NAD) over time (Figure 5). In these assays, the rate of oxidization of NADH is dependent on the concentration of AST or ALT, which catalyze primary reactions producing Bronstead-Lowry bases (Oxaloacetate in the AST catalyzed reaction and Pyruvate in the ALT catalyzed reaction), which accept protons from NADH (Figure 5).

Before any of the serum samples were used, these assays were validated using mouse serum obtained from other experiments. The main variables that were considered were the volumes of serum and test reagents used and the incubation times. In addition, intraday and interday variability of the assays were determined.

2.3.3 Serum Creatinine Analysis

Serum creatinine was measured as a secondary measure of kidney toxicity. Creatine produced by the liver, kidneys and pancreas is converted to creatinine in muscle; the amount of creatinine produced depends on the amount of muscle tissue (Figure 6) (108). In the absence of disease, kidneys secrete creatinine at a constant rate. However, during

end stage renal failure, the glomerular filtration rate will decline leading to a decrease in creatinine secretion (108).

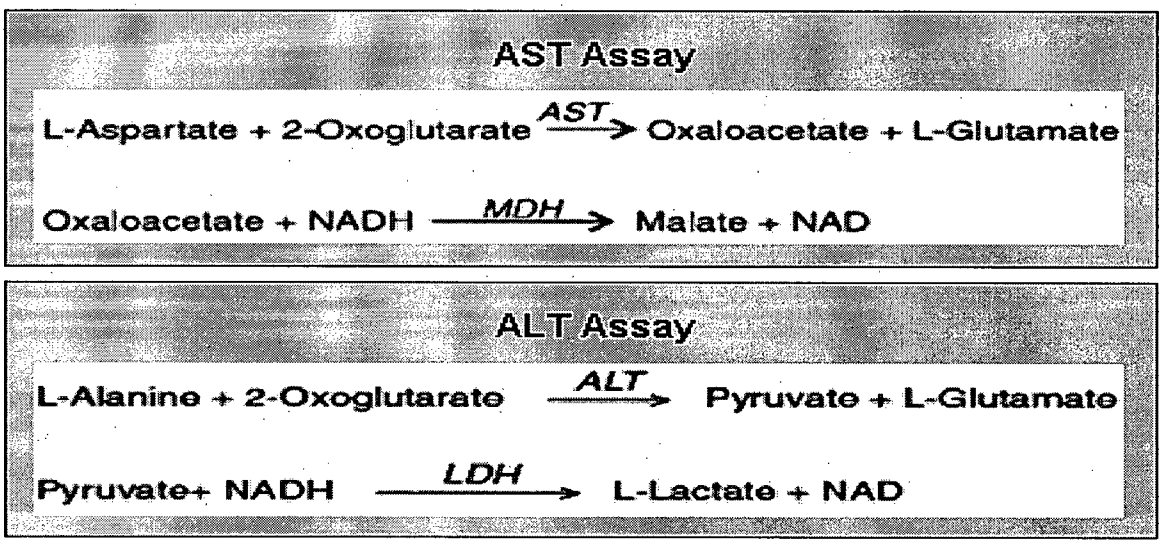

Figure 5. AST (above) and ALT (below) catalyzed chemical reactions that take place once serum is added to the AST and ALT kinetic assay kits. AST and ALT are measured indirectly by monitoring absorbance at 340nm which decreases as NADH is oxidized to NAD over time. (Figure modified from the Thermo Electron Infinity™ AST (GOT) Liquid Stable Reagent product insert (106) and the Thermo Electron Infinity™ ALT (GPT) Liquid Stable Reagent product insert (107))

Picric acid based creatinine assays are typically used to assess serum creatinine concentrations in a number of species. However, mouse serum contains chromagens which interfere in these picric acid based creatinine assays, resulting in overestimations of serum creatinine levels (109, 110). To assess serum creatinine in the nude mice, a high performance liquid chromatography (HPLC) method was developed.

Creatinine levels in serum were quantified using an HPLC method developed on a Waters 2695 Separations Module paired with a Waters 996 Photodiode Array Detector. The column chosen for this assay was a 3μm bore diameter 2.1x 50mm Waters Atlantis™ HILIC Silica column. The mobile phase used was a 97.5% acetonitrile solution

containing 0.025% ammonium formate. Creatinine standards (0µg/ml, 5µg/ml, 10µg/ml, 20µg/ml, 40µg/ml and 80µg/ml) were created in 94.5% acetonitrile from a creatinine 2mg/ml stock solution. For sample preparation, 10µl of serum was added to 190µl of 99.5% acetonitrile, vortexed, and centrifuged at 15000g at 4°C for 5min. The supernatant (~94.5% acetonitrile) from each sample was collected and placed in a HPLC autosample vial for injection. Duplicate injections of 80µl were performed for each standard and sample. The flow rate was maintained at 1ml/min resulting in the creatinine peak to elute at ~2min, which was monitored with an ultraviolet absorbance of 238nm. After every ten injections a gradient elution was run for 10min to clean the column and a quality control sample was injected to monitor the consistency of the method. Table 5 is a summary of the parameters used in this protocol.

Table 5. Parameters of the high performance liquid chromatography protocol developed to assess creatinine concentrations in murine serum.

Column Type	3µm 2.1x 50mm Waters Atlantis™ HILIC Silica column
Mobile Phase	97.5% acetonitrile solution containing 0.025% ammonium formate
Flow Rate	1ml/min
Sample Volume	80µl
Wavelength Analyzed	238nm

The HPLC method was validated using excess mouse serum collected from other experiments ongoing in the lab. This test serum was used to determine the optimum column type, mobile phase, sample preparation method, concentrations of creatinine

standards, flow rate, ultraviolet absorbance frequency, and column cleaning procedure. In addition, intraday and interday variability of the assay was determined.

Serum from control, 150mg/kg, 800mg/kg and 1200mg/kg animals were analyzed to maintain consistency with the histopathology analysis.

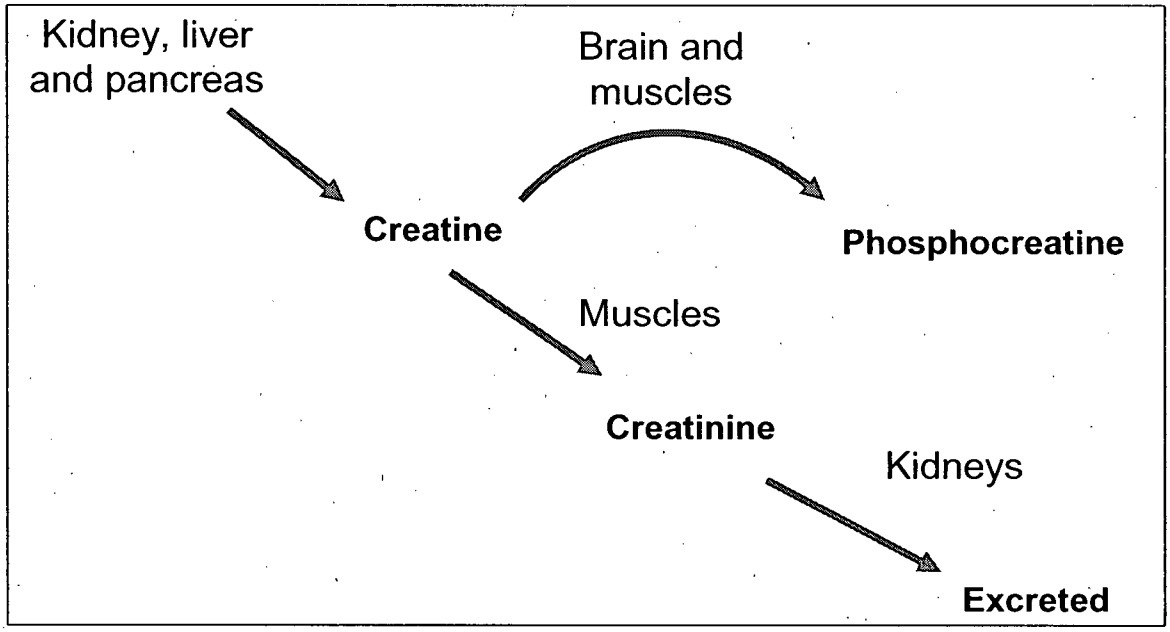

Figure 6. A summary of the pathways involved in the production and excretion of creatinine.

2.4 Comparisons between Control Animals

Once the three animal studies were completed, it was evident that the two different tumor types were contributing different levels of toxicity in the nude mouse model. This phenomenon was explored by comparing the data from the acute toxicity measurements (body mass, food consumption, water consumption and tumor volume), histopathological analysis and serum marker tests (AST, ALT and creatinine) between the three control groups from the three animal studies.

These experiments were warranted as all animals within the three animal studies experienced the same living, handling and dosing conditions. In addition, all animals analyzed were terminated on day 30 of their respective studies at which time tissues and serum were harvested.

2.5 Statistical Analysis and Removal of Outliers

All of the data collected from each experiment was analyzed using the SigmaStat 3.0 software. Groups were first compared by one-way ANOVA. If statistical significance was observed ($P<0.05$), a subsequent Tukey Test was implicated to determine which groups were significantly different from each other.

For each of the parameters measured, treatment groups would sometimes have a single animal, which would not follow the same trends as the rest of the group. In this study, these animals were considered outliers if the majority of results collected from the animal (results from multiple days) did not fall in the designated range: (Group Average + 2 Standard Deviations (STD)) - (Group Average – 2STD). The results collected for identified outlier animals were not included in group averages and calculations of variance.

Section 3

Results

3.1 Tumor growth and toxicity in the PC-3 and LNCaP human prostate tumor xenograft models, after administration of escalating doses of CsCl.

3.1.1 PC-3 Solid Tumor Xenograft Study

The study of CsCl in PC-3 bearing mice produced some very interesting results at the highest doses tested. Mice administered 1000mg/kg and 1200mg/kg CsCl displayed a significant reduction in % average initial body mass compared to the control, from day 5 and day 8 onwards, respectively (Figure 7). However, the magnitude of changes in body mass observed upon CsCl administration did not extend beyond the designated cutoff considered to be toxic (% average initial body mass was not reduced below 80% for any of the animals); thus, euthanization was not performed.

In terms of food consumption, there was no difference between any of the treatment groups and the control (Figure 8). Alternatively, water consumption increased significantly in the 1200mg/kg, 1000mg/kg and 800mg/kg groups compared to the control, from day 3 onwards for the 1200mg/kg and 1000 mg/kg groups and from day 17 onwards for the 800mg/kg group (Figure 9). The 300 mg/kg group also displayed a significant elevation in water consumption compared to the control, from day 3 to day 10 (Figure 9).

A significant reduction in % average initial tumor volume was observed in the three highest dosed groups when compared to the control. The 1200mg/kg group displayed a significant reduction in tumor growth compared to the control from day 5 onwards (Figure 10).

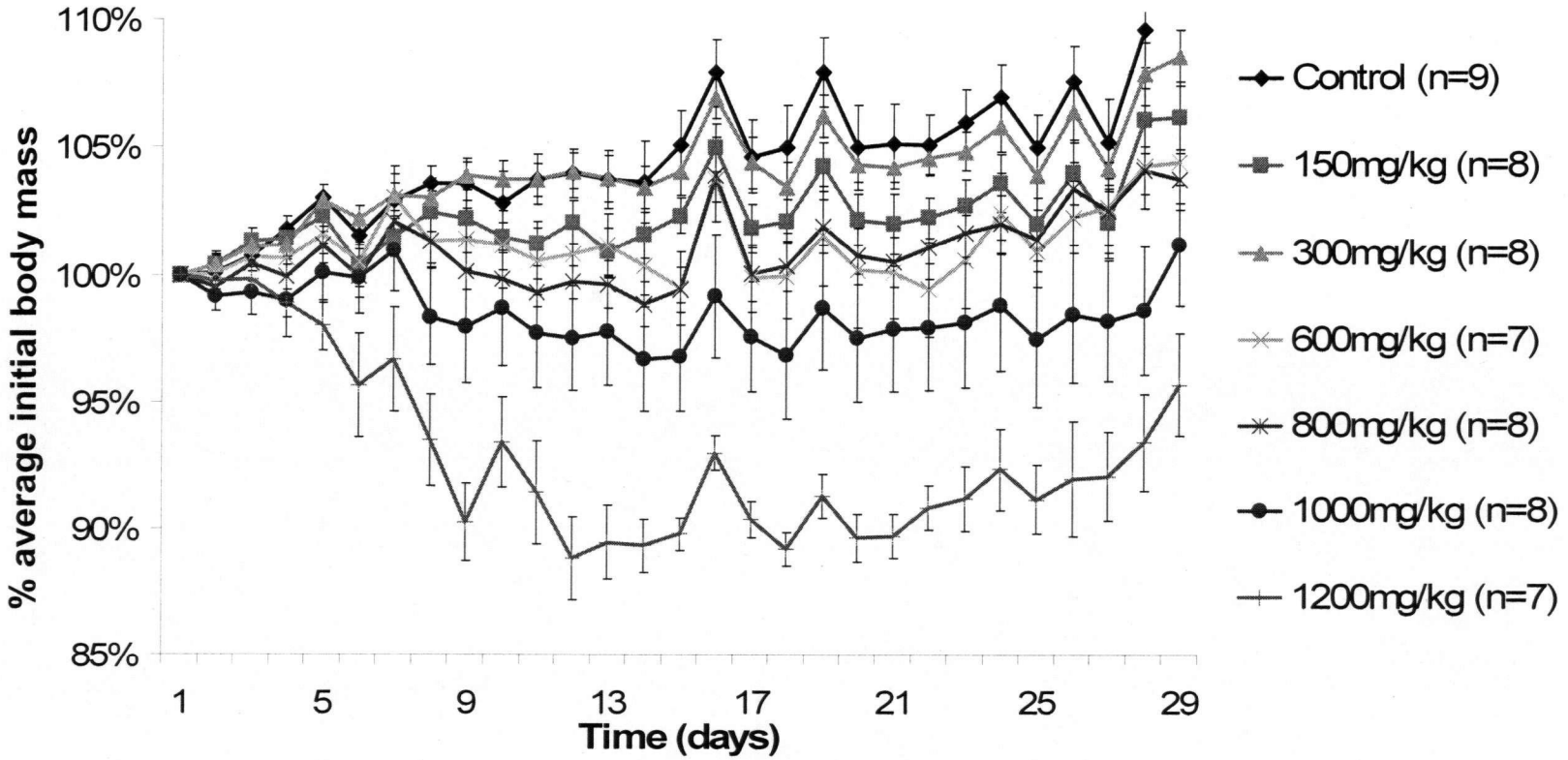

Figure 7. Percent average initial body mass over time of nude mice bearing a PC-3 tumor xenograft for control (vehicle) and treatment groups (150mg/kg-1200mg/kg CsCl). All mice were administered vehicle or CsCl daily for 30 days. Results are represented as mean value ± standard error of the mean. Statistical analysis using one way ANOVA indicates a significant difference between the control and treatment groups beginning on day 5 and extending to the end of the study ($P<0.05$). Pair-wise multiple comparison via Tukey test indicates a difference between the 1200mg/kg group and the control from day 5 until the end of the study ($P<0.05$), and a difference between the 1000mg/kg group and the control from day 8 until the end of the study ($P<0.05$).

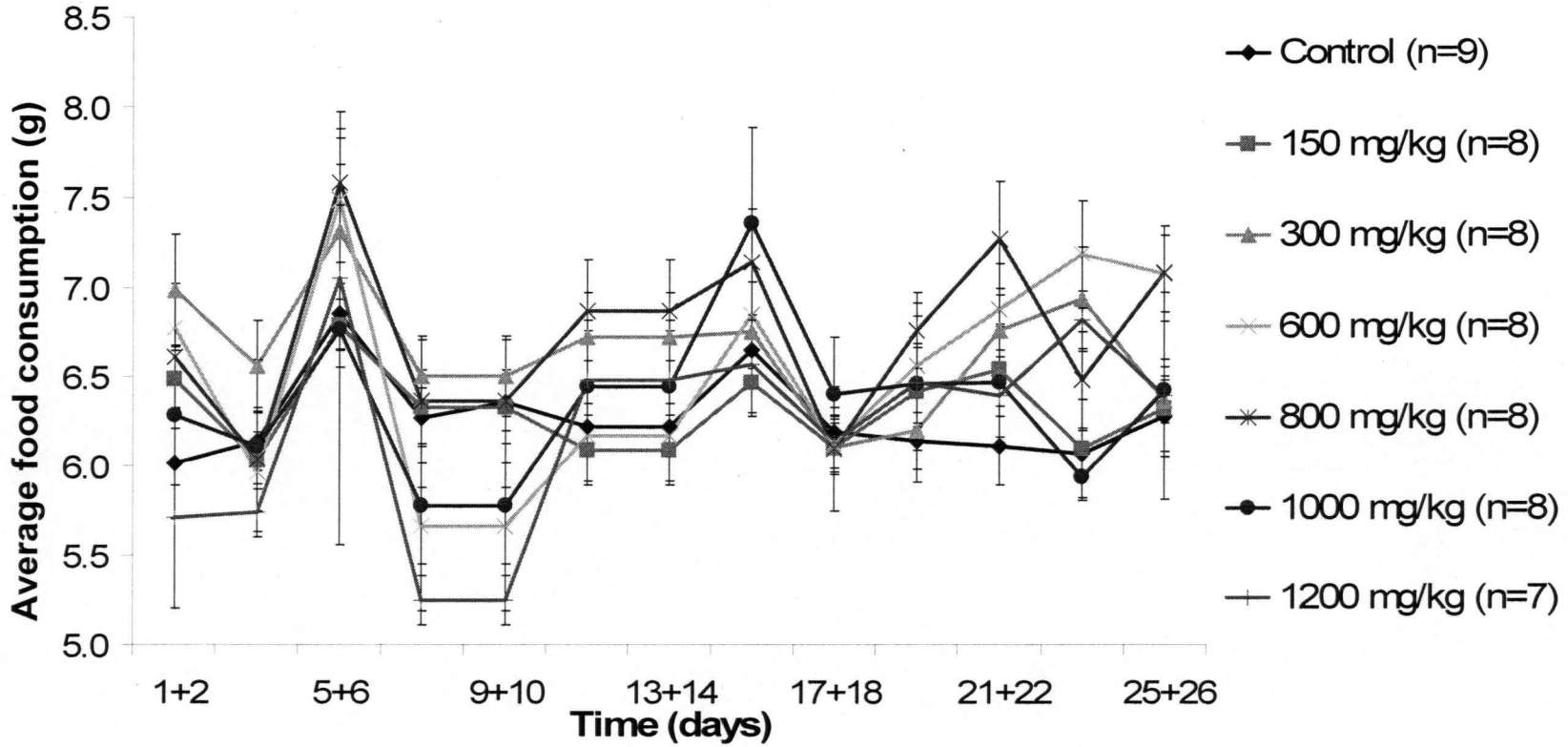

Figure 8. Average food consumption over time of nude mice bearing a PC-3 tumor xenograft for control (vehicle) and treatment groups (150mg/kg-1200mg/kg CsCl). All mice were administered vehicle or CsCl daily for 30 days. Results are represented as mean value ± standard error of the mean. There was no statistical difference between any of the groups ($P>0.05$).

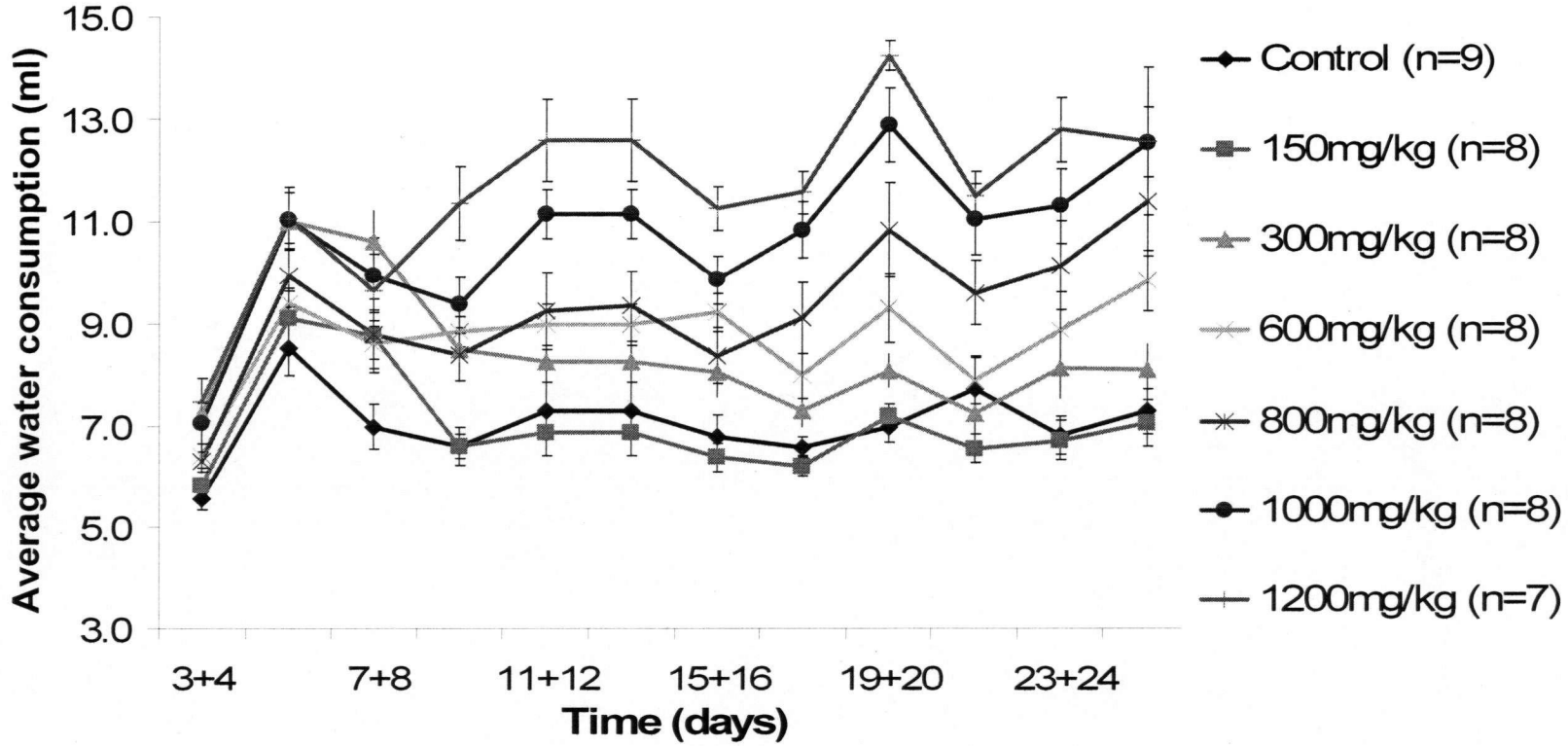

Figure 9. Average water consumption over time of nude mice bearing a PC-3 tumor xenograft for control (vehicle) and treatment groups (150mg/kg-1200mg/kg CsCl). All mice were administered vehicle or CsCl daily for 30 days. Results are represented as mean value ± standard error of the mean. Statistical analysis using one way ANOVA indicates a significant difference between the control and treatment groups beginning on day 3 and extending to the end of the study ($P<0.05$). Pair-wise multiple comparison via Tukey test indicates a difference between the 1200mg/kg group and the control from day 3 until the end of the study ($P<0.05$), a difference between the 1000mg/kg group and the control from day 3 until the end of the study ($P<0.05$), a difference between the 800mg/kg group and the control from day 17 until the end of the study ($P<0.05$), and a difference between the 300mg/kg group and the control from day 3 to day 10 ($P<0.05$).

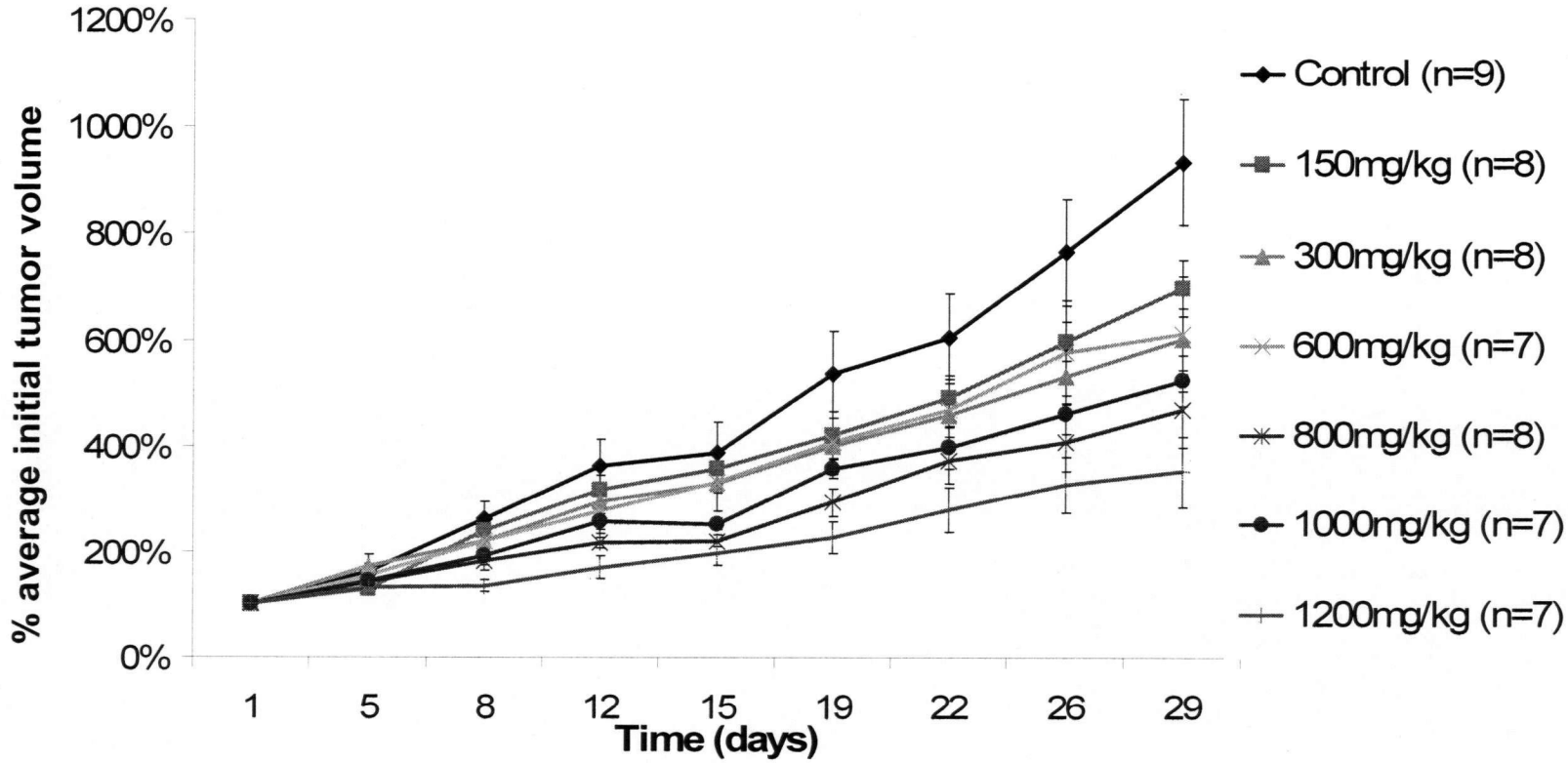

Figure 10. Percent average initial tumor volume over time of nude mice bearing a PC-3 tumor xenograft for control (vehicle) and treatment groups (150mg/kg-1200mg/kg CsCl). All mice were administered vehicle or CsCl daily for 30 days. Results are represented as mean value ± standard error of the mean. Statistical analysis using one way ANOVA indicates a significant difference between the control and treatment groups beginning on day 5 and extending to the end of the study ($P<0.05$). Pair-wise multiple comparison via Tukey test indicates a difference between the 1200mg/kg group and the control from day 5 until the end of the study ($P<0.05$), a difference between the 1000mg/kg group and the control from day 26 until the end of the study ($P<0.05$), and a difference between the 800mg/kg group and the control from day 12 to the end of the study ($P<0.05$).

Likewise the 1000mg/kg and 800mg/kg groups showed significant reductions in tumor growth compared to the control from day 26 and day 12 onwards, respectively (Figure 10).

3.1.2 LNCaP Solid Tumor Xenograft Study

Administration of CsCl in combination with the effects of LNCaP tumor burden was quite toxic in the nude mouse model. The 1200mg/kg, 1000mg/kg and 800mg/kg treatment groups were removed from the study, when one or more animals in each group saw a reduction in body mass below 80% of their initial body mass and were subsequently euthanized (Figure 11). The 1200mg/kg and 1000mg/kg groups were both discontinued on day 15 and the 800mg/kg group was removed on day 19 (Figure 11). The animals in these groups that did not show this significant reduction in body mass on the described days remained in the study until this toxicity point was reached. On average, animals from the 1200mg/kg and 1000mg/kg groups remained in the study for 21 days and animals of the 800 mg/kg group remained in the study for 27 days.

Although the 1200mg/kg, 1000mg/kg and 800mg/kg groups were removed prior to the completion of the study, each of these groups showed a significant reduction in % average initial body mass compared to the control. This reduction in body mass was first observed on day 6 for the 1200mg/kg group, day 7 for the1000mg/kg group, and day 16 for the 800mg/kg group, and remained significantly different for each group until their removal from the study (Figure 11).

There was no significant difference in food consumption or water consumption between any of the treatment groups and the control (except on day 3+4 where the 600mg/kg group had a significant increase in food consumption) (Figures 12, 13).

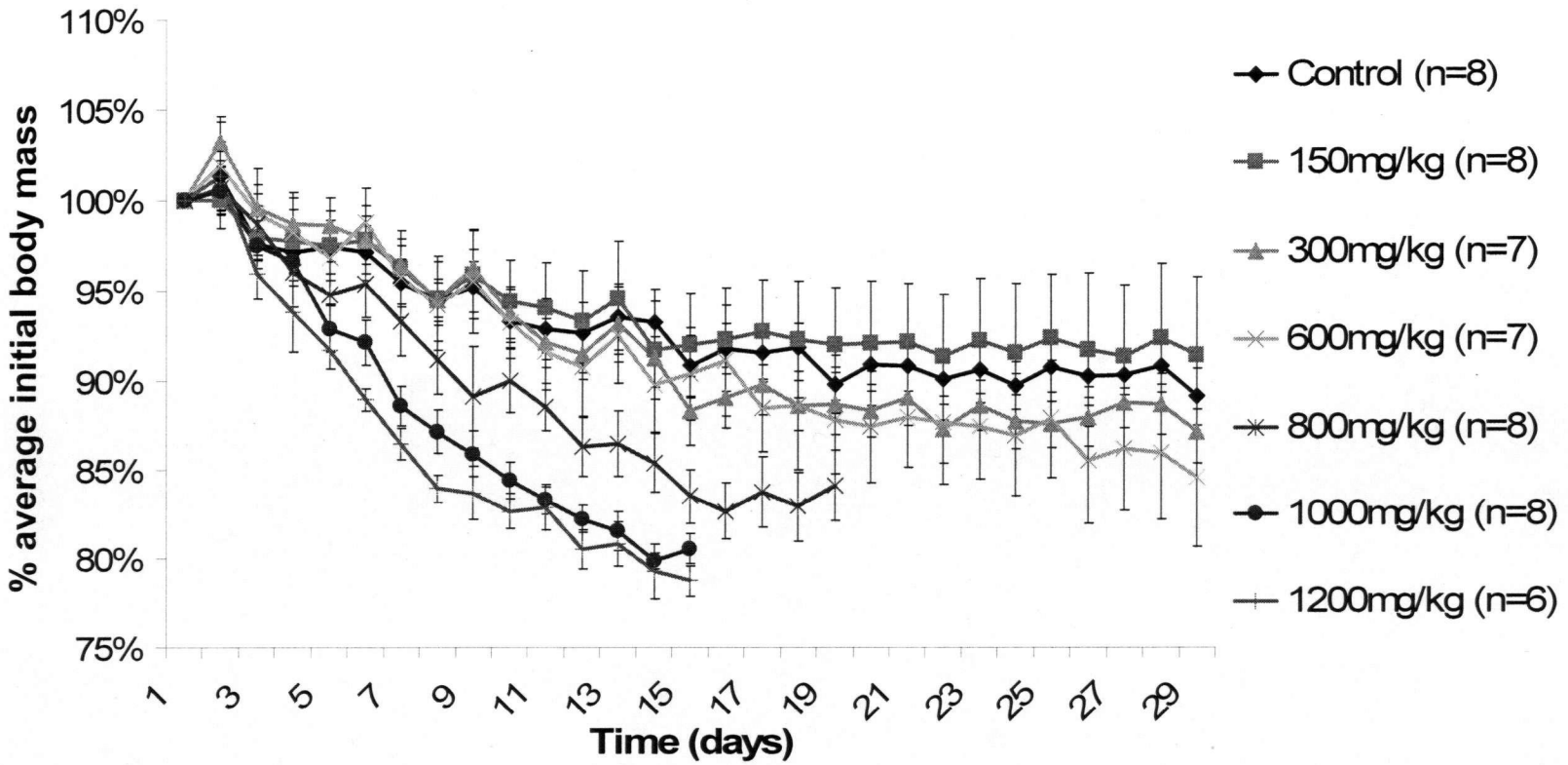

Figure 11. Percent average initial body mass over time of nude mice bearing a LNCaP tumor xenograft for control (vehicle) and treatment groups (150mg/kg-1200mg/kg CsCl). Most mice were administered vehicle or CsCl daily for 30 days; the 800mg/kg, 1000mg/kg and 1200mg/kg treatment groups were removed halfway through the study because the % average initial body mass of the mice dropped below 80%. Results are represented as mean value ± standard error of the mean. Statistical analysis using one way ANOVA indicates a significant difference between the control and treatment groups beginning on day 6 and extending to day 19 ($P<0.05$). Pair-wise multiple comparison via Tukey test indicates a difference between the 1200mg/kg group and the control from day 6 to day 15 ($P<0.05$), a difference between the 1000mg/kg group and the control from day 7 to day 15($P<0.05$), and a difference between the 800mg/kg group and the control from day 16 to day 19 ($P<0.05$).

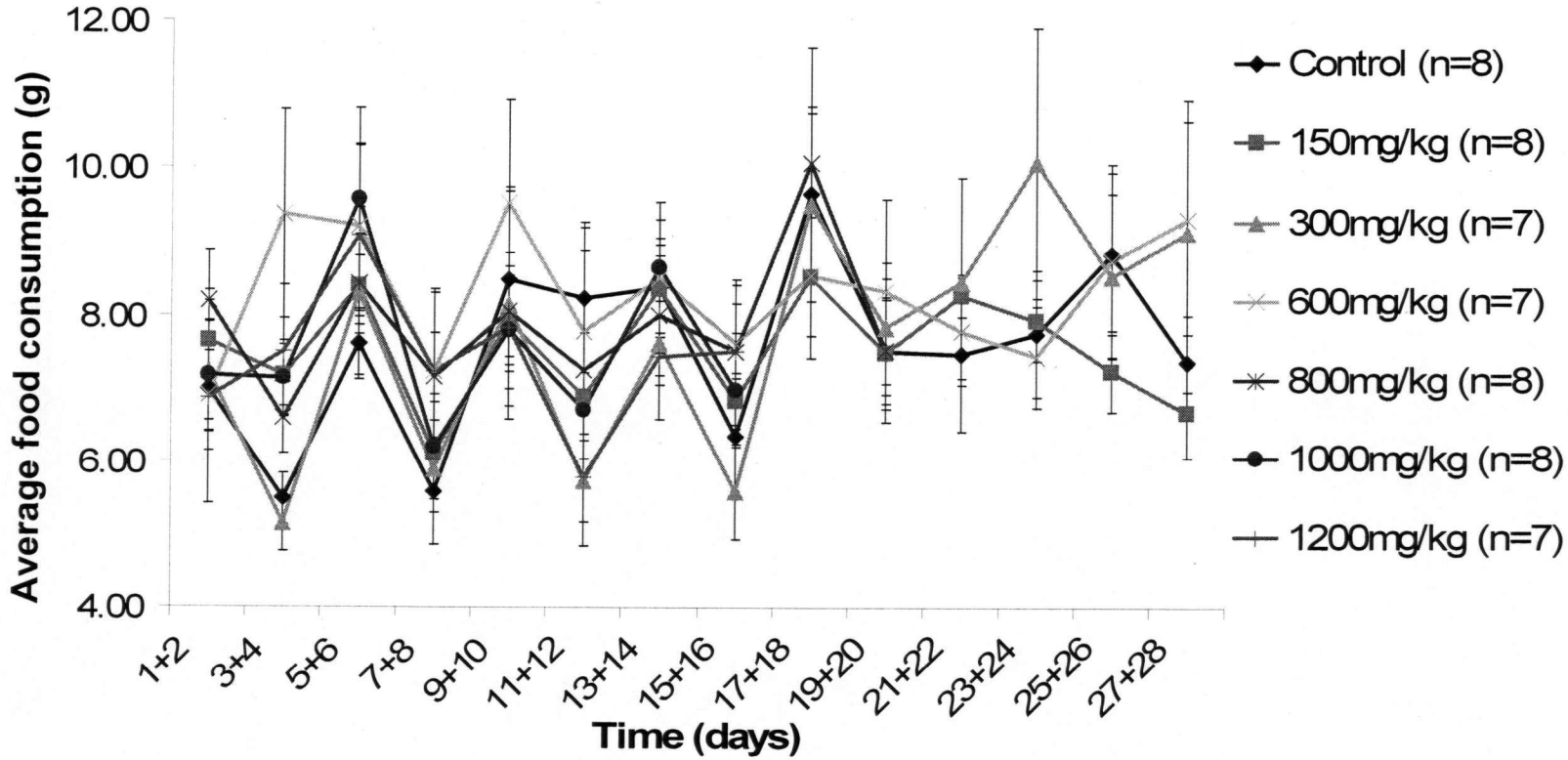

Figure 12. Average food consumption over time of nude mice bearing a LNCaP tumor xenograft for control (vehicle) and treatment groups (150mg/kg-1200mg/kg CsCl). Most mice were administered vehicle or CsCl daily for 30 days; the 800mg/kg, 1000mg/kg and 1200mg/kg treatment groups were removed halfway through the study because the % average initial body mass of the mice dropped below 80%. Results are represented as mean value ± standard error of the mean. Statistical analysis using one way ANOVA indicates a significant difference between the control and treatment groups on day 3+4 ($P<0.05$). Pair-wise multiple comparisons via Tukey test indicates a difference between the 600mg/kg group and the control ($P=0.008$).

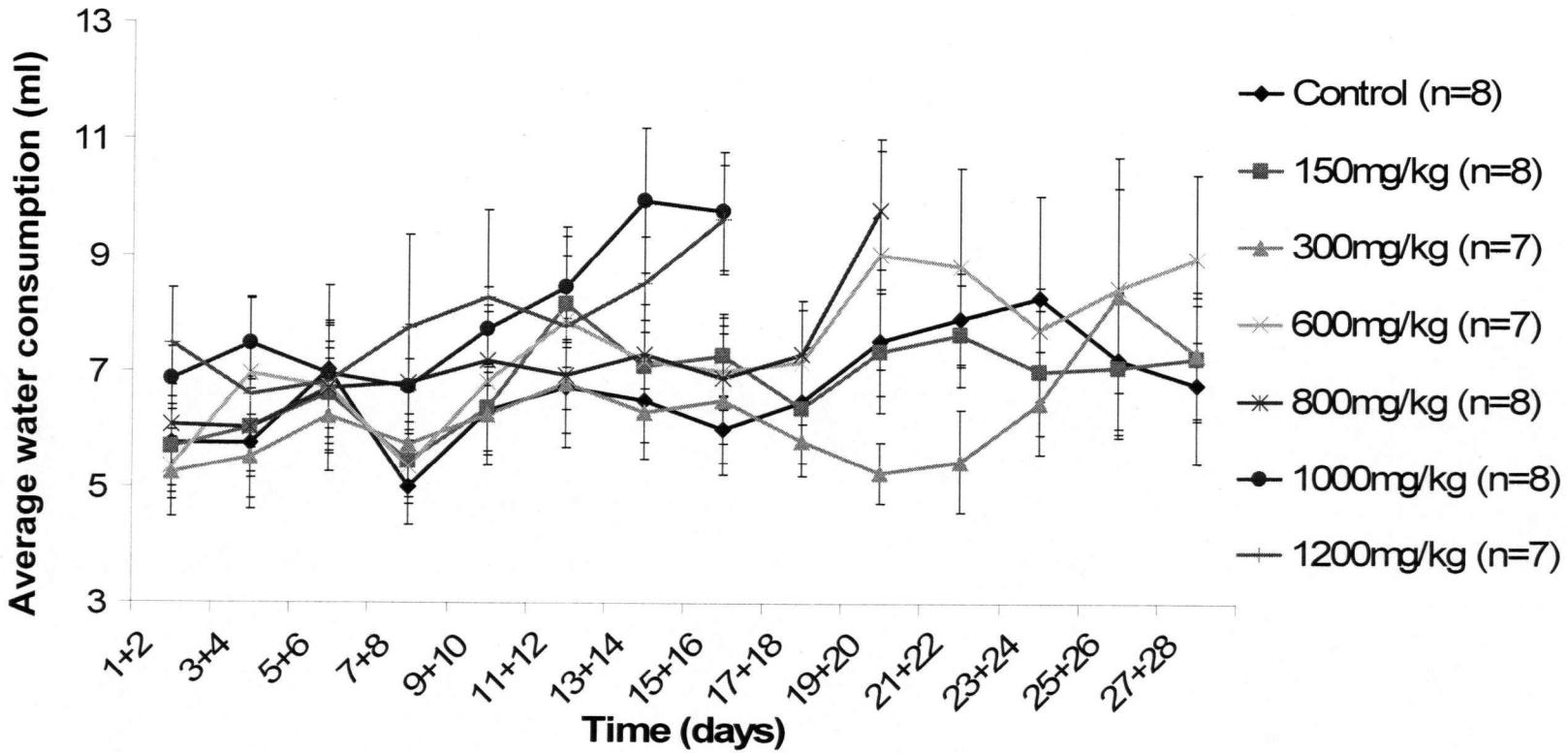

Figure 13. Average water consumption over time of nude mice bearing a LNCaP tumor xenograft for control (vehicle) and treatment groups (150mg/kg-1200mg/kg CsCl). Most mice were administered vehicle or CsCl daily for 30 days; the 800mg/kg, 1000mg/kg and 1200mg/kg treatment groups were removed halfway through the study because the % average initial body mass of the mice dropped below 80%. Results are represented as mean value ± standard error of the mean. There was no statistical difference between any of the groups ($P>0.05$).

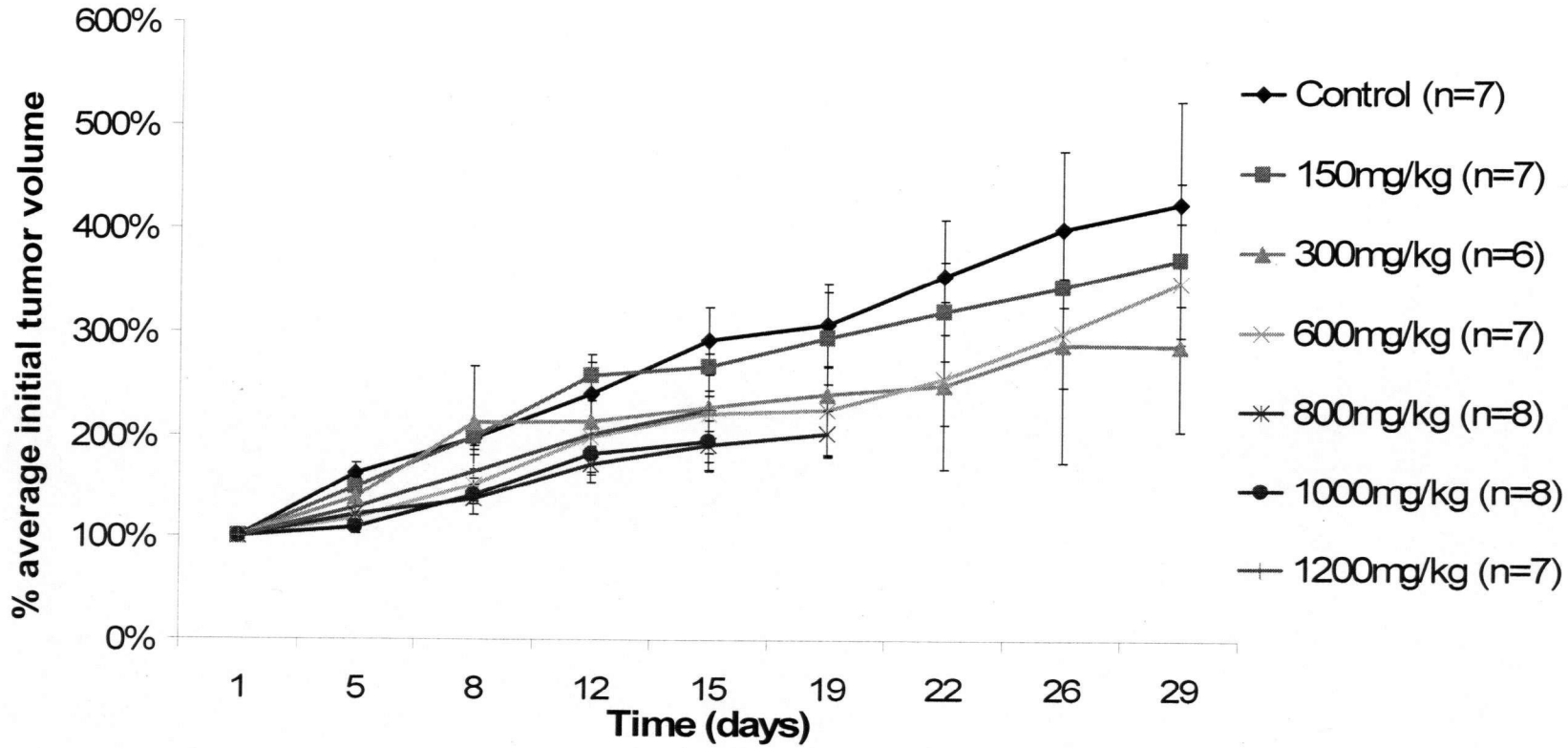

Figure 14. Percent average initial tumor volume over time of nude mice bearing a LNCaP tumor xenograft for control (vehicle) and treatment groups (150mg/kg-1200mg/kg CsCl). Most mice were administered vehicle or CsCl daily for 30 days; the 800mg/kg, 1000mg/kg and 1200mg/kg treatment groups were removed halfway through the study because the % average initial body mass of the mice dropped below 80%. Results are represented as mean value ± standard error of the mean. There was no statistical difference between any of the groups ($P>0.05$

In terms of water consumption, there appears to be a trend that suggests an increase in water consumption in the two groups that received the highest concentrations of CsCl, four days prior to their removal from the study (Figure 13)

Unlike the PC-3 xenograft, the LNCaP xenograft was less responsive to the CsCl treatment. Only on day 5 did any of the treatment groups have a significant reduction in % average initial tumor volume compared to the control group (1000mg/kg, 800mg/kg and 600mg/kg groups) (Figure 14).

3.1.3 Non-tumor Bearing Nude Mouse Study

The third study involving non-tumor bearing mice provided insight into the toxicity of CsCl alone without a confounding tumor burden. When CsCl was chronically administered to these animals, it was discovered that none of the treatment groups displayed any significant difference in % average initial body mass when compared to the control (Figure 15). Even animals receiving the highest concentrations of CsCl, showed a similar increase in body mass compared to the control mice, which was not observed in either of the previous two studies.

There was no difference in food consumption between any of the treatment groups and the control animals (Figure 16). However, water consumption was significantly elevated beginning on day 15 in animals receiving 1200mg/kg and 1000mg/kg CsCl (Figure 17). Water consumption was also elevated in animals receiving 800mg/kg CsCl from day 21 to 27 (Figure 17).

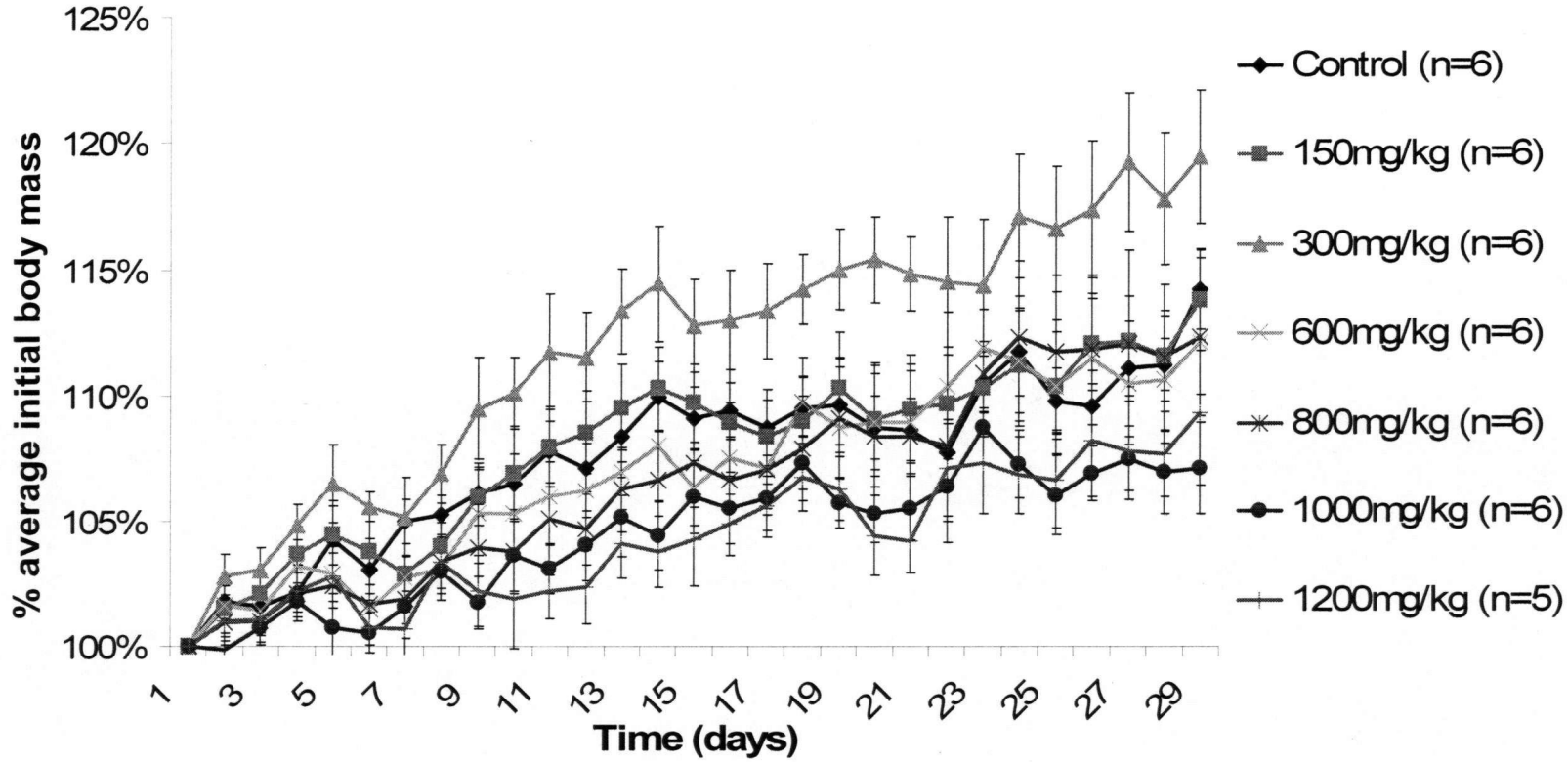

Figure 15. Percent average initial body mass over time of tumor free nude mice for control (vehicle) and treatment groups (150mg/kg-1200mg/kg CsCl). All mice were administered vehicle or CsCl daily for 30 days. Results are represented as mean value ± standard error of the mean. Statistical analysis using one way ANOVA indicates no difference between the control and treatment groups for the duration of the study ($P>0.05$).

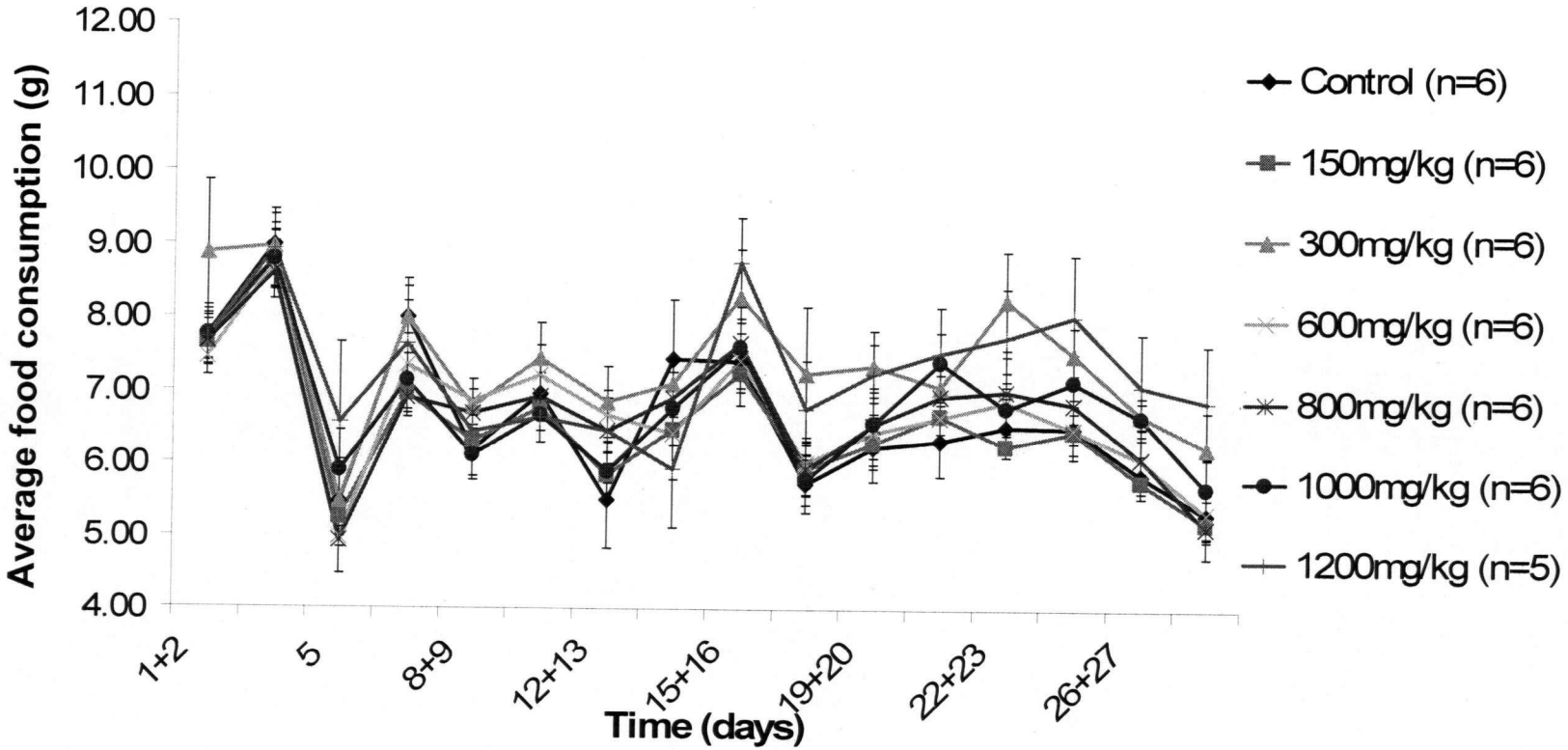

Figure 16. Average food consumption over time of tumor free nude mice for control (vehicle) and treatment groups (150mg/kg-1200mg/kg CsCl). All mice were administered vehicle or CsCl daily for 30 days. Results are represented as mean value ± standard error of the mean. There was no statistical difference between any of the groups ($P>0.05$).

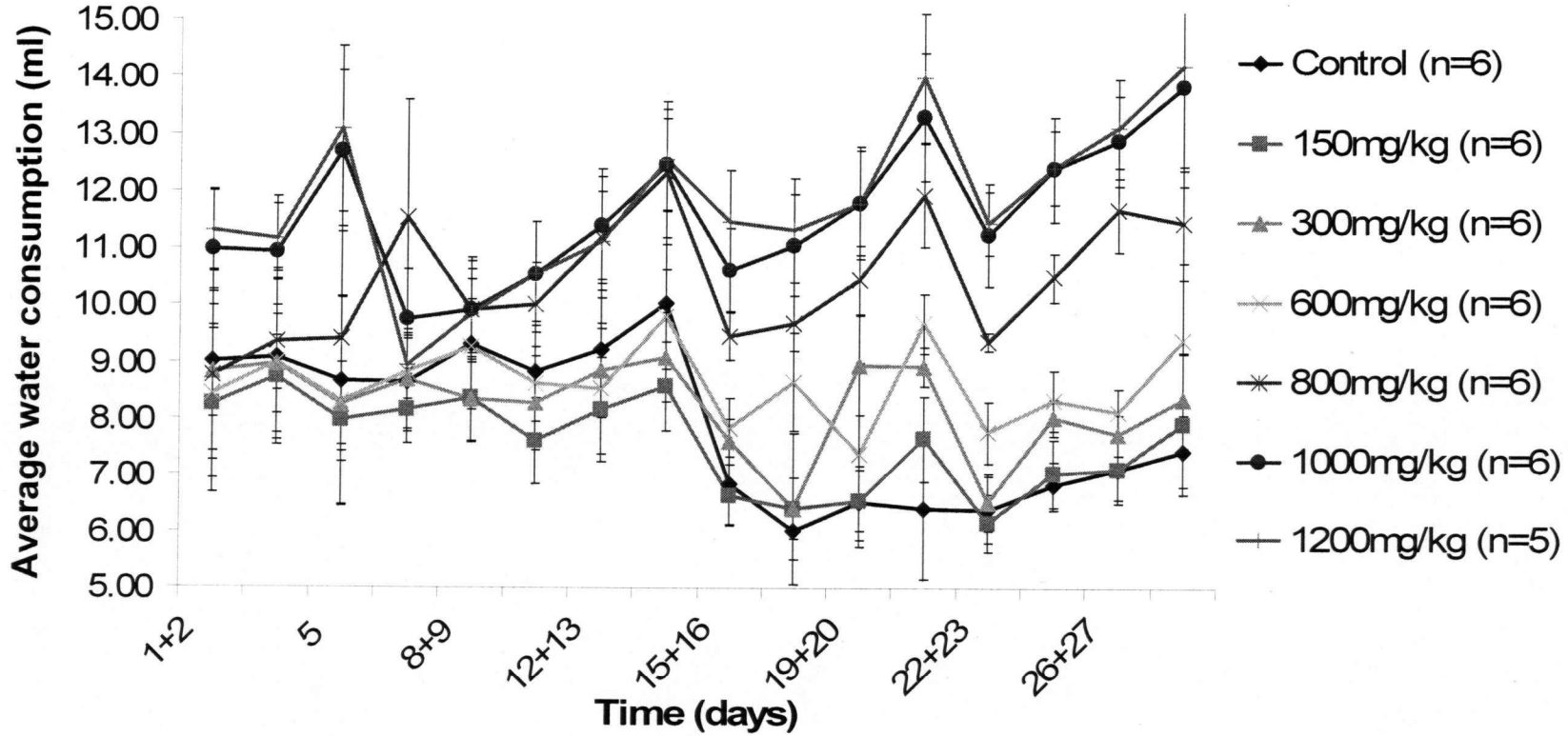

Figure 17. Average water consumption over time of tumor free nude mice for control (vehicle) and treatment groups (150mg/kg-1200mg/kg CsCl). All mice were administered vehicle or CsCl daily for 30 days. Results are represented as mean value ± standard error of the mean. Statistical analysis by way of one way ANOVA indicates a significant difference between the control and treatment groups beginning on day 15 and extending to the end of the study ($P<0.05$). Pair-wise multiple comparison via Tukey test indicates a difference between the 1200mg/kg group and the control from day 15 until the end of the study ($P<0.05$), a difference between the 1000mg/kg group and the control from day 15 until the end of the study ($P<0.05$), and a difference between the 800mg/kg group and the control from day 21 to day 27 ($P<0.05$).

3.2 Investigation of organ and tissue specific toxicity from CsCl (histopathology and serum marker tests) in human prostate tumor xenograft bearing nude mice

3.2.1 Histopathology

Tissues were collected from each of the animals in the three CsCl dose titration studies for histopathological analysis. Of the eight tissues examined, abnormalities were only observed in the hearts and small intestines. Fibrin clots present in the aorta, atrium or ventricles were found in animals from all three studies (Figure 18). Although fibrin clots can form post-mortem, there appears to be a higher incidence of fibrin clots in animals receiving 800-1200mg/kg CsCl compared to control animals in both the PC-3 and LNCaP studies (Figure 19). This same trend was not observed in mice without tumors; fibrin clots were present in 33% of the animals within in each treatment group (Figure 19).

Atrophy of the mucosal epithelium and villi, as well as the presence of inflammatory infiltrate of the submucosa of the small intestine were observed in both control and CsCl treated mice of the three studies (Figure 20). There appeared to be no evident trend in the incidence of these abnormalities across the different treatment groups and the control group in each of the three studies (Figures 21, 22, 23).

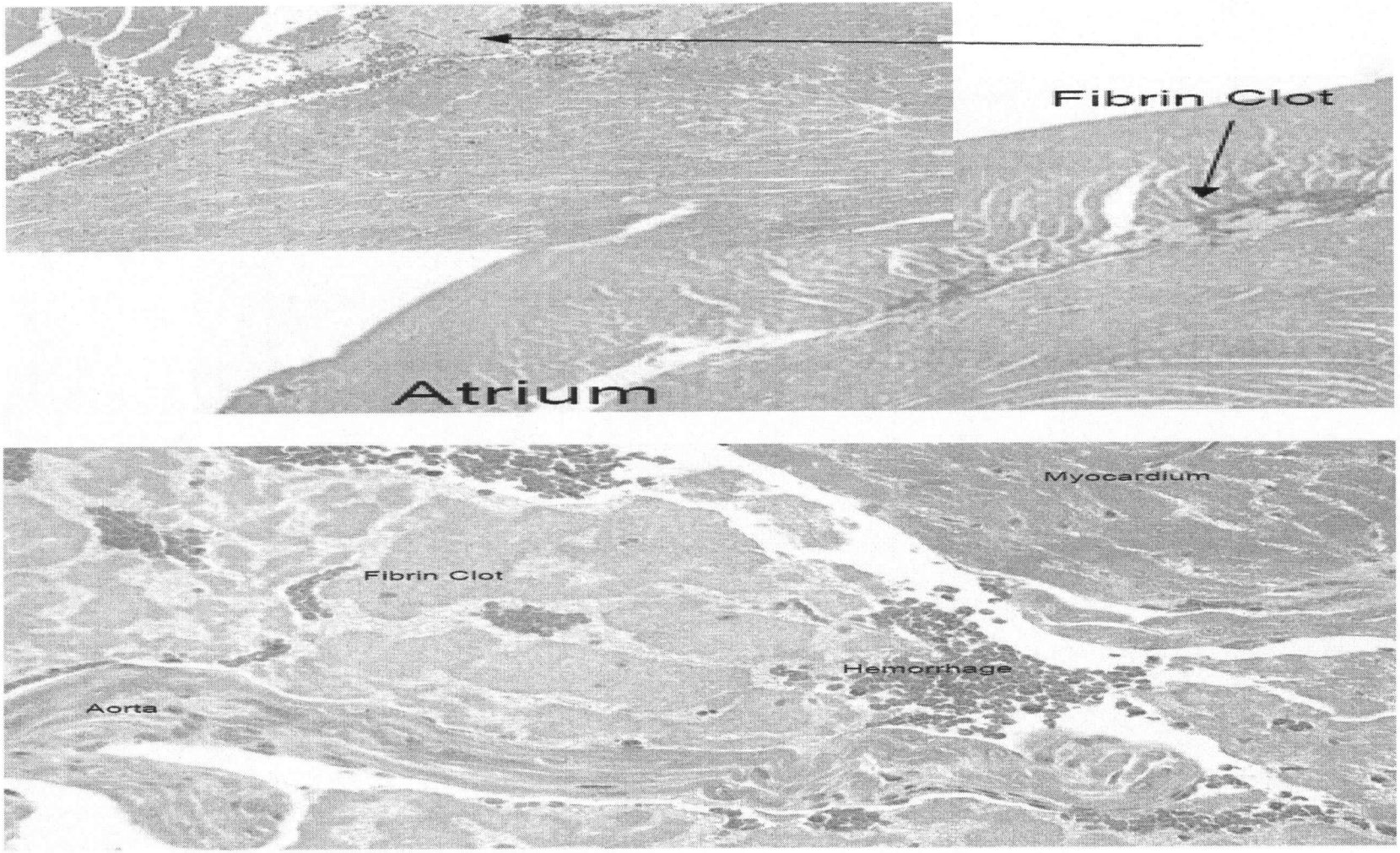

Figure 18. Images of cardiac fibrin clots discovered post-mortem in a nude mouse of the PC-3 study.

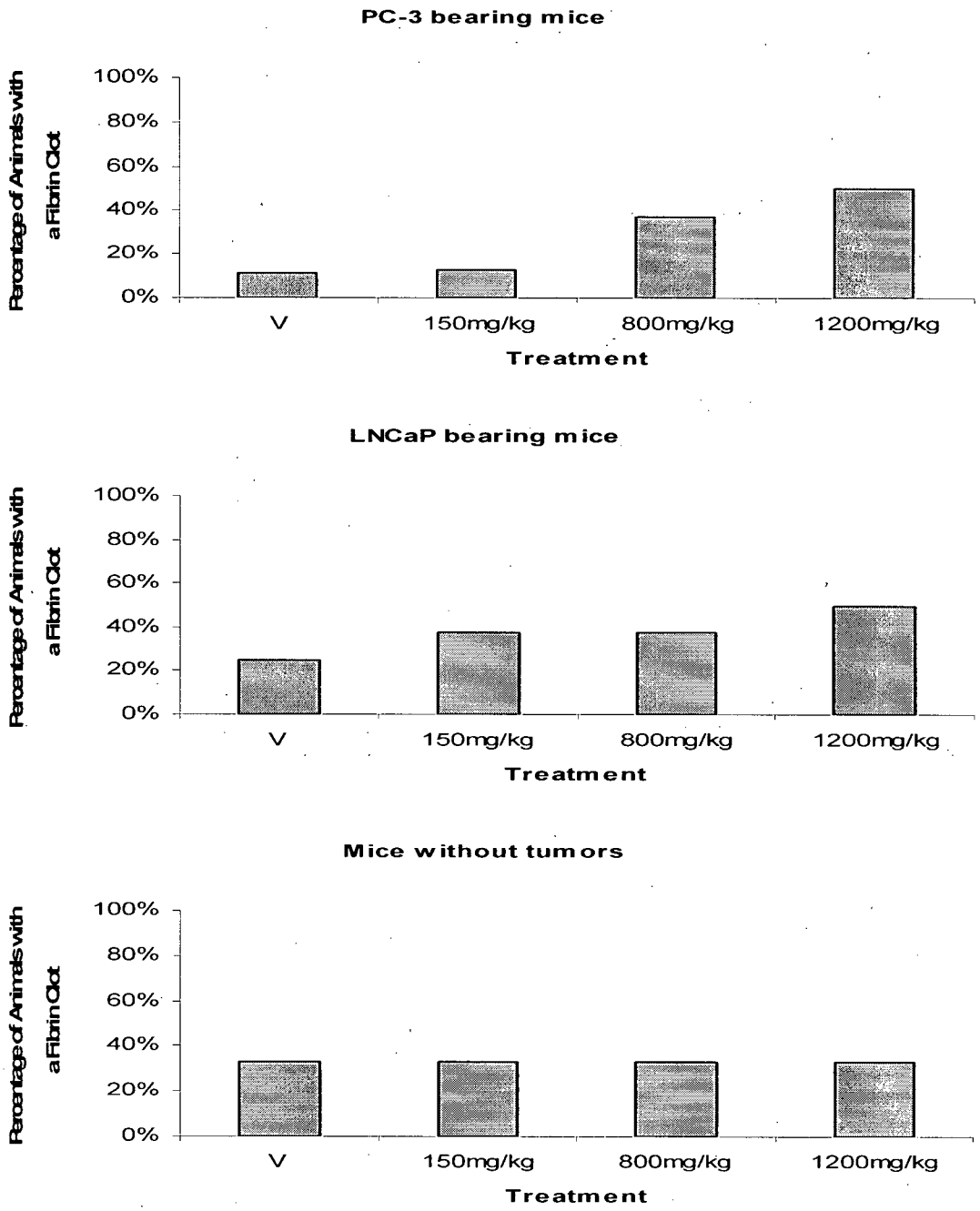

Figure 19. Percentage of nude mice from the three studies (PC-3, LNCaP, non-tumor bearing) with the presence of post-mortem fibrin clots for control (vehicle) and treatment groups (150mg/kg, 800mg/kg, 1200mg/kg CsCl). Most mice were administered vehicle or CsCl daily for 30 days; the 800mg/kg and 1200mg/kg treatment groups of the LNCaP study were removed halfway through the study because the % average initial body mass of the mice dropped below 80%

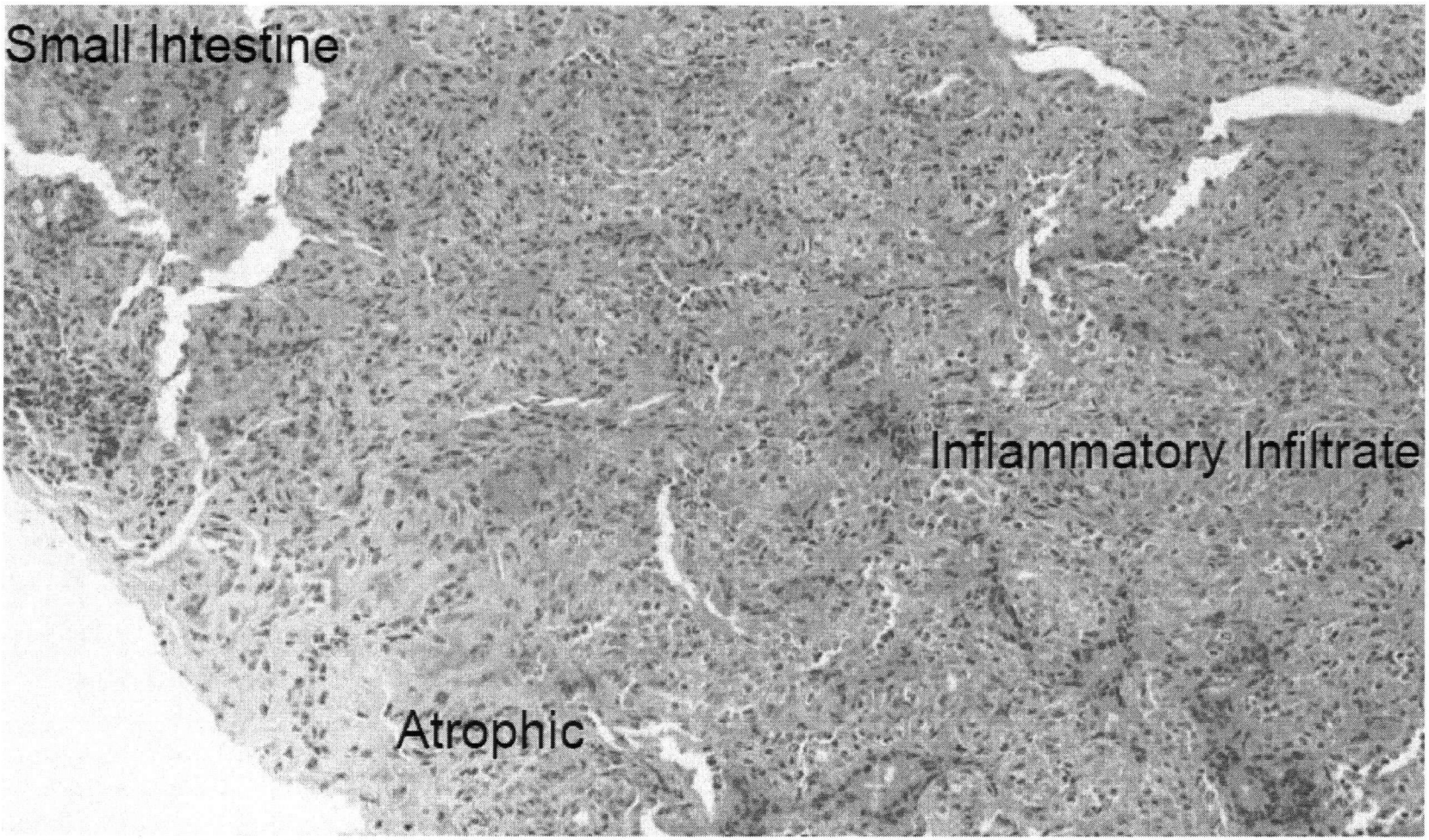

Figure 20. Image of abnormalities of the small intestine discovered post-mortem in a nude mouse of the PC-3 study

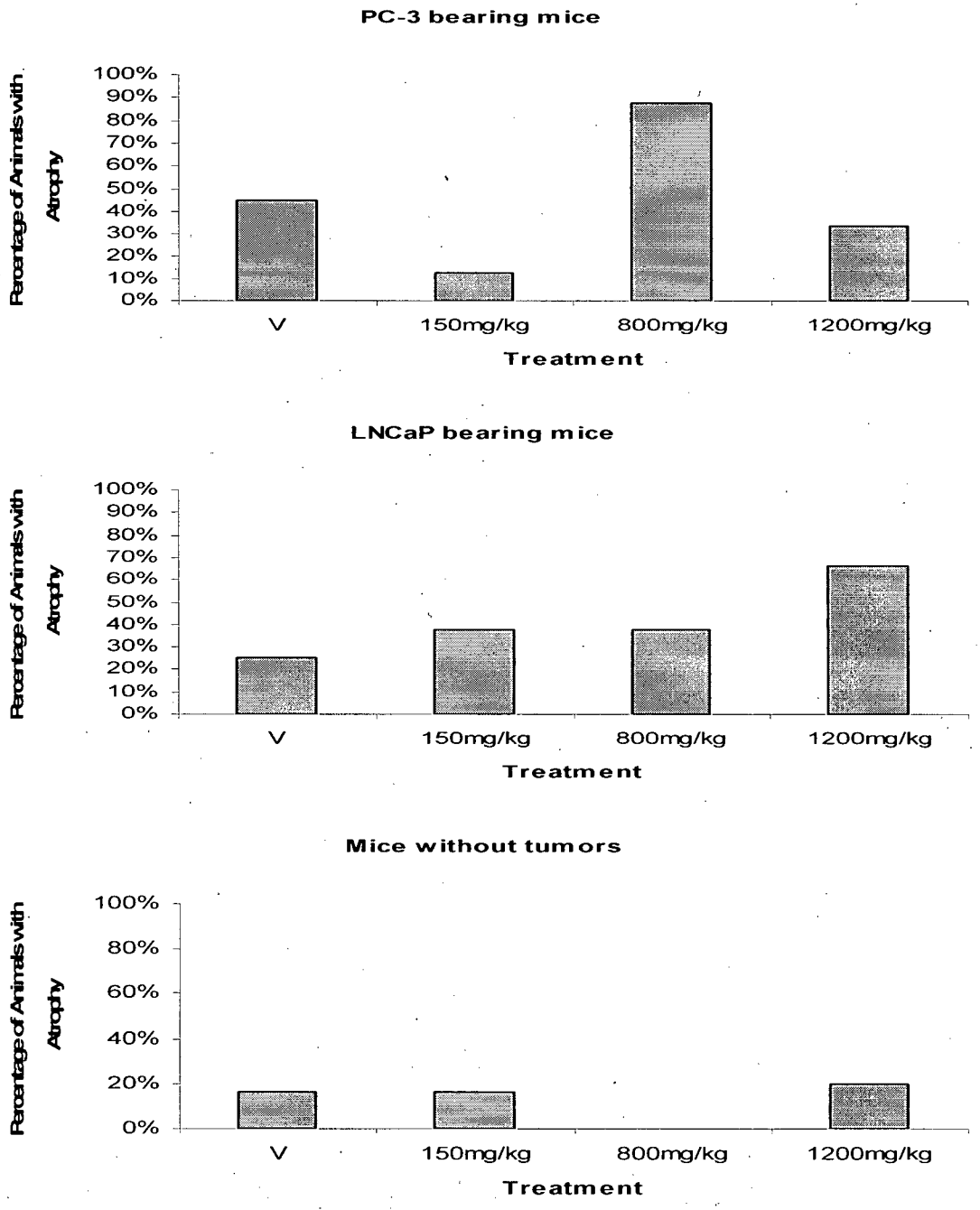

Figure 21. Percentage of nude mice from the three studies (PC-3, LNCaP, non-tumor bearing) with the presence of atrophy of mucosal epithelium of the small intestine for control (vehicle) and treatment groups (150mg/kg, 800mg/kg, 1200mg/kg CsCl). Most mice were administered vehicle or CsCl daily for 30 days; the 800mg/kg and 1200mg/kg treatment groups of the LNCaP study were removed halfway through the study because the % average initial body mass of the mice dropped below 80%.

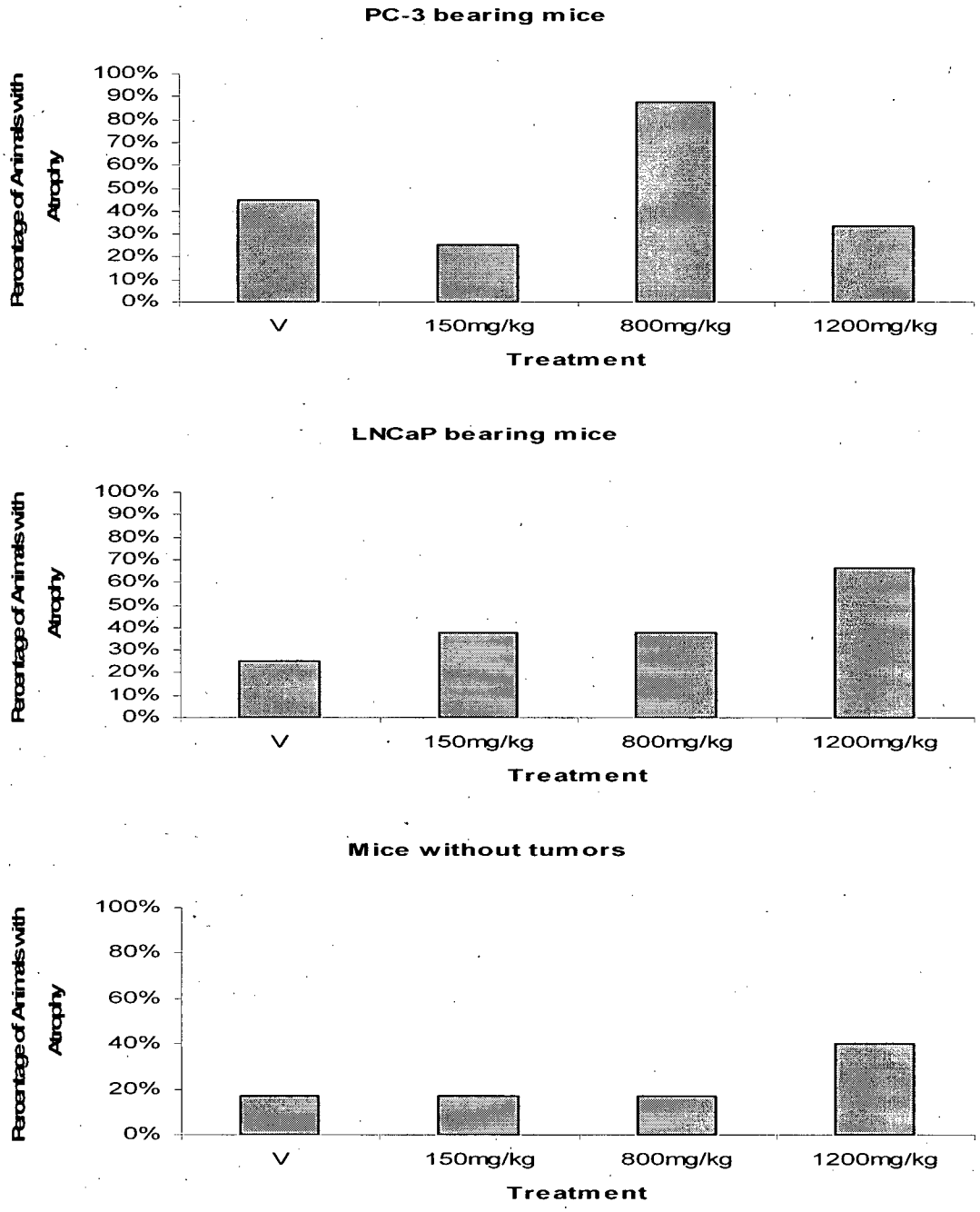

Figure 22. Percentage of nude mice from the three studies (PC-3, LNCaP, non-tumor bearing) with the presence of atrophy of villi of the small intestine for control (vehicle) and treatment groups (150mg/kg, 800mg/kg, 1200mg/kg CsCl). Most mice were administered vehicle or CsCl daily for 30 days; the 800mg/kg and 1200mg/kg treatment groups of the LNCaP study were removed halfway through the study because the % average initial body mass of the mice dropped below 80%.

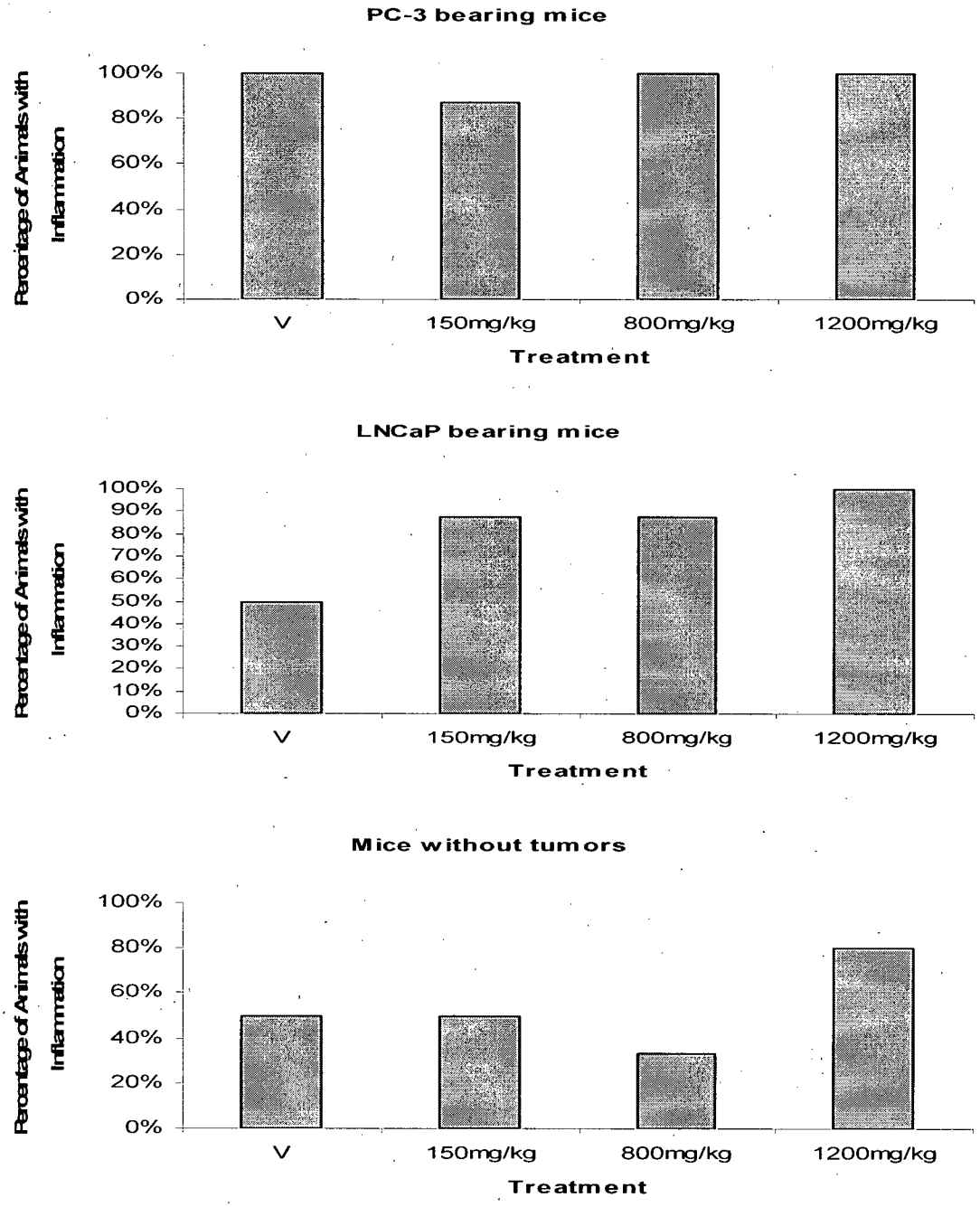

Figure 23. Percentage of nude mice from the three studies (PC-3, LNCaP, non-tumor bearing) with the presence of inflammatory infiltrate of the small intestine for control (vehicle) and treatment groups (150mg/kg, 800mg/kg, 1200mg/kg CsCl). Most mice were administered vehicle or CsCl daily for 30 days; the 800mg/kg and 1200mg/kg treatment groups of the LNCaP study were removed halfway through the study because the % average initial body mass of the mice dropped below 80%.

3.2.2 Serum AST/ALT

Serum collected from animals in the three CsCl dose titration studies was analyzed for AST and ALT levels as secondary measures of cellular and tissue damage. Specifically, these two markers were used to assess damage to the heart, liver, skeletal muscle, kidney and erythrocytes. Serum from the CsCl treated PC-3, LNCaP and non-tumor bearing mice showed no difference in the levels of these markers as compared to the control animals within each study (Figures 24, 25, 26).

3.2.3 Serum Creatinine

Serum collected from the animals was also analyzed for creatinine levels as a measure of kidney toxicity. Figure 27 illustrates the chromatograms of a creatinine spiked standard and of a serum sample. In each chromatogram, the peak eluting just after 2 minutes is creatinine (Figure 27). The peak that elutes before creatinine is cytosine (~1.69 min), which was intended to be used as an internal standard until problems arose with variable basal levels of cytosine present in the serum samples (Figure 27). The two peaks that elute after creatinine in the serum sample are unknown artifacts (Figure 27).

Figure 28 represents the standard curve developed for the serum creatinine assay. One can observe the highly linear relationship between peak area and creatinine concentration (R^2= 0.9997) (Figure 28). The Limit of Detection (LOD) and Limit of Quantification (LOQ) of this assay were 1.27ug/ml and 4.23ug/ml, respectively. The intraday and interday Percent Coefficient of Variance (%CV) were 3.16% and 0.93%, respectively.

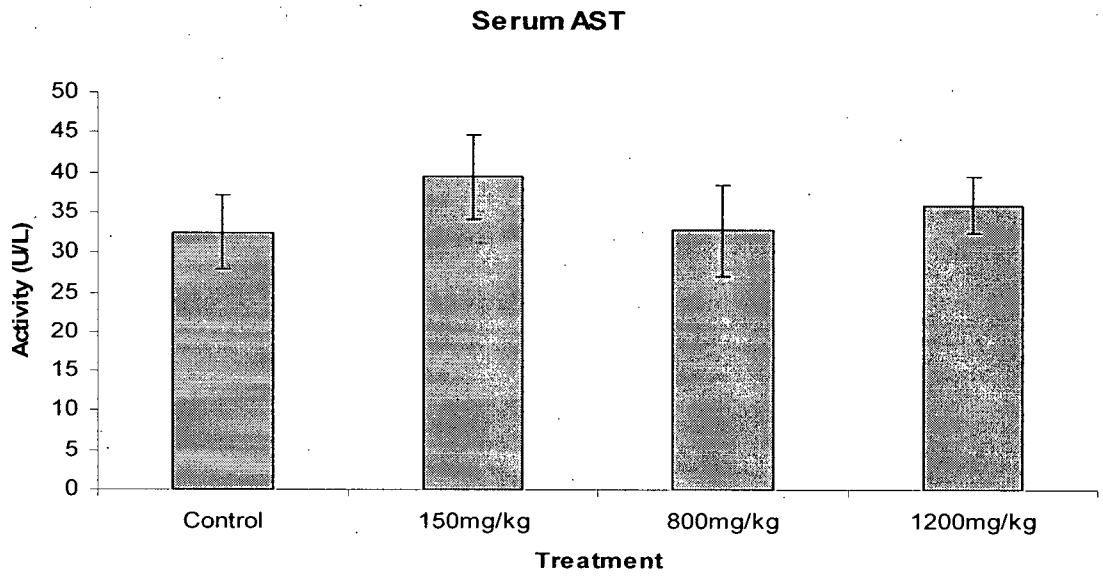

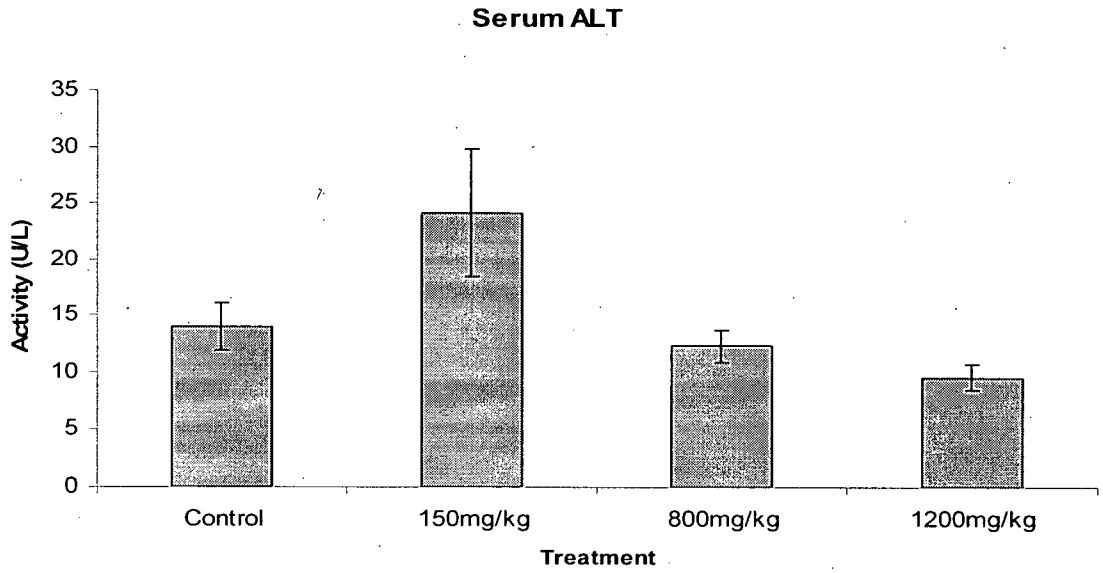

Figure 24. Serum AST and ALT levels of nude mice bearing a PC-3 xenograft for control (vehicle) and treatment groups (150mg/kg, 800mg/kg, 1200mg/kg CsCl). All mice were administered vehicle or CsCl daily for 30 days. Results are represented as mean value ± standard error of the mean. Statistical analysis using one way ANOVA indicates no difference in AST or ALT levels between the control and treatment groups (P=0.726, P=0.067, respectively).

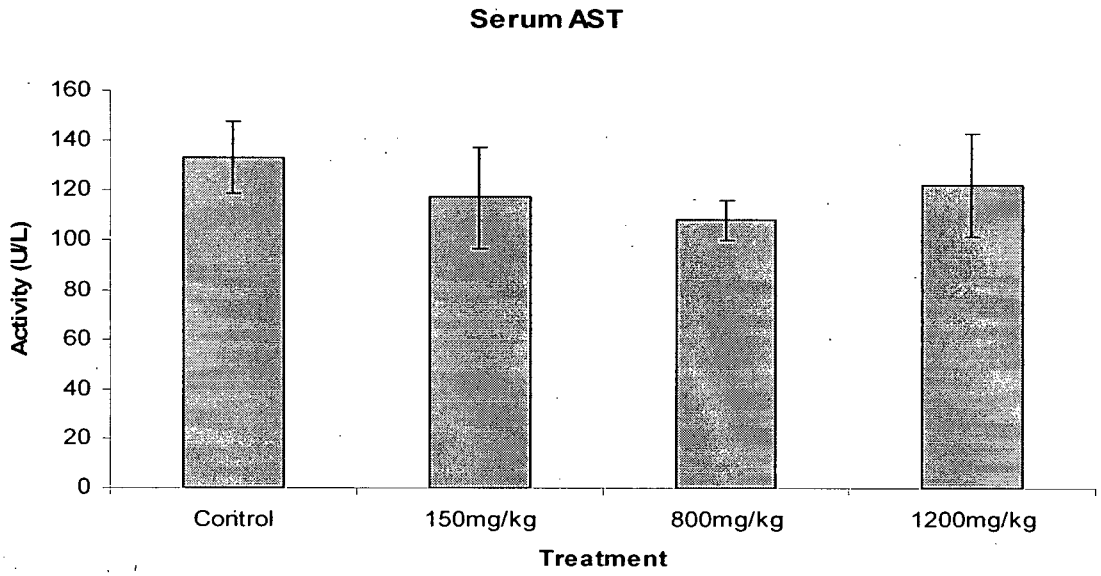

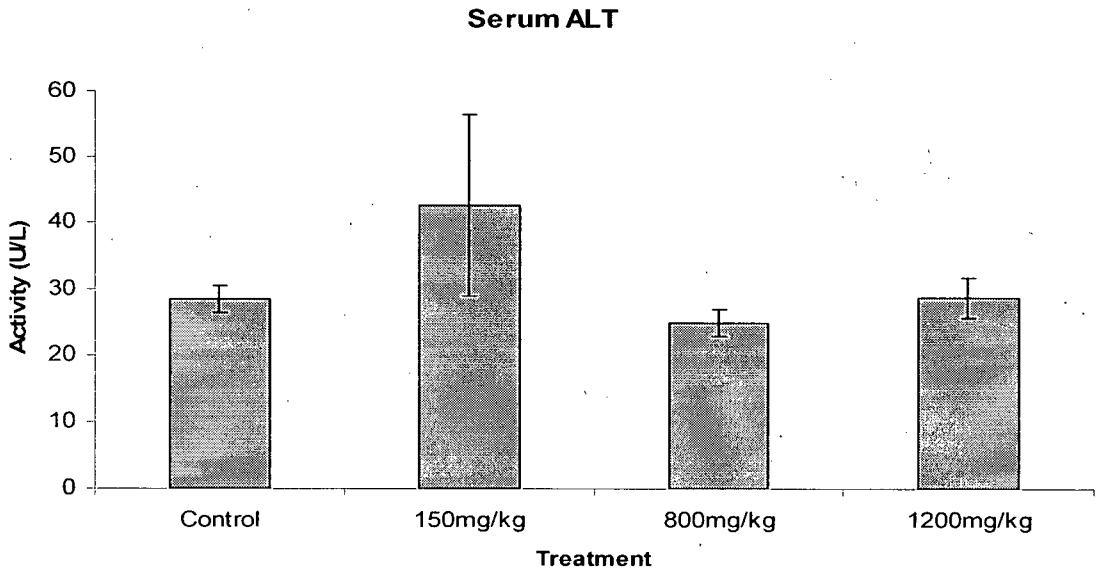

Figure 25. Serum AST and ALT levels of nude mice bearing a LNCaP xenograft for control (vehicle) and treatment groups (150mg/kg, 800mg/kg, 1200mg/kg CsCl). Most mice were administered vehicle or CsCl daily for 30 days; the 800mg/kg and 1200mg/kg treatment groups were removed halfway through the study because the % average initial body mass of the mice dropped below 80%. Results are represented as mean value ± standard error of the mean. Statistical analysis using one way ANOVA indicates no difference in AST or ALT levels between the control and treatment groups (P=0.736, P=0.569, respectively).

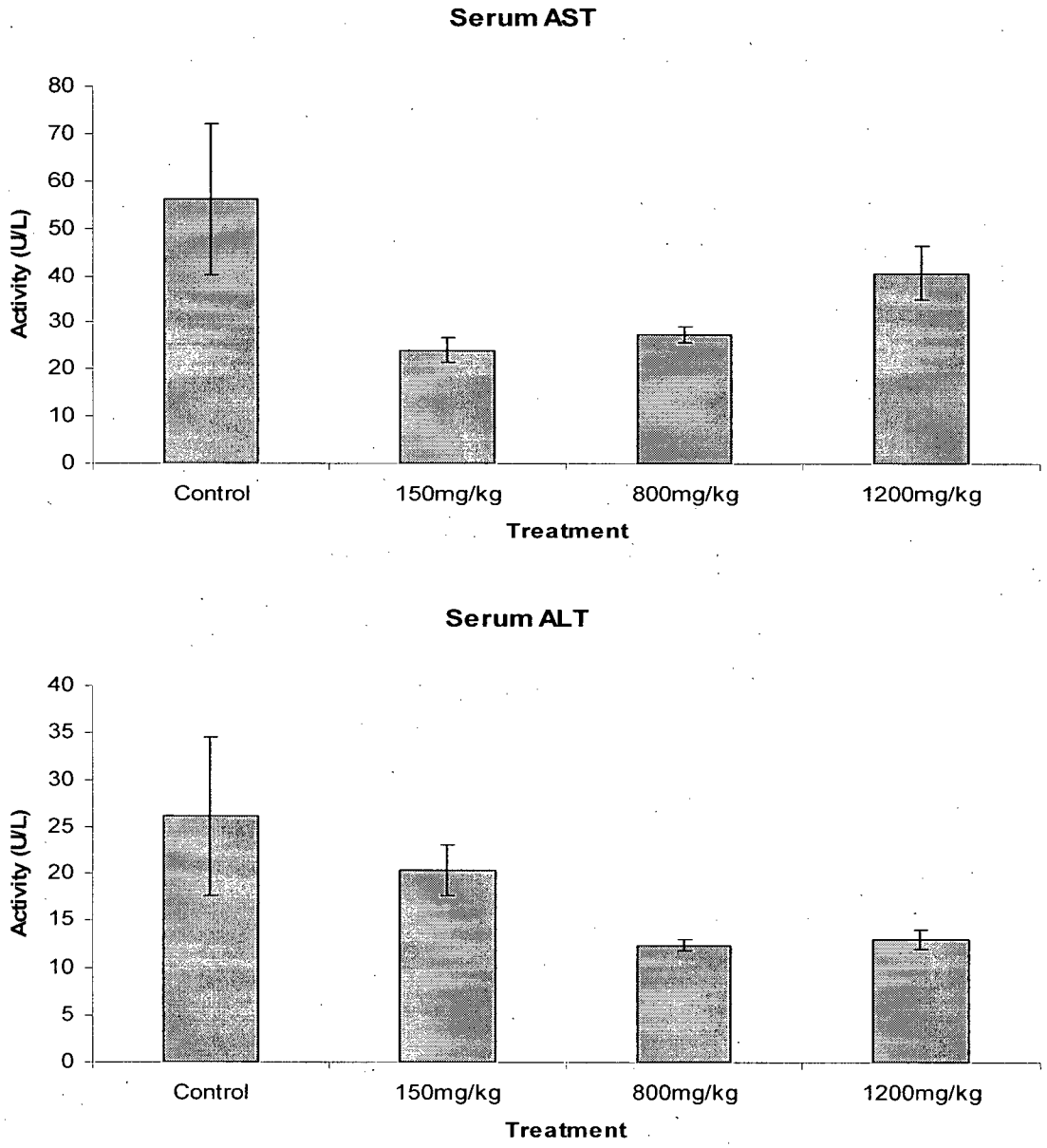

Figure 26. Serum AST and ALT levels of tumor free nude mice for control (vehicle) and treatment groups (150mg/kg, 800mg/kg, 1200mg/kg CsCl). All mice were administered vehicle or CsCl daily for 30 days. Results are represented as mean value ± standard error of the mean. Statistical analysis using one way ANOVA indicates no difference in AST levels between the control and treatment groups (P=0.085). However, there was a statistical difference in ALT levels between the 150mg/kg and 800mg/kg group (P=0.029).

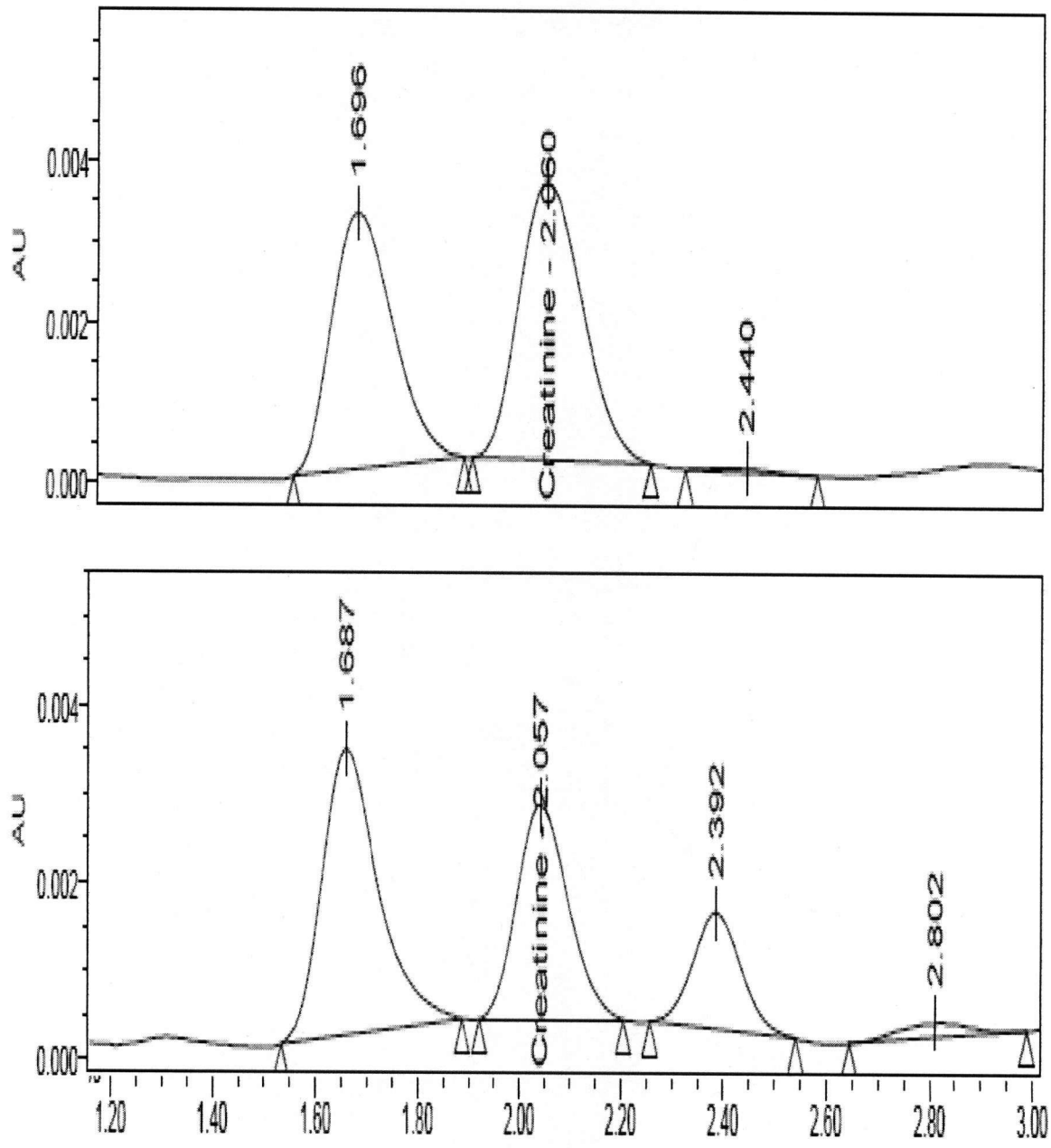

Figure 27. Chromatograms of a creatinine spiked standard (above) and a serum sample (below) using Hydrophilic Interaction Chromatography. In the two chromatograms, cytosine elutes at ~1.69 min and creatinine elutes at ~2.06 min. In the chromatogram of the serum sample, the two substances that elute at ~2.39 and ~2.80 min are unknown artifacts.

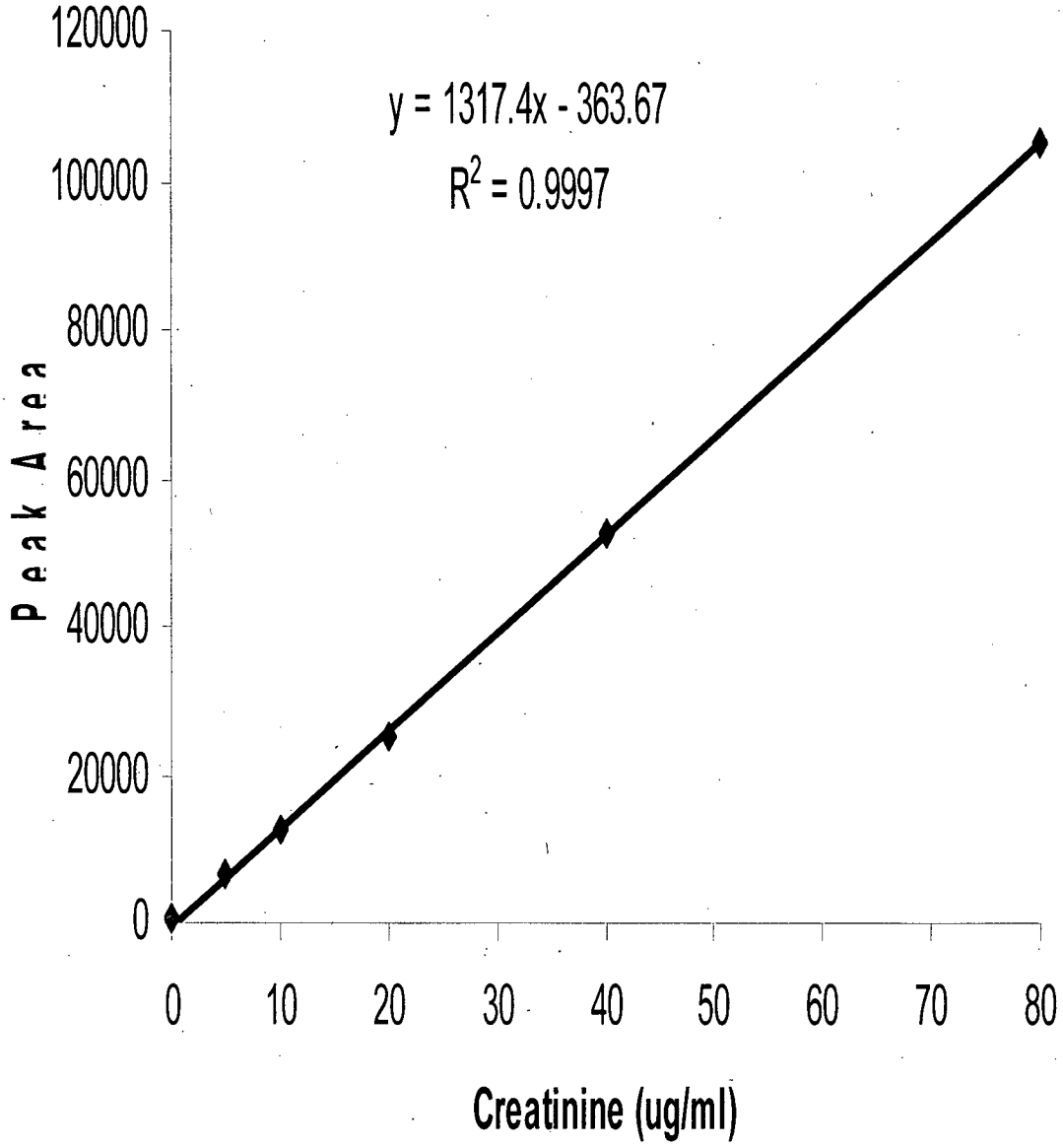

Figure 28. Standard curve for the serum creatinine HPLC assay. Standards were created in 94.5% acetonitrile. The standard curve has R^2= 0.9997, a LOD= 1.27ug/ml and LOQ= 4.23ug/ml. The intraday and interday %CV for this assay were 3.16% and 0.93%, respectively.

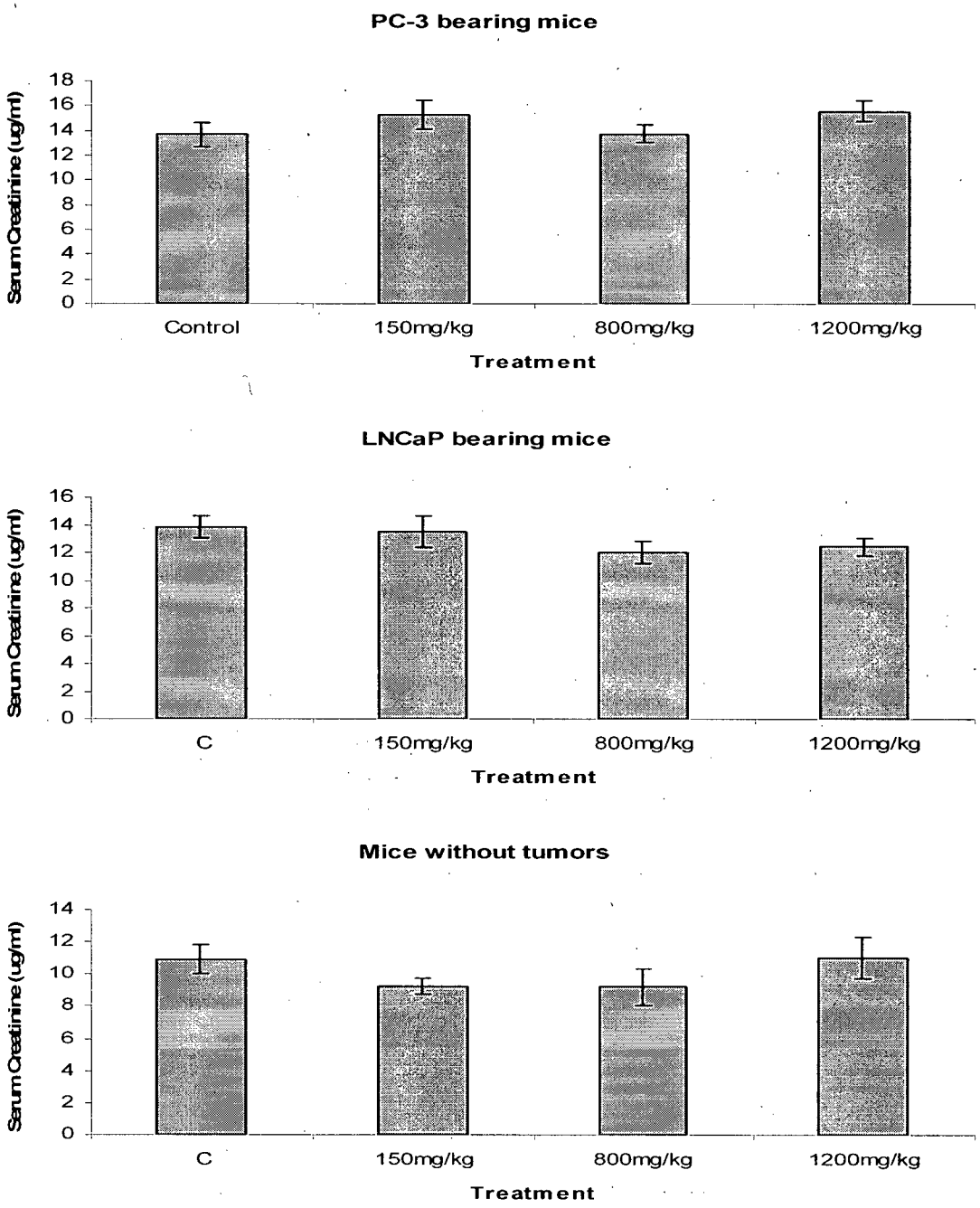

Figure 29. Serum creatinine levels of nude mice from the three studies (PC-3, LNCaP, non-tumor bearing) for control (vehicle) and treatment groups (150mg/kg, 800mg/kg, 1200mg/kg CsCl). Most mice were administered vehicle or CsCl daily for 30 days; the 800mg/kg and 1200mg/kg treatment groups of the LNCaP study were removed halfway through the study because the % average initial body mass of the mice dropped below 80%. Results are represented as mean value ± standard error of the mean. Statistical analysis using one way ANOVA indicates no difference between the control and treatment groups for any of the studies ($P>0.05$).

There was no difference in serum creatinine levels between the treatment groups and the controls within each of the three studies (Figure 29).

3.2.4 Bladder Crystals and Viscous Mucosal Fluid

During the excision of prostates from the PC-3 animals, it became evident that high levels of inflammation were present in the bladders of animals that had received the higher doses of CsCl. Further investigation revealed the presence of crystals or viscous mucosal fluid in the bladders of these animals (Figure 30).

On completion of study two and three, it was realized that the presence of these crystals or viscous mucosal fluid were not restricted solely to the PC-3 study, but were present in animals from all three studies. These bladder abnormalities only existed in animals that had been administered CsCl at concentrations of 600mg/kg and higher (Figure 31).

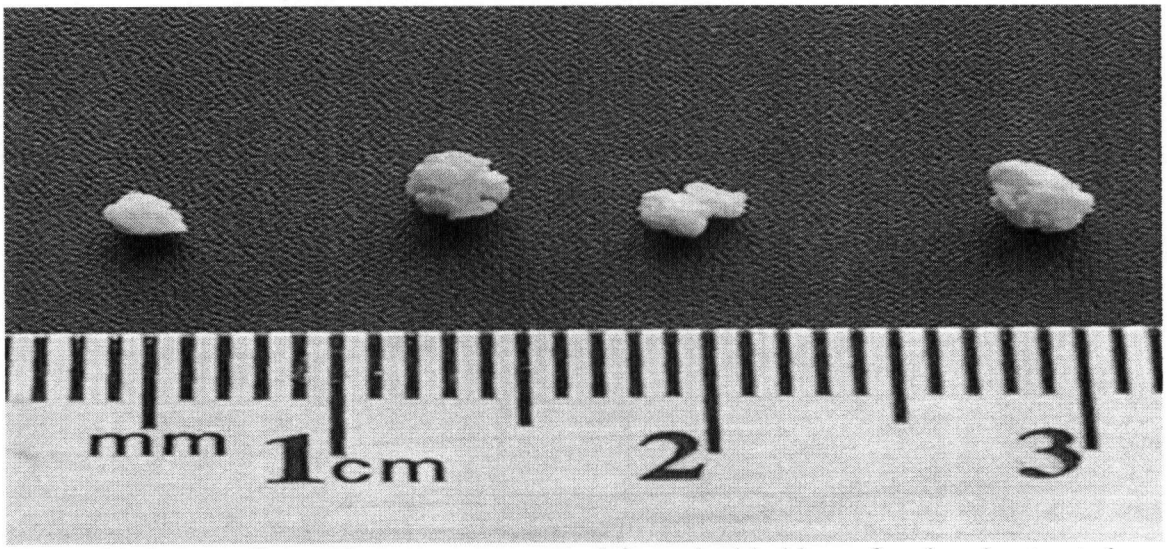

Figure 30. Image of crystal structures removed from the bladders of nude mice treated with 600mg/kg-1200mg/kg CsCl daily. These crystals were discovered in animals from the PC-3, LNCaP and non-tumor studies. In the PC-3 and non-tumor studies, these crystals were removed from the animals on day 30 during tissue collection. However, in the LNCaP study these crystals were observed as early as day 15 in animals that were euthanized (1000mg/kg and 1200mg/kg treatment groups).

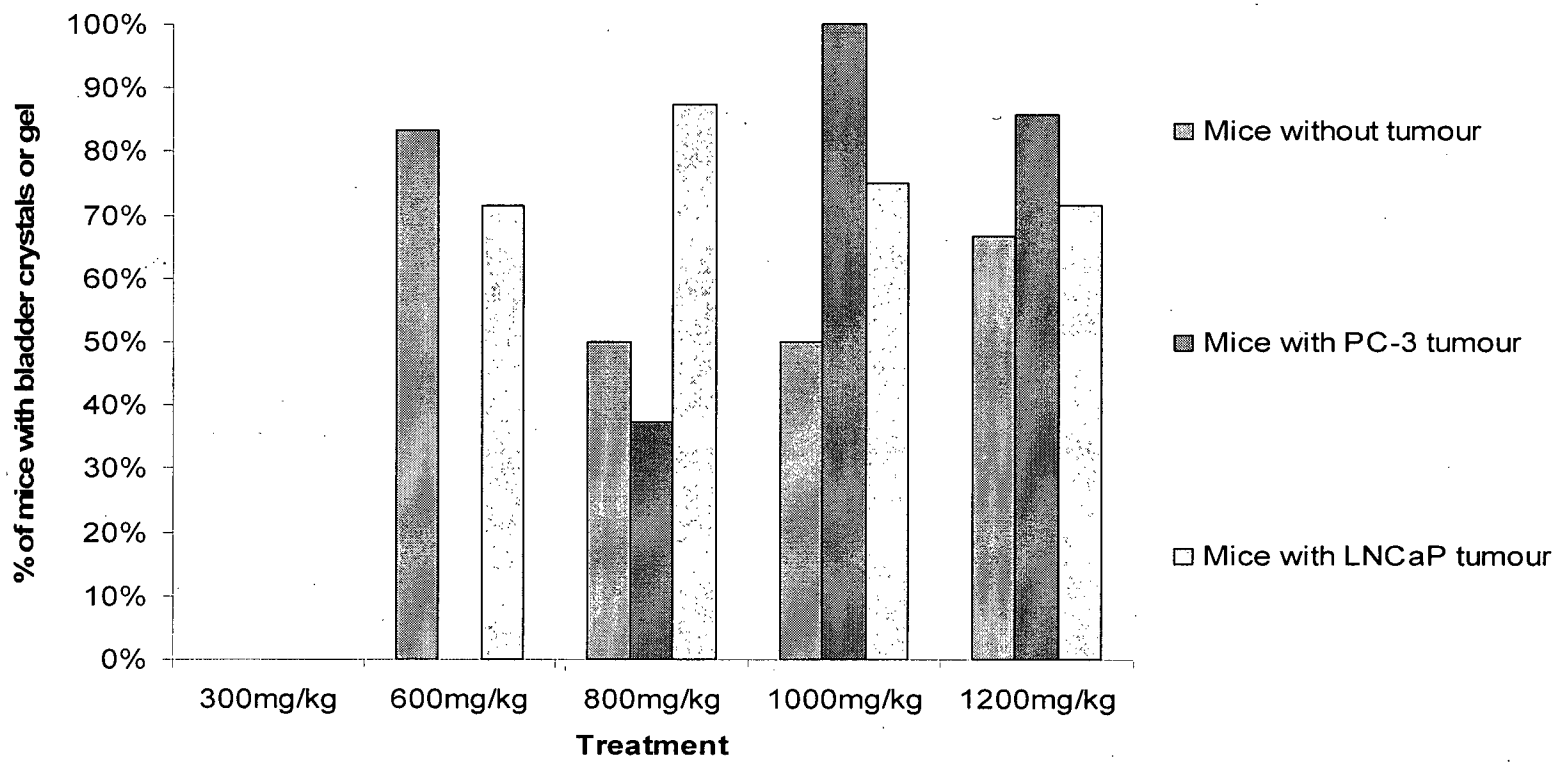

Figure 31. Percentage of nude mice with the presence of bladder crystals or viscous mucosal fluid in the PC-3, LNCaP and non-tumor studies. In the PC-3 and non-tumor studies, these crystals were removed from the animals on day 30 during tissue collection. However, in the LNCaP study these crystals were observed as early as day 15 in animals that were euthanized (1000mg/kg and 1200mg/kg treatment groups). Results are represented as percentage of mice per treatment group with the presence of bladder crystals or pus. Bladder crystals or pus may have been present in the 600mg/kg group from the PC-3 study, but unfortunately were over-looked in these animals.

3.3 Comparison of Control Animals

Upon completion of the three studies, it was apparent that the PC-3 and LNCaP xenograft models used had different tumor growth characteristics and were contributing to different levels of toxicity in the nude mice. The PC-3 xenograft model used was contrived from a single subcutaneous inoculation of PC-3 cells while the LNCaP xenograft model used was contrived from inoculation in two subcutaneous sites with LNCaP cells. By the end of the study, each LNCaP bearing mouse either represented a single tumor, or a large tumor and significantly smaller tumor. The large tumors, which were measurable on day 1 of the LNCaP study, were the only tumors tracked on animals that had two tumors propagate; the smaller tumors normally only became measurable by the end of the study, and thus were not measured throughout the study.

Through comparison of tumor results from the control group of the PC-3 study with the control group of the LNCaP study, one can observe the different growth characteristics of each tumor type relative to the other. Figure 32 illustrates the difference in average tumor volume between the PC-3 and LNCaP control groups. Although, there is no significant difference in average tumor volume between the PC-3 and LNCaP tumors when compared over a 29 day period, statistically the average tumor volume of the PC-3 group begins to depart from that of the LNCaP group from day 19 as indicated by a decreasing p-value (Figure 32). Figure 33 illustrates the difference in % average initial tumor volume between the PC-3 and LNCaP control groups. The LNCaP group shows a significant reduction in % average initial tumor volume when compared to the PC-3 group by day 29 (P=0.011) (Figure 33).

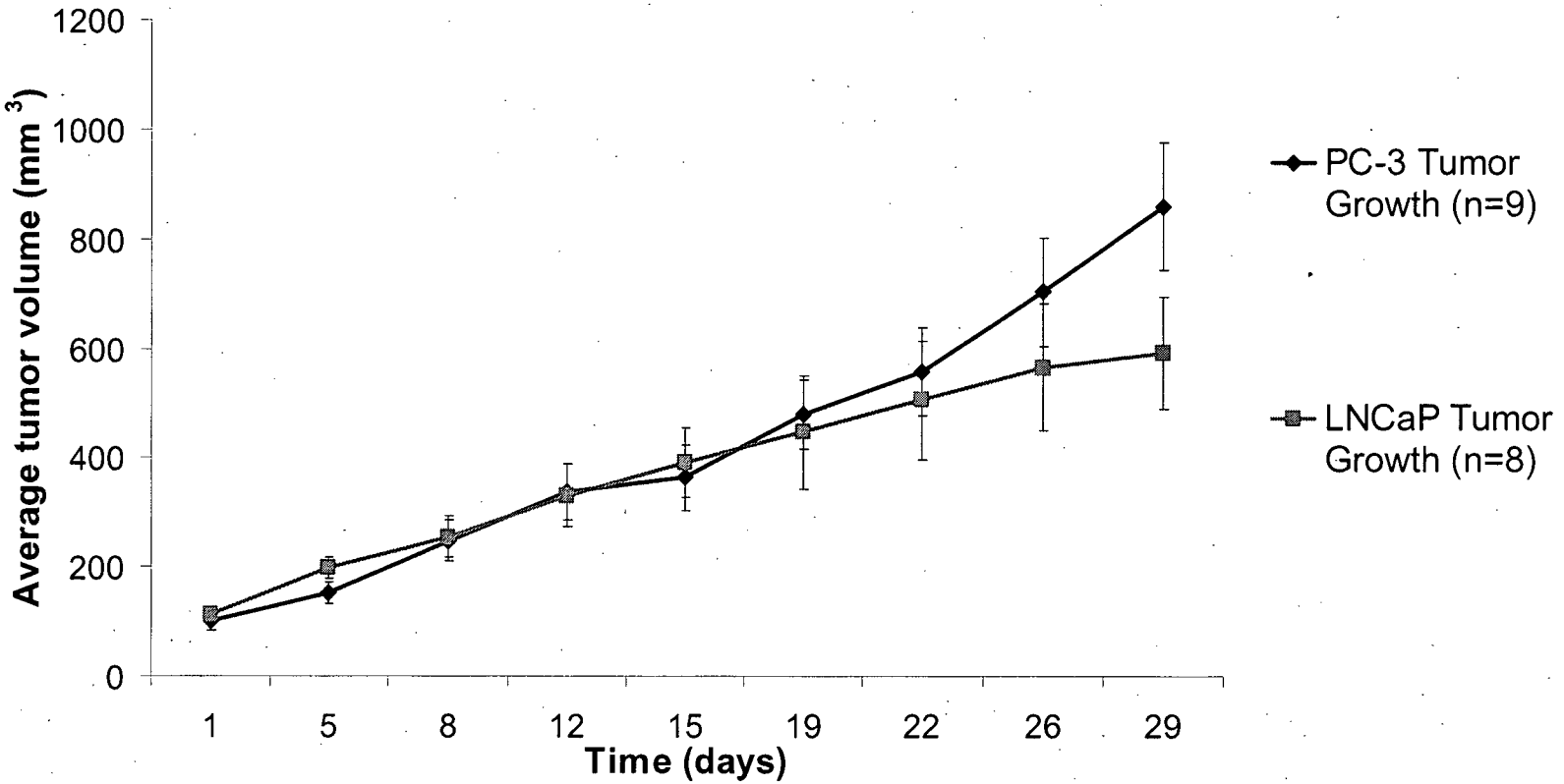

Figure 32. Average tumor volume over time of nude mice representing a PC-3 or LNCaP xenograft. Results are represented as mean value ± standard error of the mean. There was no statistical difference between the two groups (P>0.05).

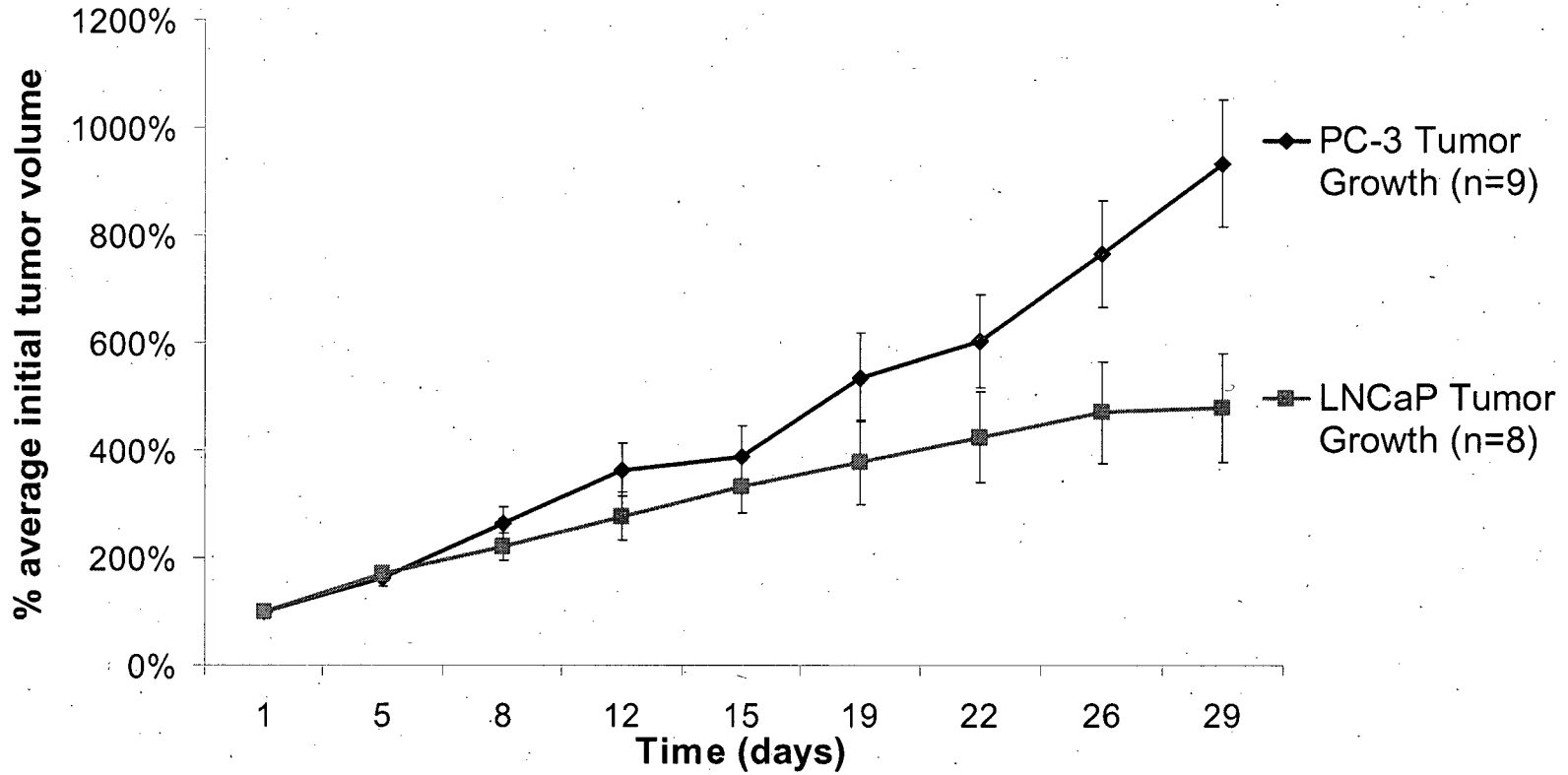

Figure 33. Percent average initial tumor volume over time of nude mice representing a PC-3 or LNCaP xenograft. Results are represented as mean value ± standard error of the mean. Statistical analysis using a Students T-Test indicates a significant difference between the two groups by the end of the study (P=0.011).

Comparison of the control groups from all three studies provided insight into the systemic burden elicited by each of the specific tumor models relative to the non-tumor bearing mice. Although there was no difference observed in food and water consumption between the three control groups (Figures 34, 35), there was a significant difference in % average initial body mass between the LNCaP animals and the animals from the other two studies (Figure 36). A dramatic loss of body mass was observed in the LNCaP animals beginning on day 3, which is not observed in the other two control groups ($P<0.05$). This decrease in body mass appears to be inversely proportional to the increase of the LNCaP tumors in these animals (Figures 32, 36). This same trend was not observed in the PC-3 bearing animals (Figures 32, 36).

Comparison of the serum from the control animals from the three studies provided some interesting insights on cellular and tissue damage possibly linked to the different tumor models. Serum from the LNCaP animals had significantly elevated AST levels ($P<0.001$), but showed no differences in ALT and creatinine levels when compared the serum from the other two control groups (Figure 37, 38).

The histopathological results from the control animals of three studies provide a trend in terms of intestinal abnormalities. The PC-3 animals have a consistently higher prevalence of atrophy to their intestinal mucosal epithelium and villi, as well as a higher prevalence of intestinal submucosal infiltrate when compared to the other two control groups (Figures 39, 40, 41). In terms of cardiac abnormalities, the PC-3 bearing animals had slightly lower prevalence of the fibrin clots compared to the other two control groups (Figure 42).

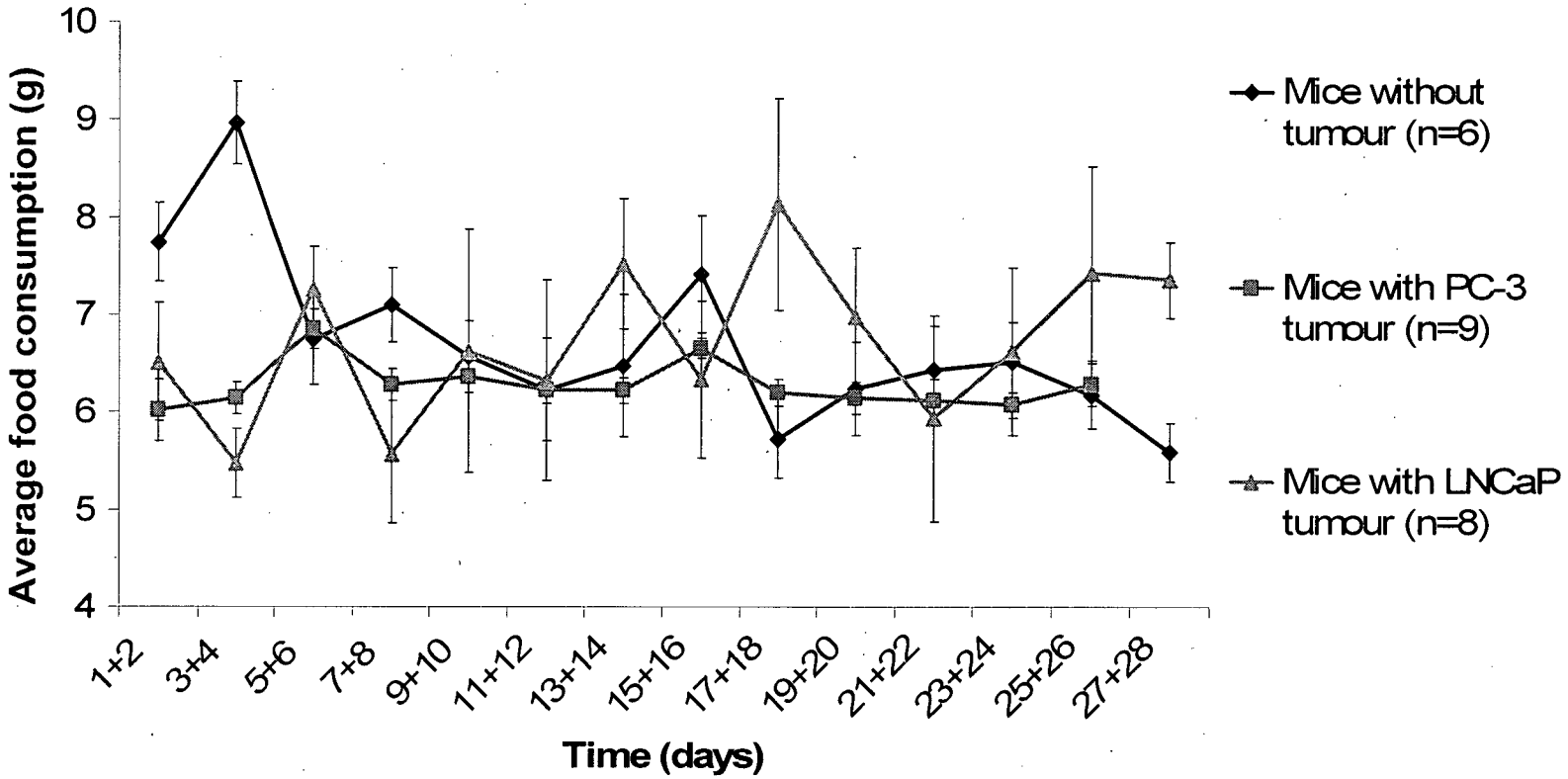

Figure 34. Average food consumption over time of nude mice from the control groups of the three CsCl dose titration studies. Results are represented as mean value ± standard error of the mean. There was no statistical difference between any of the groups ($P>0.05$).

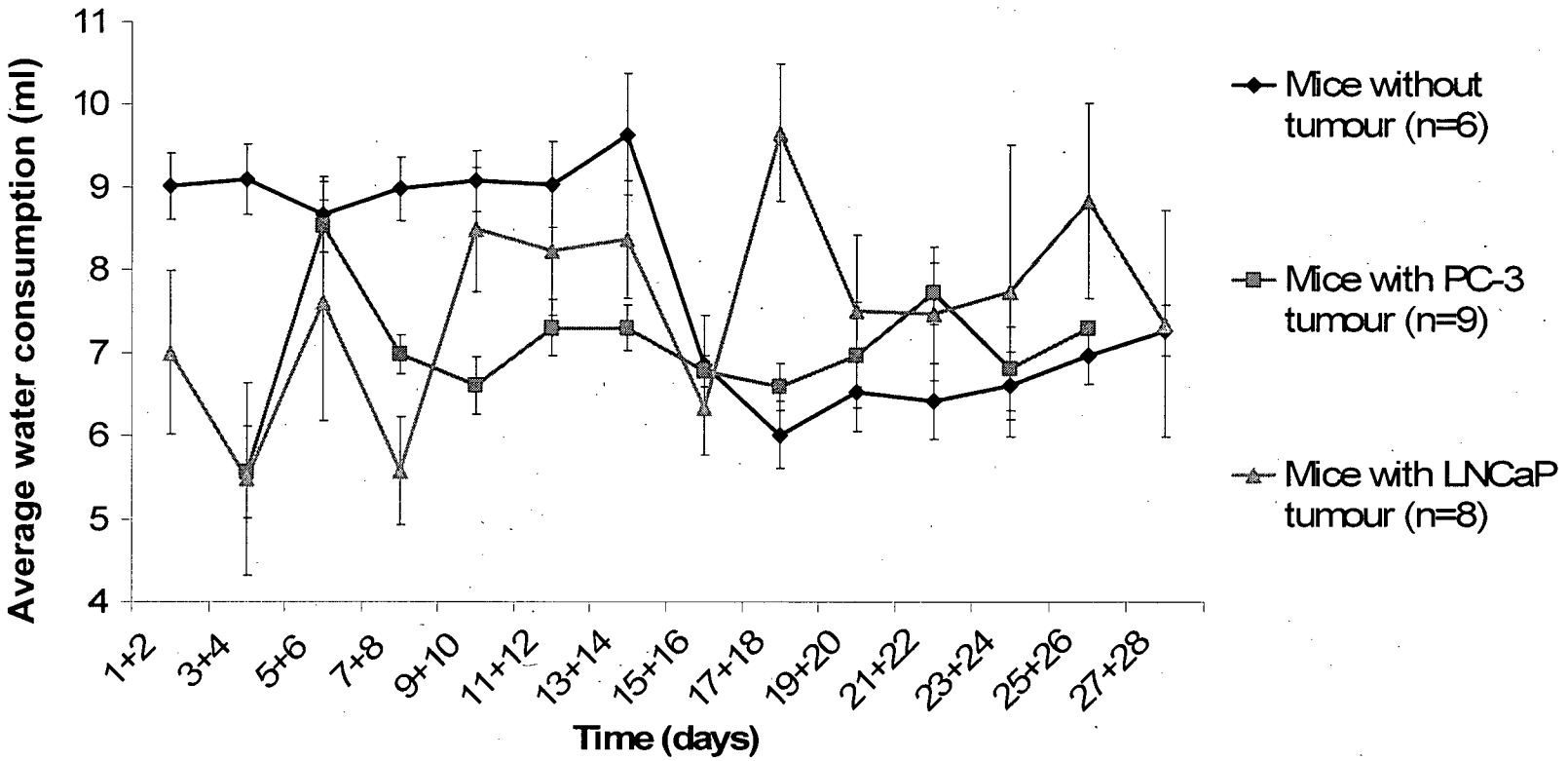

Figure 35. Average water consumption over time of nude mice from the control groups of the three CsCl dose titration studies. Results are represented as mean value ± standard error of the mean. There was no statistical difference between any of the groups ($P>0.05$).

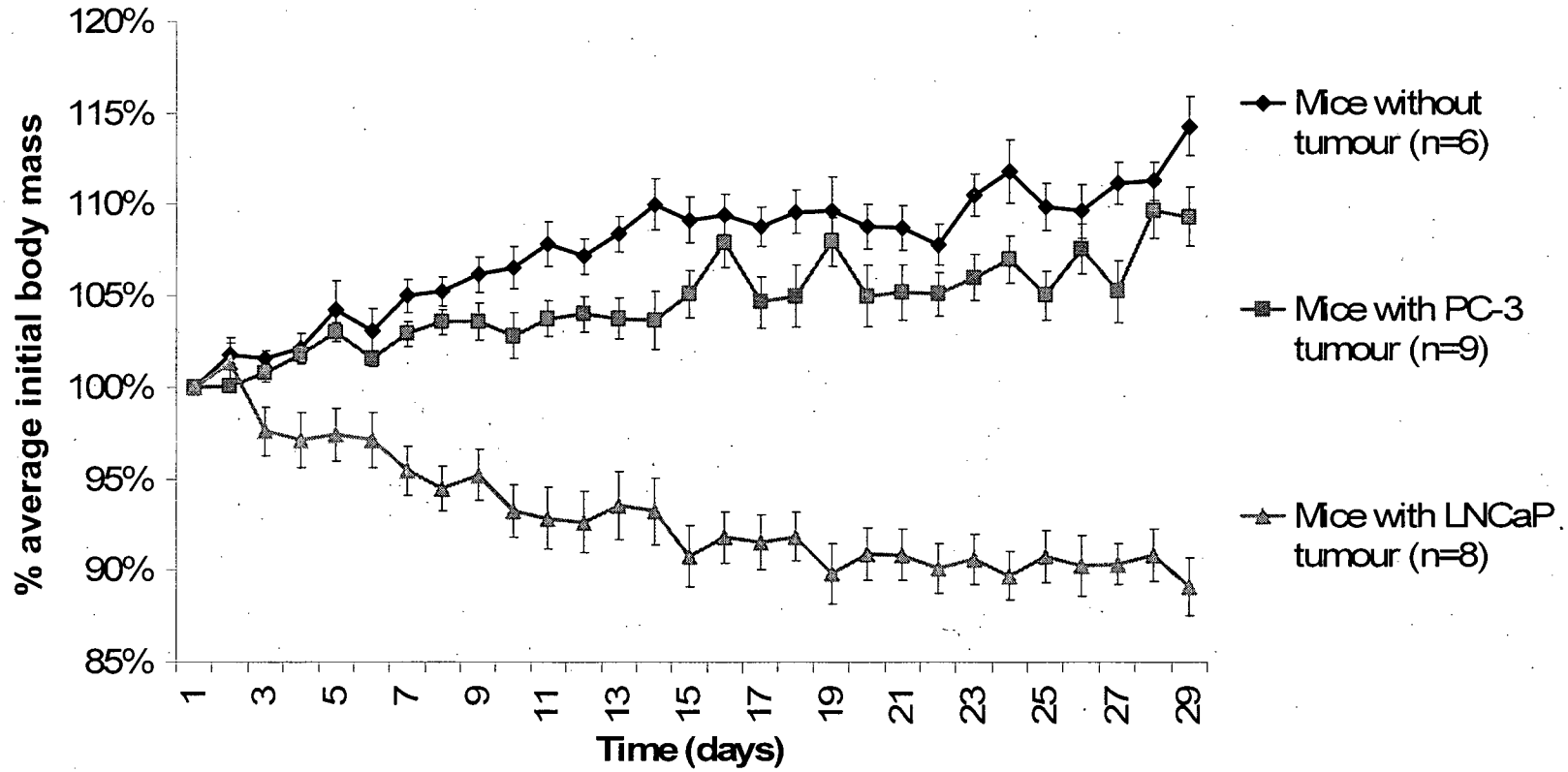

Figure 36. Percent average initial body mass over time of nude mice from the control groups of the three CsCl dose titration studies. Results are represented as mean value ± standard error of the mean. Statistical analysis using one way ANOVA indicates a significant difference between the treatment groups beginning on day 3 and extending to the end of the study ($P<0.05$). Pair-wise multiple comparison via Tukey test indicates a difference between the LNCaP control group and the other two control groups from day 3 until the end of the study ($P<0.05$).

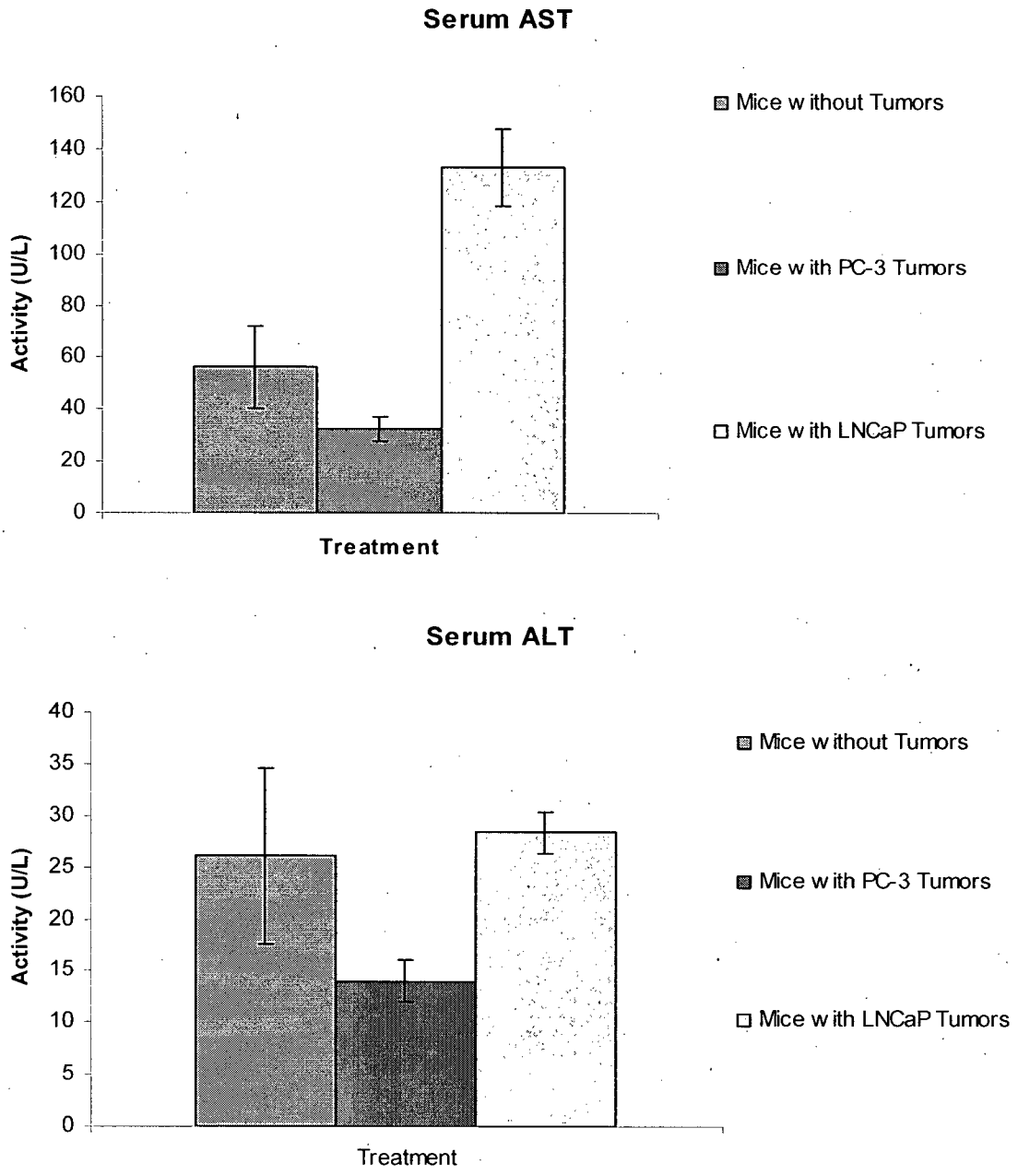

Figure 37. Serum AST and ALT levels of nude mice from the control groups of the three CsCl dose titration studies. Results are represented as mean value ± standard error of the mean. Statistical analysis using one way ANOVA indicates a significant difference in AST between the treatment groups ($P<0.05$). Pair-wise multiple comparisons via Tukey test indicates a difference in AST levels between the LNCaP group and the other two groups ($P<0.001$). There is no statistical difference in ALT levels between any of the treatment groups ($P = 0.068$).

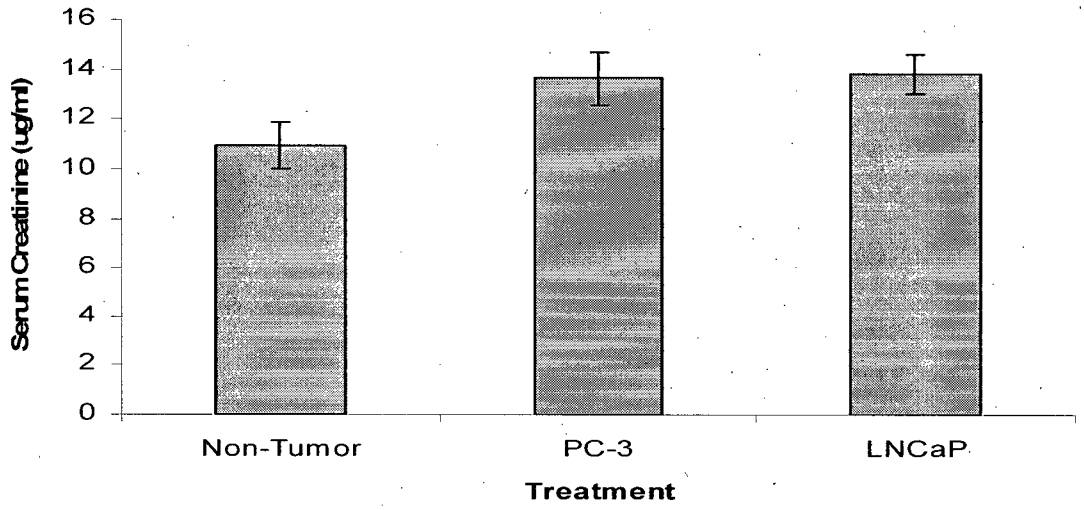

Figure 38. Serum creatinine levels of nude mice from the control groups of the three CsCl dose titration studies. Results are represented as mean value ± standard error of the mean. Statistical analysis using one way ANOVA indicates no statistical difference between any of the treatment groups (P=0.107).

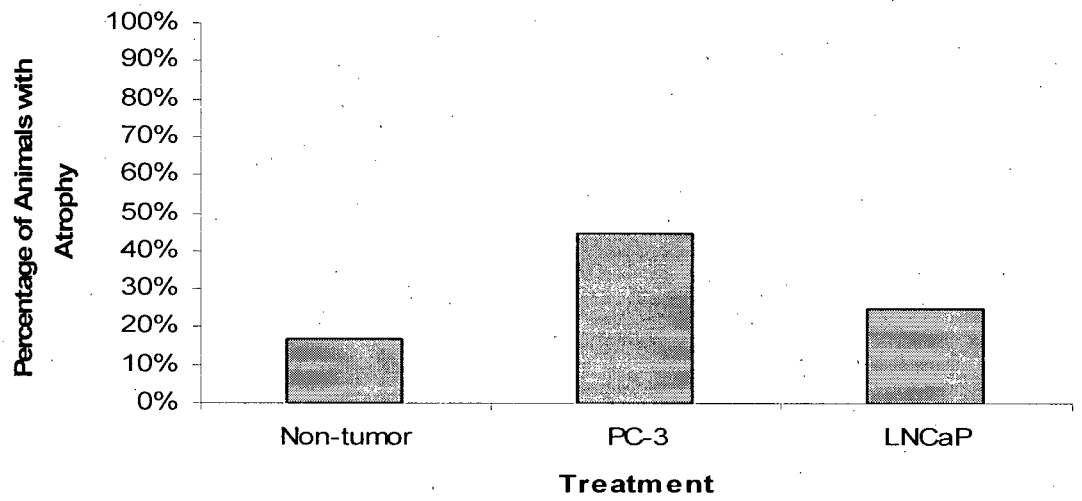

Figure 39. Presence of atrophy of the intestinal mucosal epithelium in nude mice from the control groups of the three CsCl dose titration studies. Results are represented as percentage of mice per treatment group with the presence of atrophy of the intestinal mucosal epithelium

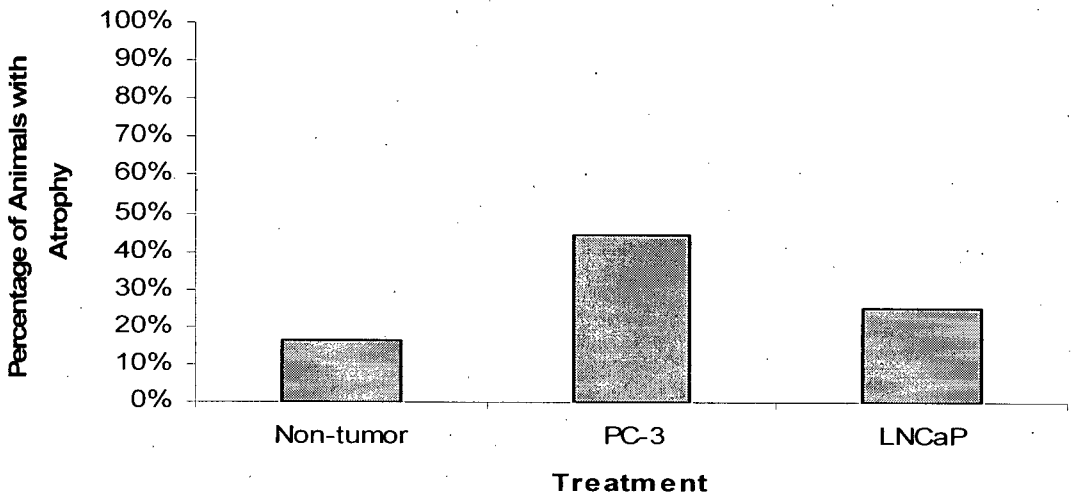

Figure 40. Presence of atrophy of the intestinal villi in nude mice from the control groups of the three CsCl dose titration studies. Results are represented as percentage of mice per treatment group with the presence of atrophy of the intestinal villi

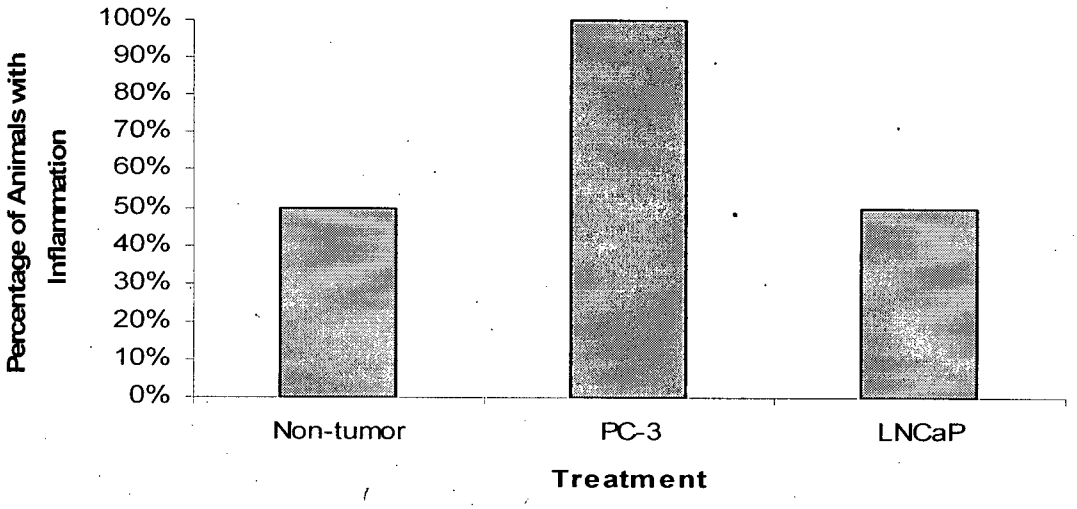

Figure 41. Presence of intestinal submucosal infiltrate in nude mice from the control groups of the three CsCl dose titration studies. Results are represented as percentage of mice per treatment group with the presence of intestinal submucosal infiltrate

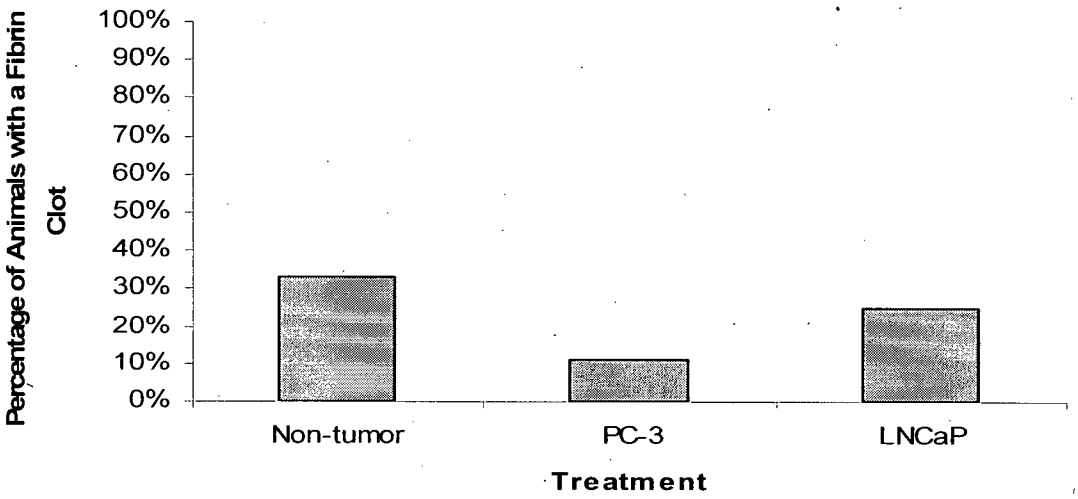

Figure 42. Presence of cardiac fibrin clots in nude mice from the control groups of the three CsCl dose titration studies. Results are represented as percentage of mice per treatment group with the presence of fibrin clots.

Section 4

Discussion

4.1 Tumor growth and toxicity in the PC-3 and LNCaP human prostate tumor xenograft models, after administration of escalating doses of CsCl.

In the present study, CsCl was able to significantly slow the growth of the PC-3 tumor model when administered at 800mg/kg to 1200mg/kg. This same therapeutic effect was not observed in the LNCaP model. However, it should be noted that the animals in the LNCaP study, which received the highest dosages (800mg/kg-1200mg/kg) of CsCl were euthanized halfway through the study, and thus, did not receive the same number of CsCl treatments as the PC-3 bearing animals.

A speculative mechanism for CsCl's therapeutic effect may be similar to its mechanism for disrupting cardiac function. In the heart, CsCl has been shown to block a number of potassium channels including Kir2.1, Kir3.1/Kir3.4 and channels involved in transient outward potassium current (111-117). CsCl has also been shown to slow the rate of inactivation of the HERG potassium channel, which is involved in the onset of long QT syndrome (111, 118). Each of the described channels play a role in repolarizing cardiac cells back to their resting potential during an action potential (116, 118, 119). Thus, the effects of CsCl on these channels are likely linked to the propagation of cardiac arrhythmias which have been observed in animal models and in some humans receiving the CsCl treatment. Like cardiac cells, some of these inward rectifying potassium channels have been described in cancer cells, where they maintain the resting potential of these cells at depolarized levels to ensure unlimited tumor growth (120, 121). Although, these channels have not yet been described in prostate cancer cells, their existence could provide a mechanism for the observed effects of CsCl. If PC-3 cells express higher levels of these channels than LNCaP cells, one could hypothesize their presence as a possible

rationale for CsCl's therapeutic effects in reducing the PC-3 tumor growth while not hindering the growth of the LNCaP tumor.

There appeared to be a number of acute toxicological effects of CsCl in the athymic nude mouse model, specifically, increased water consumption, the presence of bladder crystals and viscous mucosal fluid, and a decrease in body mass. Animals receiving the three highest dosages of CsCl in both PC-3 and non-tumor study demonstrated a significant increase in water consumption. These results were not observed in the LNCaP study, perhaps due to the early removal of the animals of interest. It appears that CsCl could be dehydrating the animals, possibly through dieresis. However, this claim cannot be confirmed as urination was not measured.

The presence of bladder crystals or viscous mucosal fluid in animals from all three studies was an unexpected finding. The formation of these crystals appears to be directly dependent on the concentration of CsCl administered; crystals were only observed in animals that were administered 600mg/kg to 1200mg/kg CsCl. However, the number of animals representing these crystals did not increase with administration of increased CsCl concentration. Although it is not known when these crystals first began to form in the mice, their presence was observed as early as day 15 in the euthanized animals of the LNCaP study. Some of these crystals were occupying up to 60-80% of the volume within the bladders of these animals.

Unfortunately, these bladder crystals were overlooked in the 600mg/kg dosed animals of the PC-3 study. As the PC-3 study was the first study completed out of the three animal studies and the 600mg/kg group was the first group euthanized within this study,

we did not recognize the presence of bladder inflammation during the organ harvesting of these animals.

It will be of interest to determine the composition of these crystals to help rationalize the role of CsCl in their formation. Infrared spectroscopy has been performed on the bladder crystals, however, the obtained spectrums are difficult to interpret as they do not match up with known bladder/kidney crystal spectrums. Some of the crystals have been sent to a collaborating researcher in the United States for further analysis in regards to their composition. In hindsight, it may have been beneficial to harvest bladder tissue from the affected animals for additional histopathology analysis.

A significant decrease in body mass was observed in animals receiving the higher concentrations of CsCl in both the PC-3 and LNCaP studies, (Figures 7, 11). However, non-tumor bearing mice appeared to tolerate these concentrated doses. Although there was a dose dependent trend in loss of body mass of these animals, no groups were statistically different from the control by the end of the study (Figure 15). This result indicates that the significant decreases in mass of the nude mouse model, as observed in the PC-3 and LNCaP studies, is likely to be due to the additive systemic burden and/or toxicity of the combination of both tumor and CsCl (Figures 7, 11).

4.2 Investigation of organ and tissue specific toxicity from CsCl (histopathology and serum marker tests) in human prostate tumor xenograft bearing nude mice

Histopathological analysis identified abnormalities in the hearts and small intestines of animals in the three studies. The abnormalities observed in the hearts manifested as fibrin clots. The prevalence of animals with fibrin clots increased in a dose dependent fashion

in both the PC-3 and LNCaP studies. However, in the non-tumor bearing study, there was no difference in the prevalence of animals with fibrin clots between the controls and the treated animals; 33% of the animals in each group displayed these clots. Based on this observation, it is difficult to determine if these fibrin clots were caused by CsCl or formed post-mortem from cardiac punctures, since they were so prevalent in the control group of the non-tumor bearing study. However, it is difficult to ignore that the PC-3 and LNCaP bearing animals treated with 800 and 1200mg/kg CsCl, had a consistently higher prevalence of clots when compared to their control groups, respectively, and with the control of the non-tumor bearing study. From this observation, it appears that fibrin clot formation shows some dependence on both the presence of a tumor and the dose of CsCl administered. Interestingly, the cardiac abnormalities in the human clinical case studies, were caused by CsCl doses that were similar to the 800 and 1200mg/kg doses (if human to mouse body surface area dose conversion is implemented), which resulted in the highest prevalence of animals with fibrin clots in the PC-3 and LNCaP studies (15-18, 20, 22, 23).

Abnormalities observed in the small intestines of animals from the three studies manifested as atrophy of the mucosal epithelium and villi as well as inflammatory infiltrate of the submucosa. There were no consistent trends in the incidence of intestinal abnormalities within the three animal studies. Only in the LNCaP study did the incidence of animals with these abnormalities increase in a dose response fashion with increased CsCl administration. A large number of animals in all three studies had inflammatory infiltrate of the intestinal submucosa, which was not conserved to any one treatment group within the studies.

There were no differences observed in serum AST and ALT levels between any of the treatment groups as compared with the control group in the three studies. These results indicate that CsCl treatment at the concentrations administered, did not cause considerable structural damage to the heart, liver, skeletal muscle, kidney and erythrocytes.

The HPLC assay developed to assess serum creatinine levels was sufficiently optimized before running the samples, based on the peak separation, the standard curve, LOD, LOQ and %CV achieved. The addition of an internal standard within this assay may have increased its accuracy; however, we experienced difficulty in identifying a suitable internal standard. The results show that serum creatinine levels were not significantly different between the treatment groups and the control within each of the three studies. Such results indicate that the CsCl treatment at the concentrations administered did not result in a reduction in glomeruli filtration in the animals.

4.3 Comparison of Control Animals

There is a distinctive differential impact of the two tumor types on body mass. The results suggest that there are clear differences in the system burden manifested in nude mice bearing PC-3 and LNCaP prostate cancer tumors. Although tumor growth was less rapid in LNCaP bearing animals as compared to animals bearing PC-3 tumors, LNCaP bearing animals were visibly thinner and weaker. In addition, a distinct decrease in body mass over time in LNCaP bearing animals was observed, which appears to be inversely related to tumor growth. This phenomenon was not observed in PC-3 bearing animals as their body mass increased over time similar to control animals regardless of increase in

tumor volume and greater levels of intestinal abnormalities. Interestingly, there was no difference observed in food consumption in LNCaP bearing mice compared to control animals, despite their loss of body mass, however, it is possible that the methods used in this study to measure this parameter were not sensitive enough to detect these changes. LNCaP bearing mice had significantly increased serum AST levels but showed not differences in serum ALT and creatinine levels when compared to PC-3 and control mice. These results indicate potential cardiac, skeletal muscle or erythrocyte damage in animals which could potentially be linked to the observed toxicity within these animals.

The loss of body mass attributed to the LNCaP tumor has been described previously in other tumor bearing animals with cancer linked cachexia. Cachexia affects more than half of all cancer patients and is the cause of 20% of cancer-related deaths (122). It is characterized as complex metabolic syndrome which incurs anorexic effects followed by a progressive depletion of adipose and muscle mass which ultimately increases morbidity and mortality amongst cancer patients (122-124). Weight loss is the typical marker for cachexia as it is easy to measure and clinically relevant in terms of toxicity.

To fully characterize the LNCaP xenograft model as a model for cachexia, a more comprehensive *in vivo* study must be completed, involving the measurement of adipose and muscle mass post-mortem, immunohistochemistry analysis on adipose and muscle tissue for markers of cachexia, and serum analysis for markers of cachexia. Investigation of the cytokines, interleukin-6 (IL-6), interleukin-1β (IL-1β) and tumor necrosis factor α (TNF-α), would be of particular interest in the LNCaP bearing mice. These specific cytokines have been associated with cachexia in animal models (125, 126) and have also been shown to regulate growth and are expressed by prostate cancer cells. IL-6 has also

been shown to be positively correlated with neuroendocrine differentiation and androgen independent prostate cancer progression (127). Alternatively, IL-1β and TNF-α have been shown to reduce proliferation of the LNCaP cells *in vitro* (128, 129).

4.4 Conclusions

This study is the first to provide a detailed investigation into the therapeutic and acute toxicological effects of CsCl in human prostate tumor xenograft models. Although CsCl appears to have some therapeutic benefit in treating prostate cancer, a number of toxicological effects were also observed in conjunction with its administration, including loss of body mass, increase of water consumption, fibrin clot formation and bladder crystal formation. Interestingly, one of most life threatening of these toxicological effects from CsCl, specifically, a loss in body mass, was not observed in disease free animals receiving the CsCl treatment. This observation indicates some interplay between CsCl administration and the presence of a tumor compounding to culminate this effect.

Comparison of control animals from the three studies provided some provoking findings in terms of tumor specific toxicity. The results provoke further study of the LNCaP tumor model to rationalize its possible role in the induction of cachexia-like symptoms and serve as a potential *in vivo* model for this significant and life threatening cancer-related health problem.

4.5 Significance and Limitations of the Results

As there have not been any epidemiological studies completed in regards to the use of CsCl by cancer patients, like many other alternative cancer treatments, it is difficult to

provide an estimate on the number of users of this therapy. However, we conducted this research as warranted by the unregulated availability of these products through the internet and the potential harm they may be causing due to their potential toxicity. In addition, it is important to assess the potential therapeutic effects of CsCl and weigh the risk to benefit ratio for its use as an anti-cancer product in the hope of increasing the limited arsenal of chemotherapeutic compounds against this devastating disease.

The results from this preclinical study provide some insight on the therapeutic and toxicological effects of concentrated, repeated doses of orally administered CsCl in human prostate xenograft models. CsCl was shown to reduce the growth rate of the PC-3 human prostate cancer tumor, but was also shown to elicit certain levels of toxicity in the nude mouse model at the same dosages. This information is important for individuals considering the use of this alternative therapy. An additional, serendipitous, finding of this study was the differences in tumor induced toxicity by the PC-3 and LNCaP prostate cancer xenografts. These effects have not been described previously in the scientific literature and should be further studied.

The limitations of results of this study are a product of the models used and the experimental design. The PC-3 and LNCaP cell lines used in these experiments were both isolated from metastasized sites and not from primary tumors. In other words, both of these cell lines represent rapidly dividing, late stage prostate cancer, and thus, do not provide information on the therapeutic effects of chemotherapeutic agents on early stage prostate cancer. Another limitation of using these cell lines, and of cell lines in general, is the formation of subpopulations of cells through selection processes as a consequence of cell culturing techniques. Experimentation, *in vitro* and *in vivo*, on different

subpopulations of the same cell line using the same protocol can render different results. As both the PC-3 and LNCaP cells used in these experiments had been passaged at least 25 times prior to inoculation, it is possible that the cells injected into the athymic nude mice in this study were subpopulations of each respective cell line.

The athymic nude mouse prostate cancer xenograft model is routinely used to analyze the therapeutic and toxicological effects of anticancer agents. However, as this an *in vivo* model for prostate cancer, the drug effects observed do not always match the effects of the same drugs in human clinical trials. In some instances, drugs that have an optimal therapeutic effect in the athymic nude mouse prostate cancer xenograft model, show only minimal effects in humans.

An additional limitation of this *in vivo* model is the use of the immunocompromised animals. The immunocompromised status of these animals allows them to inoculated with human prostate cancer cells without rejection, but prevents the researcher from analyzing the effects of their therapy on the immune system. Once prostate tumors propagate within these animals, the studies are usually limited to one month due to the aggressive growth rate of most prostate cancer cell lines. This is a further limitation of this model, as it prevents long term studies.

There were steps in the experimental design that in hindsight, may limit the results of this study. Firstly, the procedure to measure food and water consumption (weighing the food pellets and water bottles on a top loading scale) may have overestimated these two parameters and may have lacked the sensitivity to detect small differences between groups. Partly uneaten food pellets may have been missed and not weighed, and water may have been spilled either by the animals or the experimenter. Ultimately, the use of

metabolic cages would have increased the accuracy of the measurements and allowed the experimenter to also collect urine and feces for further toxicological analysis. However, the use of metabolic cages would have been considerably more expensive and unpractical considering the number of animals surveyed. Secondly, in each of the animal studies, bladder tissue should have been removed from controls and animals that displayed bladder crystals or viscous mucosal fluid. With the bladder tissue, histopathological analysis could help further delineate the cause of these bladder crystals and viscous mucosal fluid. Finally, the dosages of CsCl that were chosen to administer to the animals may have not covered the range of human dosages if a proper conversion is undertaken. Although the doses of CsCl used in the human clinical case studies are similar to some of the doses used in our study (if human to mouse body surface area dose conversion is implemented), other factors must be considered, such as half-life which is quite different between humans (~65.5-96 days) and mice (~3-6 days) (90-93, 96, 97). For this reason, one has to refrain from making direct inferences from the results in terms of the dosages administered, to the potential physiological complications in humans at similar dosages.

4.6 Future Studies

Although oral administration of CsCl in solution appeared to elicit some toxicity, it did elicit some therapeutic effect in the PC-3 model. Future studies could investigate the reduction of CsCl's toxicity while maintaining or enhancing its therapeutic effect. The first series of experiments would need to investigate CsCl's distribution within the animal; what tissues is it accumulating in and how does this information relate to the observed therapeutic and toxicological effects observed in this study and in other

scientific literature. If CsCl is accumulating in the tumors, experiments could investigate the presence of potassium channels that regulate cellular resting potential (Kir2.1, Kir3.1/3.4, HERG) as a possible mechanism for CsCl's therapeutic effect, in the PC-3 and LNCaP prostate cancer cell lines. In addition, tumor tissue microarrays could be constructed and subsequently probed for specific growth and apoptotic regulating proteins to determine if CsCl is affecting specific biochemical pathways. Other tissues, in which CsCl is determined to accumulate in, could also be used in microarray experiments to determine CsCl's toxicological effect in these tissues.

A further toxicological study would need to investigate the dose effects of CsCl on the murine cardiac system. It would be important to determine whether the dosages of CsCl that reduce tumor volume, also affect cardiac output as observed in canine experiments. In addition, this study could further analyze the effects of CsCl on the renal system to fully understand its role in the production of the observed bladder crystals.

Ultimately, if CsCl is shown to directly reduce tumor volume, while eliciting toxicity in specific organs, studies could investigate the integration of CsCl into drug carrier molecules to reduce its toxicity. If CsCl could be loaded inside a drug carrier molecule with targeted specificity, it may be possible to implement the direct release of CsCl at the site of the tumor. In this mode it is possible that CsCl could be used as a viable chemotherapeutic agent.

Finally, a comprehensive investigation into the toxicological effects of the LNCaP tumor on the nude mouse model could be conducted. Results from the current study provide some evidence that the LNCaP model may elicit cachexic-like symptoms in nude

mice. To date, none of the established human prostate cancer models have been identified and/or reportedly characterized with an associated cachexia.

4.7 Synopsis

CsCl has been used by some cancer patients as an alternative treatment to their conventional therapy, however, it has not been previously determined as to whether CsCl consumption is beneficial or deleterious. The purpose of the research conducted as part of this thesis was to assess the therapeutic and toxicological effects of oral CsCl administration in mice bearing prostate cancer tumors. Although there were some confounding factors within this study that may have compromised the accuracy of the results, the overall design of this study was very thorough and provides a detailed analysis of the effects of CsCl therapy *in vivo*. The results of this study have shown that oral CsCl may have some therapeutic effect against advanced prostate cancer, however, its administration also elicits specific toxicities, including loss of body mass, increase of water consumption, fibrin clot formation and bladder crystal formation. One should be cautious when translating the therapeutic and toxicological effects observed in the treated animals to humans as establishing CsCl dose conversion from one species to another is difficult.

We have shown that CsCl therapy may be associated with some therapeutic effect while also eliciting significant signs of toxicity. Therefore, future work could shed light as to whether this effect is real and whether the associated toxicity can be reduced while maintaining this effect.

References

1. Brewer AK. The "High pH Therapy" for cancer tests on mice and humans. Pharmacol Biochem Behav. 1984;21 Suppl 1:1-5

2. Cesium package. Essence-of-life.com Website. Available at: http://www.essense-of-life.com/info/cesium.htm. Accessibility verified on January 12, 2007.

3. CT-Cesium. Healthau.com website. Available at: http://healthau.com/shop/rt/index.html (dietary supplements). Accessibility verified on January 12, 2007.

4. New liquid ionic cesium chloride. Rainbowminerals.net website. Available at: http://www.rainbowminerals.net/Minerals/cesium.html. Accessibility verified on January 12, 2007.

5. Sartori HE. Cesium therapy in cancer patients. Pharmacol Biochem Behav. 1984;21 Suppl 1:11-3.

6. Messiha FS, El-Domeiri A, Sproat HF. Effects of lithium and cesium salts on sarcoma-I implants in the mouse. Neurobehav Toxicol 1979;1: 27-31.

7. El-Domeiri AA, Messiha FS, Hsia WC. Effect of alkali metal salts on Sarcoma I in A/J mice. J Surg Oncol. 1981;18(4):423-9.

8. Tufte MJ, Tufte FW, Brewer AK. The response of colon carcinoma in mice to cesium, zinc and vitamin A. Pharmacol Biochem Behav. 1984;21 Suppl 1:25-6.

9. Tufte FW, Tufte MJ. The effects of zinc gluconate, vitamin A and caesium salts on colon carcinoma in mice. Cytobios. 1984;39(155-156):177-82.

10. Pinsky C, Bose R. Pharmacological and toxicological investigations of cesium. Pharmacol Biochem Behav. 1984;21 Suppl 1:17-23

11. Senges JC, Sterns LD, Freigang KD, Bauer A, Becker R, Kubler W, Schoels W. Cesium chloride induced ventricular arrhythmias in dogs: three-dimensional activation patterns and their relation to the cesium dose applied. Basic Res Cardiol. 2000;95(2):152-62.

12. Jones DL, Petrie JP, Li HG. Spontaneous, electrically, and cesium chloride induced arrhythmia and afterdepolarizations in the rapidly paced dog heart. Pacing Clin Electrophysiol. 2001;24(4 Pt 1):474-85.

13. Satoh D, Zipes TP. Cesium-induced atrial tachycardia degenerating into atrial fibrillation in dogs: atrial torsades de pointes? J Cardiovasc Electrophysiol. 1998;9(9):970-5.

14. Bai R, Lu J, Pu J, Liu N, Zhou Q, Ruan Y, Niu H, Zhang C, Wang L, Kam R. Left ventricular epicardial activation increases transmural dispersion of repolarization in healthy, long QT, and dilated cardiomyopathy dogs. Pacing Clin Electrophysiol. 2005;28(10):1098-106.

15. Pinter A, Dorian P, Newman D. Cesium-induced torsades de pointes. N Engl J Med. 2002;346(5):383-4.

16. Dalal AK, Harding JD, Verdino RJ. Acquired long QT syndrome and monomorphic ventricular tachycardia after alternative treatment with cesium chloride for brain cancer. Mayo Clin Proc. 2004;79(8):1065-9.

17. Samadani U, Marcotte P. Zero efficacy with cesium chloride self-treatment for brain cancer. Mayo Clin Proc. 2004;79(12):1588.

18. Lyon AW, Mayhew WJ. Cesium toxicity: a case of self-treatment by alternate therapy gone awry. Ther Drug Monit. 2003;25(1):114-6.

19. Centeno JA, Pestaner JP, Omalu BI, Torres NL, Field F, Wagner G, Mullick FG. Blood and tissue concentration of cesium after exposure to cesium chloride: a report of two cases. Biol Trace Elem Res. 2003;94(2):97-104

20. Saliba W, Erdogan O, Niebauer M. Polymorphic ventricular tachycardia in a woman taking cesium chloride. Pacing Clin Electrophysiol. 2001;24(4 Pt 1):515-7.

21. Olshansky B, Shivkumar K. Patient--heal thyself? Electrophysiology meets alternative medicine. Pacing Clin Electrophysiol. 2001;24(4 Pt 1):403-5.

22. Vyas H, Johnson K, Houlihan R, Bauer BA, Ackerman MJ. Acquired long QT syndrome secondary to cesium chloride supplement. J Altern Complement Med. 2006;12(10):1011-4.

23. Curry TB, Gaver R, White RD. Acquired long QT syndrome and elective anesthesia in children. Paediatr Anaesth. 2006;16(4):471-8.

24. Hanahan D, Weinburg RA. The hallmarks of cancer. Cell. 2000;100(1):57-70.

25. Parkin DM, Bray F, Ferlay J, Pisani P. Global cancer statistics, 2002. CA Cancer J Clin. 2005;55(2):74-108.

26. Delongchamps NB, Singh A, Haas GP. The role of prevalence in the diagnosis of prostate cancer. Cancer Control. 2006;13(3):158-68.

27. Routh JC, Leibovich BC. Adenocarcinoma of the prostate: epidemiological trends, screening, diagnosis, and surgical management of localized disease. Mayo Clin Proc. 2005;80(7):899-907.

28. Schwartz GG. Vitamin D and the epidemiology of prostate cancer. Semin Dial. 2005;18(4):276-89.

29. Jemal A, Tiwari RC, Murray T, Ghafoor A, Samuels A, Ward E, Feuer EJ, Thun MJ; American Cancer Society. Cancer statistics, 2004. CA Cancer J Clin. 2004;54(1):8-29.

30. Edwards BK, Brown ML, Wingo PA, Howe HL, Ward E, Ries LA, Schrag D, Jamison PM, Jemal A, Wu XC, Friedman C, Harlan L, Warren J, Anderson RN, Pickle LW. Annual report to the nation on the status of cancer, 1975-2002, featuring population-based trends in cancer treatment. J Natl Cancer Inst. 2005;97:1407-1427.

31. Carter BS, Beaty TH, Steinberg GD, Childs B, Walsh PC. Mendelian inheritance of familial prostate cancer. Proc Natl Acad Sci U S A. 1992;89: 3367-3371.

32. Lichtenstein P, Holm NV, Verkasalo PK, Iliadou A, Kaprio J, Koskenvuo M, Pukkala E, Skytthe A, Hemminki K. Environmental and heritable factors in the causation of cancer—analyses of cohorts of twins from Sweden, Denmark, and Finland. N Engl J Med. 2000;343:78-85.

33. Miller DG. On the nature of susceptibility to cancer: the presidential address. Cancer. 1980;46:1307-1318.

34. Hughes C, Murphy A, Martin C, Sheils O, O'Leary J. Molecular pathology of prostate cancer. J Clin Pathol. 2005;58(7):673-84.

35. Grandori C, Mac J, Siebelt F, Ayer DE, Eisenman RN. Myc-Max heterodimers activate a DEAD box gene and interact with multiple E box-related sites in vivo. EMBO J. 1996;15(16):4344-57.

36. Bubendorf L, Kononen J, Koivisto P, Schraml P, Moch H, Gasser TC, Willi N, Mihatsch MJ, Sauter G, Kallioniemi OP. Survey of gene amplifications during prostate cancer progression by high-throughout fluorescence in situ hybridization on tissue microarrays. Cancer Res. 1999 Feb 15;59(4):803-6. Erratum in: Cancer Res 1999;59(6):1388.

37. Konishi N, Shimada K, Ishida E, Nakamura M. Molecular pathology of prostate cancer. Pathol Int. 2005;55(9):531-9.

38. Karg A, Dinc ZA, Basok O, Ucvet A. MUC4 expression and its relation to ErbB2 expression, apoptosis, proliferation, differentiation, and tumor stage in non-small cell lung cancer (NSCLC). Pathol Res Pract. 2006;202(8):577-83.

39. Isaacs JT. The biology of hormone refractory prostate cancer. Why does it develop? Urol Clin North Am. 1999;26(2):263-73.

40. McDonnell TJ, Troncoso P, Brisbay SM, Logothetis C, Chung LWK, Hsieh JT, Tu SM, Campbell ML. Expression of the protooncogene bcl-2 in the prostate and its association with emergence of androgen-independent prostate cancer. Cancer Res. 1992;52:6940-6944

41. Nupponen N, Visakorpi T. Molecular biology of progression of prostate cancer. Eur Urol. 1999;35(5-6):351-4.

42. Schulz WA, Burchardt M, Cronauer MV. Molecular biology of prostate cancer. Mol Hum Reprod. 2003;9(8):437-48.

43. Cairns P, Okami K, Halachmi S, Halachmi N, Esteller M, Herman JG, Jen J, Isaacs WB, Bova GS, Sidransky D. Frequent inactivation of PTEN/MMAC1 in primary prostate cancer. Cancer Res. 1997;57(22):4997-5000.

44. Navone NM, Troncoso P, Pisters LL, Goodrow TL, Palmer JL, Nichols WW, von Eschenbach AC, Conti CJ. p53 protein accumulation and gene mutation in the progression of human prostate carcinoma. J Natl Cancer Inst. 1993;85(20):1657-69.

45. Whang YE, Wu X, Suzuki H, Reiter RE, Tran C, Vessela RL, Said JW, Isaacs WB, Sawyers CL. Inactivation of the tumor suppressor PTEN/NMAC1 in advanced human prostate cancer through loss of expression. Proc. Natl Acad. Sci. USA 1998;95:5246-5250.

46. Santos AF, Huang H, Tindall DJ. The androgen receptor: a potential target for therapy of prostate cancer. Steroids. 2004 Feb;69(2):79-85.

47. Chatterjee B. The role of the androgen receptor in the development of prostatic hyperplasia and prostate cancer. Mol Cell Biochem. 2003;253(1-2):89-101.

48. Heinlein CA, Chang C. Androgen receptor in prostate cancer. Endocr Rev. 2004;25(2):276-308.

49. Sharifi N, Farrar WL. Androgen receptor as a therapeutic target for androgen independent prostate cancer. Am J Ther. 2006;13(2):166-70.

50. Javidan J, Deitch AD, Shi XB, de Vere White RW. The androgen receptor and mechanisms for androgen independence in prostate cancer. Cancer Invest. 2005;23(6):520-8.

51. Pienta KJ, Smith DC. Advances in prostate cancer chemotherapy: a new era begins. CA Cancer J Clin. 2005;55(5):300-18

52. Feldman BJ, Feldman D. The development of androgen-independent prostate cancer. Nat Rev Cancer 2001;1:34–45.

53. Nelson WG, De Marzo AM, Isaacs WB. Prostate cancer. N Engl J Med 2003;349:366–381.

54. Debes JD, Tindall DJ. Mechanisms of androgen-refractory prostate cancer. N Engl J Med 2004;351:1488–1490.

55. Kirby RS, Christmas TJ, Brawer MK. Prostate Cancer, Second Edition. Mosby Publishers, London, England, 2001

56. Hoedemaeker RF, Vis AN, Van Der Kwast TH. Staging prostate cancer. Microsc Res Tech. 2000;51(5):423-9.

57. Wallace M, Powell LL. Prostate cancer : nursing assessment, management, and care. Springer Publishers, New York, 2002

58. Schwartz K, Deschere B, Xu J. Screening for prostate cancer: who and how often? J Fam Pract. 2005;54(7):586-96.

59. Staging of prostate cancer image. US. National Cancer Institute PDQ database website. Available at: http://www.meb.unibonn.de/cancer.gov/Media/CDR0000442273.jpg. Accessibility verified on January 12, 2007.

60. Grignon DJ, Sakr WA. Pathologic staging of prostate carcinoma. What are the issues? Cancer. 1996;78(2):337-40.

61. Pisansky TM. External beam radiotherapy as curative treatment of prostate cancer. Mayo Clin Proc. 2005;80(7):883-98.

62. Bott SR, Birtle AJ, Taylor CJ, Kirby RS. Prostate cancer management: (1) an update on localised disease. Postgrad Med J. 2003;79(936):575-80.

63. Mouraviev V, Polascik TJ. Update on cryotherapy for prostate cancer in 2006. Curr Opin Urol. 2006;16(3):152-6.

64. So A, Gleave M, Hurtado-Col A, Nelson C. Mechanisms of the development of androgen independence in prostate cancer. World J Urol. 2005;23(1):1-9

65. Sonpavde G, Hutson TE, Berry WR. Hormone refractory prostate cancer: Management and advances. Cancer Treat Rev. 2006;32(2):90-100.

66. Petrylak DP. Future directions in the treatment of androgen-independent prostate cancer. Urology. 2005;65(6 Suppl):8-12.

67. Eng J, Ramsum D, Verhoef M, Guns E, Davison J, Gallagher R. A population-based survey of complementary and alternative medicine use in men recently diagnosed with prostate cancer. Integr Cancer Ther. 2003;2(3):212-6.

68. Satori HE. Practicing and Teaching Alternative Health. Available at: http://www.royalrife.com/sartori5.pdf. Accessibility verified on January 12, 2007.

69. Messiha FS. Biochemical aspects of cesium administration in tumor-bearing mice. Pharmacol Biochem Behav. 1984;21 Suppl 1:27-30

70. Messiha FS, Stocco DM. Effect of cesium and potassium salts on survival of rats bearing Novikoff hepatoma. Pharmacol Biochem Behav. 1984;21 Suppl 1:31-4.

71. Messiha FS. Effect of cesium and ethanol on tumor bearing rats. Pharmacol Biochem Behav. 1984;21 Suppl 1:35-40.

72. Guns ES, Xie X, Fedoruk M, Madera C, Cowell S, Mayer LD, Skov K, Gleave ME, Kozlowski P. pH modulation using CsCl enhances therapeutic effects of vitamin D in LNCaP tumor bearing mice. Prostate. 2005;64(3):316-22.

73. Neulieb R. Effect of oral intake of cesium chloride: a single case report. Pharmacol Biochem Behav. 1984;21 Suppl 1:15-6.

74. Pinsky C, Bose R, Taylor JR, McKee J SC, Lapointe C, Birchall J. Cesium in mammals: Acute toxicity, organ changes and tissue accumulation. J Environ Sci Health Part A Environ Sci Eng; 1981;16(5):549-567.

75. Wright AW, Graham CF. The Effect of Cesium Chloride on Transplanted Tumors of Mice. Am J Path 1933;9:789.

76. Khosid GM. Novye Dannye po Torsikologii Redkikh Metallovi ikh Soedinenii (A. I. Israel' so n, ed.) 1967 Izdatel'stvo Meditsina, Moscow

77. Sigma-Aldrich. Cesium Chloride Grade I Material Safety Data Sheet Version 1.6. Date Printed: August 12, 2006.

78. Messiha FS. Effect of separate and combined maternal ingestion of alkali metals on the developing mouse. Neurosci Biobehav Rev. 1988;12(3-4):205-8.

79. Messiha FS. A toxicology evaluation of postnatal maternal exposure to cesium. Physiol Behav. 1989;46(1):85-8.

80. Messiha FS. Developmental toxicity of cesium in the mouse. Gen Pharmacol. 1994;25(3):395-400.

81. Messiha FS. Maternal cesium chloride ingestion and the newborn. Neurosci Biobehav Rev. 1988;12(3-4):209-13.

82. Messiha FS Maternally-mediated neonatal lithium-cesium interaction in the mouse. Physiol Behav. 1989;46(1):89-95.

83. Ghosh A, Sharma A, Talukder G. Clastogenic effects of cesium chloride on mouse bone marrow cells in vivo. Mutat Res. 1990;244(4):295-8.

84. Ghosh A, Sharma A, Talukder G. Cytogenetic damage induced in vivo to mice by single exposure to cesium chloride. Environ Mol Mutagen. 1991;18(2):87-91.

85. Ghosh A, Sharma A, Talukder G. Relative protection given by extract of Phyllanthus emblica fruit and an equivalent amount of vitamin C against a known clastogen--caesium chloride. Food Chem Toxicol. 1992;30(10):865-9.

86. Ghosh A, Sen S, Sharma A, Talukder G. Inhibition of clastogenic effects of cesium chloride in mice in vivo by chlorophyllin. Toxicol Lett. 1991;57(1):11-7.

87. Ghosh A, Ghosh AK, Sharma A, Talukder G. Modification of cesium toxicity by calcium in mammalian system. Biol Trace Elem Res. 1991;31(2):139-45.

88. Santos-Mello R, Deimling LI, Almeida A. Induction of micronuclei in mouse polychromatic erythrocytes by the administration of non-radioactive CsCl by the oral and intraperitoneal route. Mutat Res. 2001;497(1-2):147-51.

89. Santos-Mello R, Schmidt T, Neuhauss E, Almeida A. Induction of micronuclei by CsCl in vivo and in vitro. Mutat Res. 1999;446(2):239-44.

90. Leggett RW, Williams LR, Melo DR, Lipsztein JL. A physiologically based biokinetic model for cesium in the human body. Sci Total Environ. 2003;317(1-3):235-55.

91. Ruhm W, Konig K, Bayer A. Long-term follow-up of the 137Cs body burden of individuals after the Chernobyl accident--a means for the determination of biological half-lives. Health Phys. 1999;77(4):373-82.

92. Lipsztein JL, Bertelli L, Oliveira CA, Dantas BM. Studies of Cs retention in the human body related to body parameters and Prussian blue administration. Health Phys. 1991;60(1):57-61.

93. Hasanen E, Rahola T. The biological half-life of 137 Cs and 24 Na in man. Ann Clin Res. 1971;3(4):236-40.

94. Cryer MA, Baverstock KF. Biological Half-Life of 137Cs in man. Health Phys. 1972;23:395-396

95. Henrichs H, Paretzke HG, Voigt G, Berg D. Measurements of Cs absorption and retention in man. Health Phys. 1989;57(4):571-8.

96. Sato I, Matsusaka N, Tsuda S, Kobayashi H, Nishimura Y. Relationship between turnover of cesium-137 and dietary potassium content in potassium-restricted mice. Radiat Res. 1997;148(1):98-100.

97. Stamatelatos IE, Kalef-Ezra J, Economides S, Yasumura S. Caesium retention during pregnancy in mice. J Environ Radioact. 1999;46:171-177

98. McKee JS, Durocher JJ, Bose R, Gusdal MI, Sharma GP, Pinsky C, Gallop D. Dynamic studies of positron-emitting putative tumor marker 132Cs in mice show differential tumor and regional uptake. Cancer Detect Prev. 1985;8(1-2):87-93.

99. Chauncey DM Jr, Hagan PL, Halpern SE, McKegney ML. Distributions of 137Cs, 201Tl, 203Hg, 203Pb and 57Co in a rat hepatoma model. Comparison with 67Ga. Invest Radiol. 1978;13(1):40-5.

100. Ando A, Ando I. Biodistributions of radioactive bipositive metal ions in tumor-bearing animals. Biometals. 1994;7(2):185-92.

101. Furchner JE, Trafton GA, Richmond CR. Distribution of Cesium^{137} After Chronic Exposure in Dogs and Mice. Proc Soc Exp Biol Med. 1964;116:375-8.

102. Horoszewicz JS, Leong SS, Kawinski E, Karr JP, Rosenthal H, Chu TM, Mirand EA, Murphy GP. LNCaP model of human prostatic carcinoma. Cancer Res. 1983;43(4):1809-18.

103. Hasenson M, Lundh B, Stege R, Carlstrom K, Pousette A. PAP and PSA in prostatic carcinoma cell lines and aspiration biopsies: relation to hormone sensitivity and to cytological grading. Prostate. 1989;14(2):83-90.

104. Kaighn ME, Narayan KS, Ohnuki Y, Lechner JF, Jones LW. Establishment and characterization of a human prostatic carcinoma cell line (PC-3). Investigative Urology 1979;17: 16-23

105. Alimirah F, Chen J, Basrawala Z, Xin H, Choubey D. DU-145 and PC-3 human prostate cancer cell lines express androgen receptor: implications for the androgen receptor functions and regulation. FEBS Lett. 2006;580(9):2294-300.

106. Thermo Electron. Infinity™ AST (GOT) Liquid Stable Reagent Product Insert. Date Accessed: December 18, 2006.

107. Thermo Electron. Infinity™ ALT (GPT) Liquid Stable Reagent Product Insert. Date Accessed: December 18, 2006.

108. Cayman Chemical. Creatinine Assay Kit Product Insert. Date Accessed: December 18, 2006.

109. Meyer MH, Meyer RA Jr, Gray RW, Irwin RL. Picric acid methods greatly overestimate serum creatinine in mice: more accurate results with high-performance liquid chromatography. Anal Biochem. 1985;144(1):285-90.

110. Yuen PS, Dunn SR, Miyaji T, Yasuda H, Sharma K, Star RA. A simplified method for HPLC determination of creatinine in mouse serum. Am J Physiol Renal Physiol. 2004;286(6):F1116-9.

111. Zhang S. Isolation and characterization of I(Kr) in cardiac myocytes by Cs+ permeation. Am J Physiol Heart Circ Physiol. 2006;290(3):H1038-49

112. Harvey RD, Ten Eick RE. Voltage-dependent block of cardiac inward-rectifying potassium current by monovalent cations. J Gen Physiol. 1989;94(2):349-61.

113. Matsuda H. Rb+, Cs+ ions and the inwardly rectifying K+ channels in guinea-pig ventricular cells. Pflugers Arch. 1996;432(1):26-33.

114. Thompson GA, Leyland ML, Ashmole I, Sutcliffe MJ, Stanfield PR. Residues beyond the selectivity filter of the K+ channel kir2.1 regulate

permeation and block by external Rb+ and Cs+. J Physiol. 2000;526 Pt 2:231-40.

115. Dibb KM, Leach R, Lancaster MK, Findlay JB, Boyett MR. Cs+ block of the cardiac muscarinic K+ channel, GIRK1/GIRK4, is not dependent on the aspartate residue at position 173. Pflugers Arch. 2000;440(5):740-4.

116. Apkon M, Nerbonne JM. Characterization of two distinct depolarization-activated K+ currents in isolated adult rat ventricular myocytes. J Gen Physiol. 1991;97(5):973-1011.

117. Lai XG, Yang J, Zhou SS, Zhu J, Li GR, Wong TM. Involvement of anion channel(s) in the modulation of the transient outward K(+) channel in rat ventricular myocytes. Am J Physiol Cell Physiol. 2004;287(1):C163-70.

118. Zhang S, Kehl SJ, Fedida D. Modulation of human ether-a-go-go-related K+ (HERG) channel inactivation by Cs+ and K+. J Physiol. 2003;548(Pt 3):691-702.

119. Oliver D, Baukrowitz T, Fakler B. Polyamines as gating molecules of inward-rectifier K+ channels. Eur J Biochem. 2000;267(19):5824-9.

120. Conti M. Targeting K+ channels for cancer therapy. J Exp Ther Oncol. 2004;4(2):161-6.

121. Bianchi L, Wible B, Arcangeli A, Taglialatela M, Morra F, Castaldo P, Crociani O, Rosati B, Faravelli L, Olivotto M, Wanke E. herg encodes a K+ current highly conserved in tumors of different histogenesis: a selective advantage for cancer cells? Cancer Res. 1998;58(4):815-22.

122. Muscaritoli M, Bossola M, Aversa Z, Bellantone R, Rossi Fanelli F. Prevention and treatment of cancer cachexia: new insights into an old problem. Eur J Cancer 2006;42:31-41.

123. Inui A. Cancer anorexia-cachexia syndrome: current issues in research and management. CA Cancer J Clin 2002;52:72-91.

124. MacDonald N, Easson A.M, Mazurak VC, Dunn GP, Baracos VE. Understanding and managing cancer cachexia. J Am Coll Surg 2003;197:143-161.

125. Rubin H. Cancer cachexia: its correlations and causes. Proc Natl Acad Sci U S A. 2003;100:5384-5389.

126. Marks DL, Cone RD. Central melanocortins and the regulation of weight during acute and chronic disease. Recent Prog Horm Res 2001;56:59-75.

127. Deeble PD, Murphy DJ, Parsons SJ, Cox ME. Interleukin-6- and cyclic AMP-mediated signaling potentiates neuroendocrine differentiation of LNCaP prostate tumor cells. Mol Cell Biol 2001;21:8471-8482.

128. Albrecht M, Doroszewicz J, Gillen S, Gomes I, Wilhelm B, Stief T, Aumuller G. Proliferation of prostate cancer cells and activity of neutral endopeptidase is regulated by bombesin and IL-1beta with IL-1beta acting as a modulator of cellular differentiation. Prostate 2004;58:82-94.

129. Humez S, Legrand G, Vanden-Abeele F, Monet M, Marchetti P, Lepage G, Crepin A, Dewailly E, Wuytack F, Prevarskaya N. Role of endoplasmic reticulum calcium content in prostate cancer cell growth regulation by IGF and TNFalpha. J Cell Physiol 2004;201:201-13.